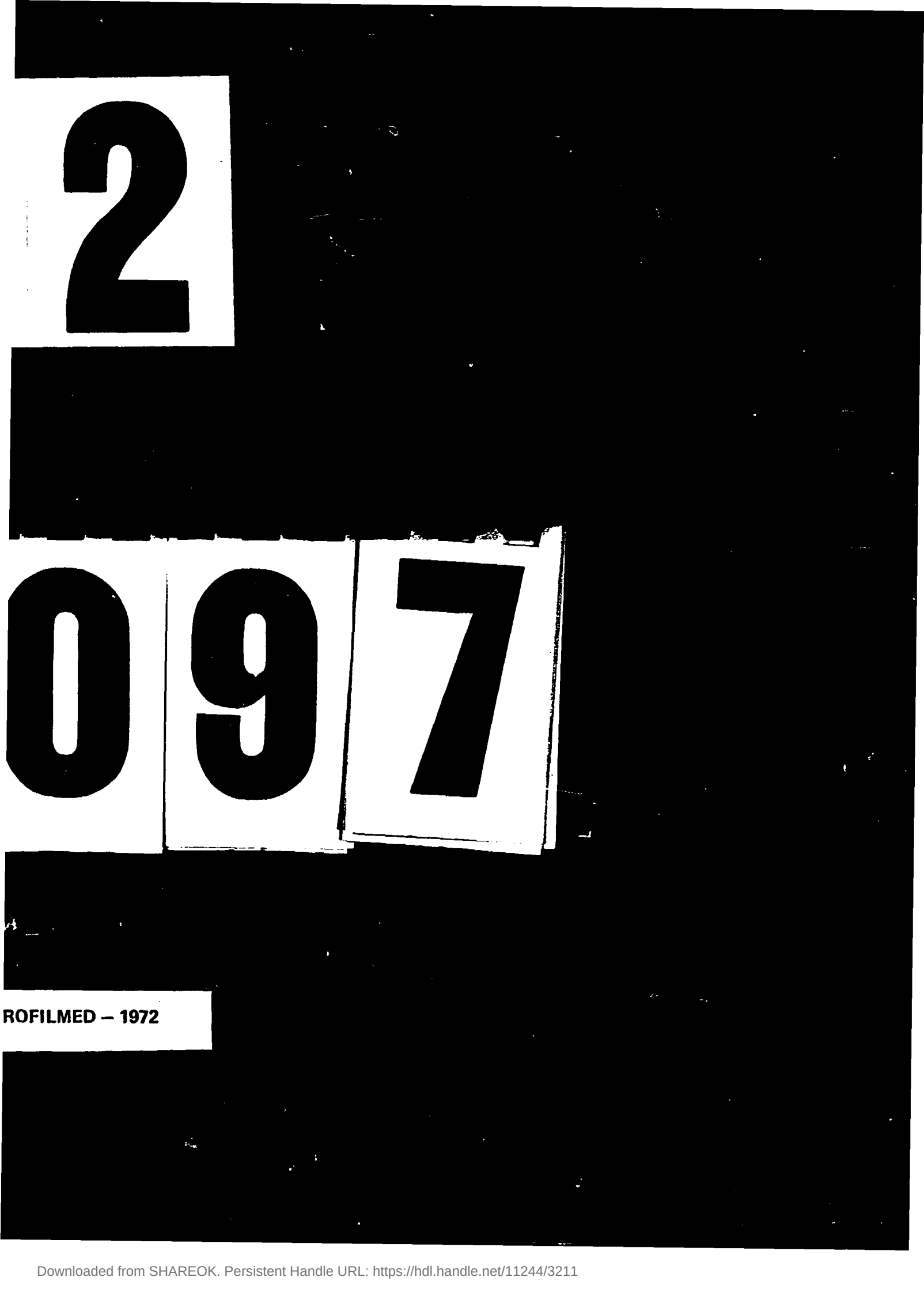

Downloaded from SHAREOK. Persistent Handle URL: https://hdl.handle.net/11244/3211

72-14,097

CHILDS, Jerry Dale, 1943-
STRUCTURAL AND SPECTRAL STUDIES OF THE CHARGE-TRANSFER COMPLEXES OF IODINE AND SULFUR DIOXIDE.

The university of Oklahoma, Ph.D., 1971
Chemistry, physical

University Microfilms, A XEROX Company, Ann Arbor, Michigan

THIS DISSERTATION HAS BEEN MICROFILMED EXACTLY AS RECEIVED

THE UNIVERSITY OF OKLAHOMA

GRADUATE COLLEGE

STRUCTURAL AND SPECTRAL STUDIES OF THE CHARGE-TRANSFER COMPLEXES OF IODINE AND SULFUR DIOXIDE

A DISSERTATION

SUBMITTED TO THE GRADUATE FACULTY

in partial fulfillment of the requirements for the

degree of

DOCTOR OF PHILOSOPHY

BY

JERRY DALE CHILDS

Norman, Oklahoma

1971

STRUCTURAL AND SPECTRAL STUDIES OF THE CHARGE-TRANSFER COMPLEXES OF IODINE AND SULFUR DIOXIDE

APPROVED BY

DISSERTATION COMMITTEE

PLEASE NOTE:

Some pages have indistinct print. Filmed as received.

UNIVERSITY MICROFILMS.

ACKNOWLEDGEMENT

The author wishes to express his appreciation to Dr. S. D. Christian and Dr. Dick van der Helm for their assistance and advice throughout the course of this research.

The many helpful suggestions of Dr. Eric Enwall, Dr. Just Grundnes, and Dr. Stanley Neely are also gratefully acknowledged.

The author is also indebted to his parents for their encouragement and assistance throughout his academic years.

The author especially wishes to thank his wife, Camilla, for her understanding and patience, and for the sacrifices she has made to make graduate study possible.

The author is grateful for support in the form of a National Science Foundation Traineeship.

TO CAMILLA

TABLE OF CONTENTS

		Page
LIST OF TABLES		vii
LIST OF ILLUSTRATIONS		x
PART I, SPECTRA AND THERMODYNAMIC CONSTANTS FOR WEAK MOLECULAR COMPLEXES OF IODINE		
Chapter		
I.	INTRODUCTION	1
II.	OBJECTIVES	24
III.	EXPERIMENTAL	25
IV.	DATA TREATMENT	40
V.	CONCLUSIONS AND DISCUSSIONS	71
PART II,	CRYSTAL AND MOLECULAR STRUCTURE OF THE CHARGE-TRANSFER COMPLEX BETWEEN TRIMETHYLAMINE AND SULFUR DIOXIDE	
VI.	INTRODUCTION	97
VII.	CRYSTAL AND MOLECULAR STRUCTURE OF TRIMETHYLAMINE·SO_2	110
VIII.	DISCUSSION OF THE STRUCTURE	131
IX.	IMPLICATIONS OF THE STRUCTURE	154
Appendix		
I.	NON-SPECIFIC EFFECTS ON SOLUBILITY	163
II.	PRIMARY DATA FROM CONVENTIONAL EXPERIMENTS OF THE BENESI-HILDEBRAND TYPE	175

Page

Appendix

III. PRIMARY DATA FROM THE POLYIODIDE SOLUBILITY METHOD. 183

IV. MULLIKEN'S VALENCE BOND RESONANCE THEORY..... 202

BIBLIOGRAPHY..... 209

LIST OF TABLES

Table		Page
1.	Free Donor Concentrations Necessary to Complex Half of the Acceptor Molecules	7
2.	Kortüm's Results for the Molecular Complexes of Iodine	20
3.	Literature Results for Various 1:1 Complexes of Iodine	21
4.	Literature Results for the Blue Shifted Iodine Band	22
5.	Extinction Coefficients at the Charge-Transfer Band and Equilibrium Constants for the 1:1 Complexes of Iodine	72
6.	Extinction Coefficients at the Charge-Transfer Band for the 1:1 Complexes of Iodine	76
7.	Extinction Coefficients at the Charge-Transfer Band for the 2:1 Complexes of Iodine	79
8.	Spectral Properties of the Blue Shifted Iodine Bands Obtained with the Solubility Method	86
9.	Spectral Properties of the Blue Shifted Iodine Bands Obtained with the Conventional Spectral Method	87
10.	Spectral and Thermodynamic Properties for the Mesitylene-Iodine System	93
11.	Correction of Observed Equilibrium Constants for Non-specific Effects	174
12.	Conventional Spectral Data for the Benzene-Iodine System at 25°C	176
13.	Conventional Spectral Data for the Toluene-Iodine System at 25°C	177
14.	Conventional Spectral Data for the o-Xylene-Iodine System at 25°C	178

Table | Page

15. Conventional Spectral Data for the m-Xylene-Iodine System at 25°C..... 179

16. Conventional Spectral Data for the p-Xylene-Iodine System at 25°C..... 180

17. Conventional Spectral Data for the Diethyl Ether-Iodine System at 15°C..... 181

18. Conventional Spectral Data for the Mesitylene-Iodine System at 25°C..... 182

19. Polyiodide Solubility Data for the System Benzene-Iodine at 25°C (Visible Region)..... 185

20. Polyiodide Solubility Data for the System Benzene-Iodine at 25°C (Ultraviolet Region)..... 186

21. Polyiodide Solubility Data for the System Toluene-Iodine at 25°C (Visible Region)..... 187

22. Polyiodide Solubility Data for the System Toluene-Iodine at 25°C (Ultraviolet Region)..... 188

23. Polyiodide Solubility Data for the System o-Xylene-Iodine at 25°C (Visible Region)..... 189

24. Polyiodide Solubility Data for the System o-Xylene-Iodine at 25°C (Ultraviolet Region)..... 190

25. Polyiodide Solubility Data for the System m-Xylene-Iodine at 25°C (Visible Region)..... 191

26. Polyiodide Solubility Data for the System m-Xylene-Iodine at 25°C (Ultraviolet Region)..... 192

27. Polyiodide Solubility Data for the System p-Xylene-Iodine at 25°C (Visible Region)..... 193

28. Polyiodide Solubility Data for the System p-Xylene-Iodine at 25°C (Ultraviolet Region)..... 194

29. Polyiodide Solubility Data for the System Pyridine-Iodine at 25°C (Visible Region)..... 195

30. Polyiodide Solubility Data for the System Pyridine-Iodine at 25°C (Ultraviolet Region)..... 196

Table Page

31. Polyiodide Solubility Data for the System Pyridine-Iodine at 15°C..... 197

32. Polyiodide Solubility Data for the System Diethyl Ether-Iodine at 15°C (Visible Region)..... 198

33. Polyiodide Solubility Data for the System Diethyl Ether-Iodine at 15°C (Ultraviolet Region)..... 199

34. Polyiodide Solubility Data for the System Mesitylene-Iodine at 25°C (Visible Region)..... 200

35. Polyiodide Solubility Data for the System Mesitylene-Iodine at 25°C (Ultraviolet Region)..... 201

36. Structural Parameters for Various Charge-Transfer Complexes..... 106

37. Crystal Data for TMA·SO_2..... 113

38. Heavy Atom Solutions for the TMA·SO_2 Structure..... 118

39. Atomic Parameters for TMA·SO_2..... 124

40. Thermal Parameters for TMA·SO_2..... 125

41. Observed and Calculated Structure Factors for TMA·SO_2... 126

42. Peak Heights of Hydrogen Atoms in the Difference Fourier 127

43. Van der Waal's Contacts Less than 4 Å..... 130

44. Charge-Transfer Bond Distances..... 135

45. Principal Axes and Direction Cosines of Anisotropic Ellipsoids..... 141

46. Angles Between Principle Axes of Anisotropic Ellipsoids and Various Vectors..... 142

47. Sulfur Dioxide Geometries..... 147

48. Mulliken's Parameters for the TMA·SO_2 Complex..... 160

LIST OF ILLUSTRATIONS

Figure		Page
1.	Spectra of the Pyridine·Iodine Complex.....	3
2.	Absorbance of Complex Versus the Concentration of the Donor.....	9
3.	Polyiodide Phase Diagram.....	28
4.	Equilibration Times in the Polyiodide Solubility Method.....	31
5.	Concentrations of Various Complexing Species in Equilibrated Polyiodide Solutions.....	34
6.	Typical Spectra Obtained with the Polyiodide Solubility Method.....	35
7.	Blue Shifted Iodine Band for the p-Xylene·Iodine Complex as Determined by the Conventional Techniques...	45
8.	Solubility Data for the Pyridine-Iodine System (Visible Spectral Region).....	51
9.	Solubility Data for the Pyridine-Iodine System (Ultraviolet Spectral Region).....	52
10.	Solubility Data for the System Benzene-Iodine (Visible Spectral Region).....	54
11.	Solubility Data for the System p-Xylene-Iodine (Visible Spectral Region).....	55
12.	Solubility Data for the System Benzene-Iodine (Ultraviolet Spectral Region).....	58
13.	Solubility Data for the System p-Xylene-Iodine (Ultraviolet Spectral Region).....	59
14.	Blue Shifted Iodine Band for the Pyridine·Iodine Complex.....	64

Figure		Page
15.	Blue Shifted Iodine Band for the Diethyl Ether·Iodine Complex.....	65
16.	Blue Shifted Iodine Band for the p-Xylene·Iodine Complex.....	67
17.	Change in Absorbance at the Blue Shifted Band Maximum Plotted Against the Corresponding Change at the Isosbestic Point for the p-Xylene·Iodine Complex.....	68
18.	Extinction Coefficient at the Maximum of the Blue Shifted Band Plotted Versus the Equilibrium Constant..	89
19.	Ultraviolet Spectra of TMA, SO_2, and TMA·SO_2.....	102
20.	Structures of the Dioxane·Br_2 and TMA·I_2 Complexes....	104
21.	Structure of the Benzene·Br_2 Complex.....	105
22.	Structure of $IrCl(CO)(SO_2)(P(C_6H_5)_3)_2$.....	109
23.	Apparatus Use to Obtain Initial TMA·SO_2 Crystals.....	111
24.	Packing of the Complex in the Unit Cell.....	130
25.	Bond Distances Observed for the TMA·SO_2 Complex.....	132
26.	Projection of the TMA·SO_2 Complex Down the N·S Bond...	133
27.	Bond Angles Observed for the TMA·SO_2 Complex.....	134
28.	Orientation of the Thermal Ellipsoids on the SO_2 Component.....	139
29.	ORTEP Drawing of the TMA·SO_2 Complex.....	140
30.	Hybridization and Molecular Orbitals of SO_2.....	152
31.	Geometry of the TMA·SO_2 Complex.....	156
32.	Energy Diagram for the TMA·SO_2 Complex.....	208

I. SPECTRA AND THERMODYNAMIC CONSTANTS FOR WEAK MOLECULAR COMPLEXES OF IODINE

CHAPTER I

INTRODUCTION

Spectral work by Benesi and Hildebrand[1] on solutions of an aromatic hydrocarbon and iodine showed the existence of an electronic absorption band which was not present in either component; this band was assumed to be characteristic of a complex between iodine and the hydrocarbon. Mulliken[2] suggested that the absorption was due to an intermolecular charge-transfer involving the partial transfer of an electron from the hydrocarbon to the iodine. The hydrocarbon thus functioned as an electron donor (Lewis base) and the iodine as an electron acceptor (Lewis acid). The resulting associated species was referred to as an electron donor-acceptor (EDA) complex. Subsequent to this work, a great number of systems involving a variety of donors and acceptors were shown to exhibit bands analogous to those found by Benesi and Hildebrand.[3] Spectral techniques rapidly developed which allowed the determination of the spectra and energetics of the various systems. While it was generally accepted that the stronger interactions of this type could be characterized with a reasonable degree of accuracy, from the start there existed skepticism concerning the reliability of

determinations made on weak complexes.[3-6] Unfortunately, the weak complexes were often the most interesting since an understanding of them might provide some insight as to the role of charge-transfer in certain biological systems and reaction mechanisms where subtle charge-transfer forces are suspected to operate.[4]

In the past few years several excellent review articles and books have been published which cover the field of EDA complexes in some detail.[3-6] In view of this, it would serve no purpose to present a comprehensive review of the literature here. However, it seems appropriate to briefly review the development of EDA theory, discuss its application to weak complexes, and present criticism of each.

Spectra of Electron Donor-Acceptor Complexes

In the electronic spectra of donor-acceptor complexes the most striking feature is the appearance of the charge-transfer band. However, for the charge-transfer complexes of iodine, there are additional interesting spectral features. These are illustrated in Figure 1 for the pyridine-iodine complex in n-heptane, which was first studied by Reid and Mulliken.[7] The Figure shows an increasing absorbance near 422 mμ due to the complexed iodine band and a decreasing absorbance near 520 mμ due to the locally excited band of uncomplexed iodine. The spectra correspond to solutions with increasing donor concentrations at a constant total iodine concentration. The curves cross near 477 mμ which is the isosbestic point for the uncomplexed and complexed iodine. The ultraviolet spectrum of this complex is characterized by an exceptionally intense charge-transfer band (235 mμ). The unusually high intensity of this band has been explained by Mulliken.[8] The derivation of equilibrium

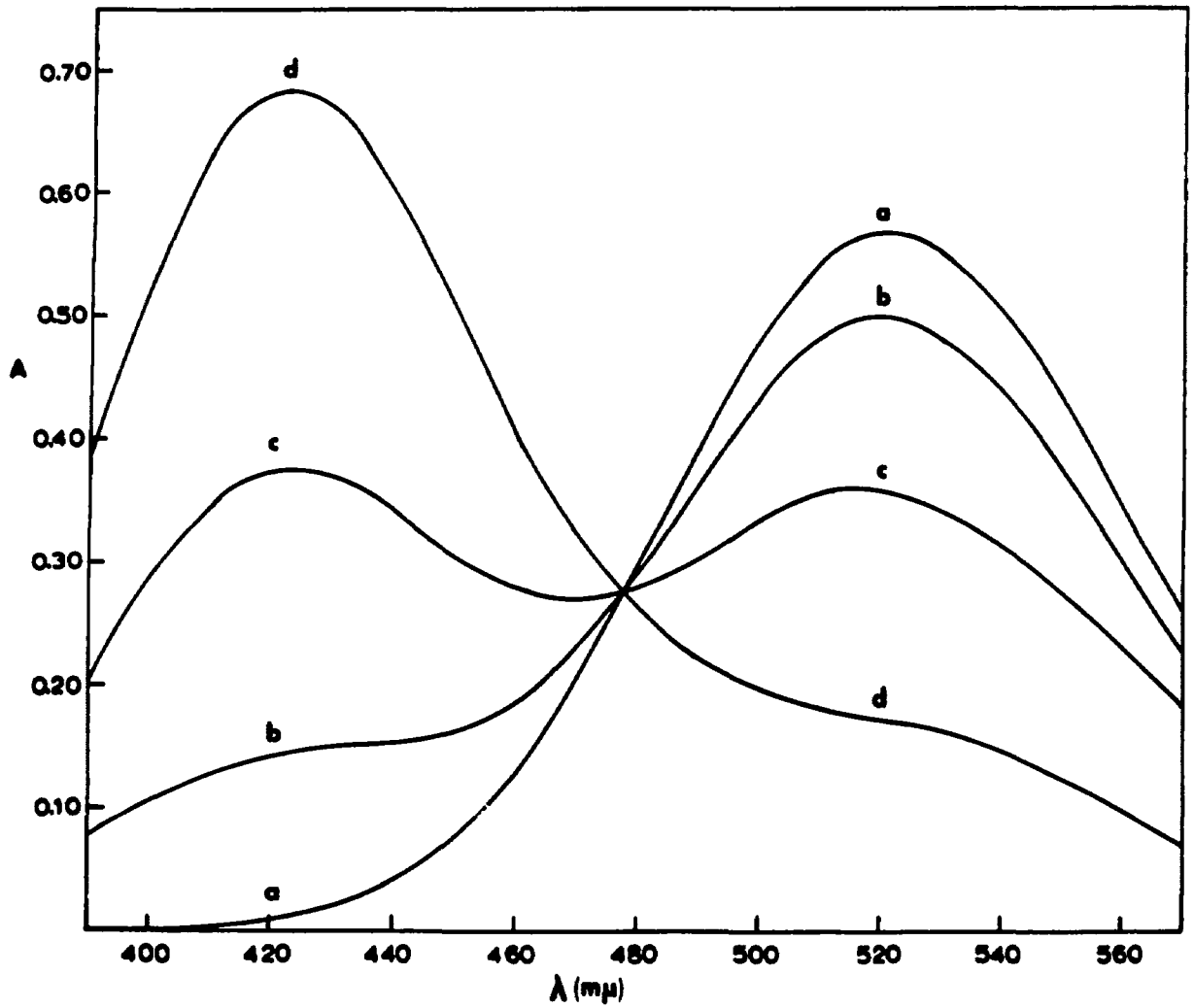

Figure 1. Visible Spectra for the Pyridine·Iodine Complex as Determined by the Usual Spectral Technique. The formal concentration of iodine is the same in all solutions. Curve a is the heptane/iodine blank; curves b, c, and d correspond to increasing pyridine concentration.

constants and extinction coefficients from spectral data has been accomplished by a variety of techniques.[3-5] Commonly, the increase in absorbance at the charge-transfer band has been followed with increasing donor concentration at constant acceptor concentration. However, the same procedure has been employed at the blue shifted iodine band for some complexes, either because the charge-transfer band is too far into the ultraviolet or because of difficulties with overlapping spectral bands. In some weak complexes (viz., aromatic hydrocarbon·iodine complexes) measurements at the blue shifted band are less sensitive than those at the charge-transfer band because of the relatively low intensity at the former. In such cases, analyses are usually performed at the charge-transfer band.

Methods of Evaluating Equilibrium Constants

In using spectral methods to study complex-formation it is necessary to infer two parameters from a set of spectral measurements at various concentrations, namely the equilibrium constant (K) and the extinction coefficient (ε) of a spectral band having an absorbance which varies in direct proportion to the concentration of the molecular complex. The Benesi-Hildebrand technique is probably the method most commonly used to obtain these properties.[1] This treatment starts with the assumption that only one equilibrium exists in solution, namely

$$A + D \rightleftarrows DA \qquad (1)$$

for which the equilibrium constant is given by

$$K_c = \frac{C_{DA}}{C_D\, C_A} \qquad (2)$$

where C_{DA} is the molar concentration of the complex and C_A and C_D are the molar concentrations of the uncomplexed donor and acceptor. Equation (2) can be rewritten in the form

$$K_c = \frac{C_{DA}}{(C_D^o - C_{DA})(C_A^o - C_{DA})} \tag{3}$$

where C_D^o and C_A^o are the initial molar concentrations of the donor and acceptor. For weak complexes (K_c < 1 ℓ/mole), $C_D^o >> C_{DA}$ so that $C_D^o \simeq C_D$ and thus equation (3) may be simplified to

$$K_c = \frac{C_{DA}}{C_D^o\,(C_A^o - C_{DA})} \tag{4}$$

Substituting for C_{DA} in equation (4) the relation between concentration and absorbance of the complex given by Beer's law ($C_{DA} = A_{DA}/\ell\varepsilon_{DA}$) yields

$$K_c = \frac{A_{DA}/\ell\varepsilon_{DA}}{C_D^o\,(C_A^o - A_{DA}/\ell\varepsilon_{DA})} \tag{5}$$

Equation (5) can be rearranged to give

$$\frac{\ell C_A^o\, C_D^o}{A_{DA}} = \frac{C_D^o}{\varepsilon_{DA}} + \frac{1}{K_c\,\varepsilon_{DA}} \tag{6}$$

and division of each term by C_D^o gives the common form of the Benesi-Hildebrand equation

$$\frac{\ell C_A^o}{A_{DA}} = \left(\frac{1}{K_c\,\varepsilon_{DA}}\right)\frac{1}{C_D^o} + \frac{1}{\varepsilon_{DA}} \quad . \tag{7}$$

Using experimentally determined values of A_{DA} at various donor concentrations (C_A^o is usually fixed), a plot of $1/C_D^o$ against $\frac{\ell C_A^o}{A_{DA}}$ can be constructed. The result should be a straight line with slope $(1/K_c\,\varepsilon_{DA})$ and intercept $(1/\varepsilon_{DA})$. There have been various modifications of this equation, probably the most important of which is the Scott equation.[9] This

equation is obtained by multiplication of Equation (7) by C_D^o

$$\frac{\ell C_D^o C_A^o}{A_{DA}} = \frac{1}{\epsilon_{DA}} C_D^o + \frac{1}{K_c \epsilon_{DA}} \quad . \tag{8}$$

This equation has been more widely used than the Benesi-Hildebrand equation since it involves an extrapolation to the dilute solution region while the Benesi-Hildebrand equation involves the reverse extrapolation. When necessary either of these equations may easily be modified to study strong complexes.[10]

Limitations of the Conventional Methods

Although these two methods of treating spectral data have been widely applied in the past, the methods have been viewed with some skepticism.[3-6] Person[11] has pointed out that the most accurate values for formation constants of a complex are obtained when the equilibrium concentration of the complex is of the same order of magnitude as the equilibrium concentration of the more dilute component. If the usual technique of a constant total concentration of acceptor is maintained while the other component is varied, then a sizeable fraction of the acceptor must be complexed in the most concentrated donor solution. In the case of weak complexes this means that the highest donor concentration must be several molar in concentration units. Table 1 illustrates this point by listing the donor concentration ($\sim\frac{1}{K_c}$) necessary to complex 50% of the acceptor. For K_c = 0.1 ℓ/mole the acceptor is 50% complexed at C_D = 10 M. As Person has pointed out, if only a small amount of complex is obtained the absorbance of the complex will vary linearly (within experimental error) with the concentration of the donor, since

TABLE 1

FREE DONOR CONCENTRATION AT WHICH HALF OF THE ACCEPTOR MOLECULES ARE IN THE COMPLEXED FORM

K(ℓ/mole)	C_D(mole/ℓ)
10.0	0.1
5.0	0.2
2.0	0.5
1.0	1.0
0.5	2.0
0.2	5.0
0.1	10.0

$$A_{DA} = \ell C_{DA} \epsilon_{DA} \simeq \ell \epsilon_{DA} K_c C_A^o C_D^o \qquad (9)$$

where $C_A \simeq C_A^o$ under these conditions. This corresponds to the limiting slope ($\ell \epsilon_{DA} K_c C_A^o$) of Figure 2. This situation is common in systems where the donor is only slightly soluble in the solvent, e.g., anthracene·I_2 in n-heptane.[12] A Scott plot of the data in Region I will result in a straight line with intercept ($1/K_c \epsilon_{DA}$) but with slope 0 (within experimental error). Thus, the product $K_c \epsilon_{DA}$ is obtained accurately but separation of the product is not possible. If the concentration of the donor is so high that all of the acceptor is in the complexed form, then further addition of donor does not significantly increase the absorbance and only the slope $1/\epsilon_{DA}$ is obtained. This corresponds to Region III of the figure. According to Person the solution with the highest initial donor concentration must lie in Region II of Figure 1 where significant curvature in the plot is observed. Only in this region can the Scott plot or other modifications be applied to separate K and ϵ.

As indicated in Table 1, equilibrium constants considerably less than 1 ℓ/mole require the use of donor concentrations well in excess of 1 M. At such concentration levels, the medium is hardly equivalent to pure solvent and it may be anticipated that both the spectral and thermodynamic properties of the solute species are significantly different from the analogous properties in dilute solution.[3-6,13] Attempts have been made to account for the effects of sizeable concentrations of dissolved solutes on specific and non-specific interaction of the solvent with the donor, acceptor and complex molecules.[14-17] Carter, Murrell and Rosch[14] define an equilibrium constant which is dependent upon the mole fraction of the "free" solvent. They consider the following

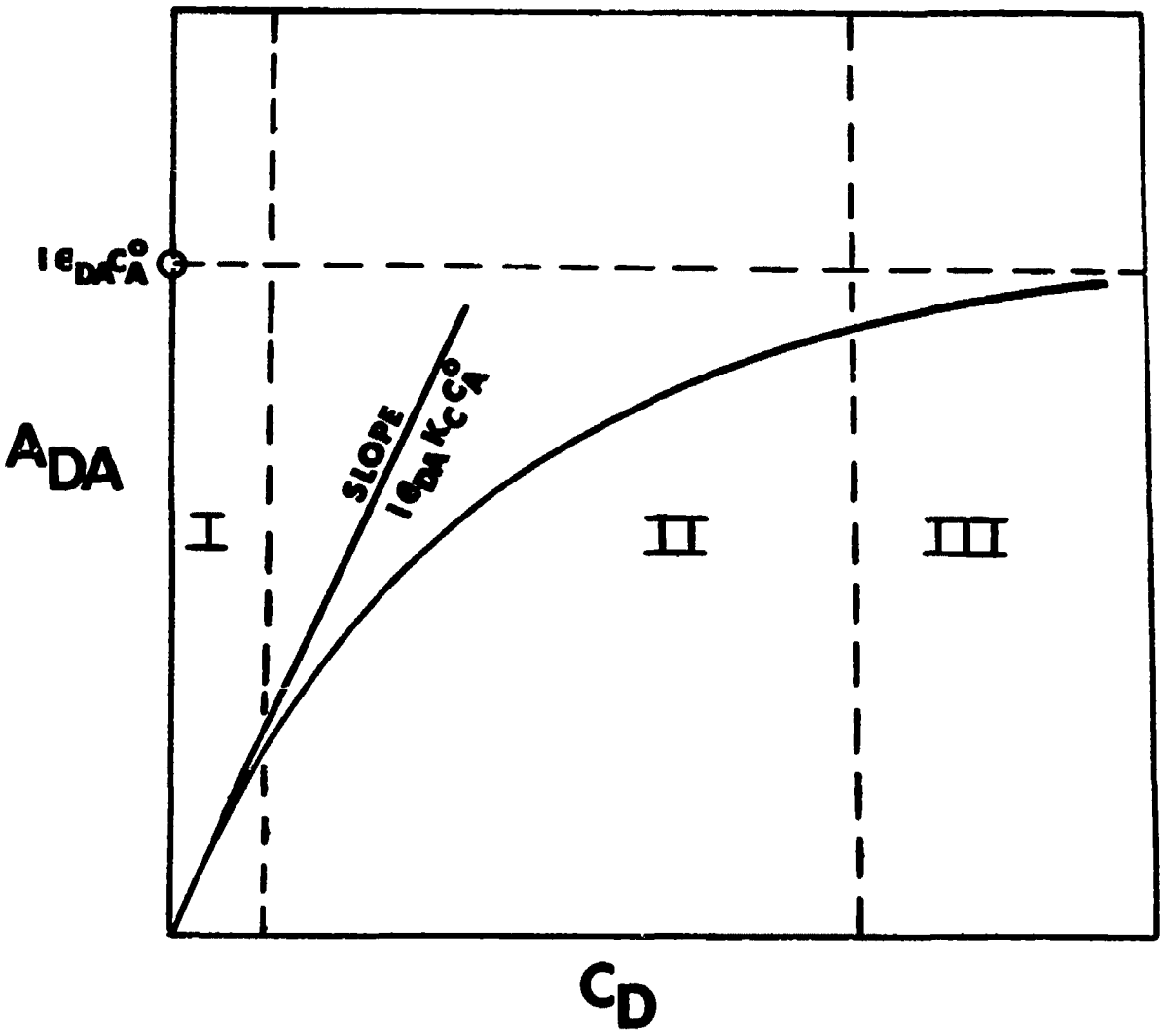

Figure 2. Absorbance of the Complex Versus the Concentration of the Donor at Fixed Acceptor Concentration, After Reference 11.

equilibrium

$$AS_n + DS_m \rightleftarrows DAS_p + qS \qquad (10)$$

where A, S, D, and DA represent the acceptor, solvent, donor and complex, respectively, and where ($q = n + m - p$). The subscripted S's indicate the extent of solvation of the various species and q is taken as a measure of the amount of solvent "squeezed" out by formation of the complex. The equilibrium constant is defined as

$$K = \frac{C_{DAS_p} X_S^q}{C_{AS_n} C_{DS_m}} \qquad (11)$$

where X_S is the mole fraction of the free solvent, defined relative to the total number of moles of D, A, and S (complexed and uncomplexed). K is defined in this way so that it has the same units as the Benesi-Hildebrand K_{B-H}. This treatment lends to a modified form of Benesi-Hildebrand equation given by

$$\frac{\ell C_D^o}{A_{DA}} = \frac{1}{C_D^o} \frac{X_S^q}{K_C \, \epsilon_{DA}} + \frac{1}{\epsilon_{DA}} \quad . \qquad (12)$$

This form differs from the original Benesi-Hildebrand equation in that it explicitly involves the mole fraction of the free solvent. According to this interpretation, if the data were analyzed according to the Benesi-Hildebrand treatment without this solven' 'ependence included, then

$$K_{B-H} = K_c - \frac{q(m + 1)}{C_S^o}$$

and $\epsilon_{B-H} = \epsilon_{DA} \left(\frac{K_c}{K_{B-H}}\right)$ where C_S^o is the total concentration of pure solvent and K_c and ϵ_{DA} are supposedly the "true" values of the equilibrium constant and extinction coefficient. Thus, the Benesi-Hildebrand treatment under-

estimates the equilibrium constant by the amount $q(m + 1)/C_S^o$ and overestimates the extinction coefficient by the ratio (K_c/K_{B-H}). In this approach, the evaluation of $q(m + 1)$ is a serious problem since there is no unambiguous way to determine a value for this quantity. For the aromatic hydrocarbon-iodine complexes, $q(m + 1)$ was obtained by varying its value until the resultant extinction coefficients were in agreement with Mulliken's predictions.[18] Thus $q(m + 1)$ becomes a parameter which may be adjusted to the extent that the experimental results fit the theory.

A less arbitrary approach to non-ideality was that of Person and Mulliken.[15] They attempted to account for the non-ideality introduced by large concentrations of the donor by considering the concentration dependence of K_x, the equilibrium constant in mole fraction units. The thermodynamic equilibrium constant defined in terms of activities is given by

$$K_a = \frac{a_{DA}}{a_D a_A} = \frac{X_{DA}\,\gamma_{DA}}{X_A X_D \gamma_A \gamma_D} = K_x\,K_\gamma$$

where the activity of a component is given by the product of the mole fraction and activity coefficient of that component. In the Benesi-Hildebrand and related methods the assumption is made that

$$\gamma_{DA} = \gamma_A \gamma_D$$

which implies $K_\gamma = 1$ over a sizable concentration range.[1] This fortuitous cancellation seems somewhat unlikely at high donor concentrations but the validity of such an assumption is difficult to assess. If K_γ is not 1, then its concentration dependence must be considered and

consequently, some assumption must be made concerning its functional form. Mulliken and Person assume K_γ to be a linear function of the donor concentration, i.e.,

$$K_\gamma = k_o (1 + bX_D) \tag{13}$$

where X_D is the mole fraction of the donor and where the standard states of all species have been taken as the pure liquids. K_γ does take the form indicated in equation (13) when calculated as a function of X_D from solubility parameters δ of the various components.[19] If equation (13) is valid, then the Scott method does not yield the true values of K_X and ε, but rather constants which are related to them by the expressions

$$\varepsilon_{Scott} = \varepsilon^o \frac{K_X^o}{K_{Scott}}$$

and

$$K_{Scott} = K_X^o + b$$

where ε_{Scott} and K_{Scott} are the values obtained from the Scott treatment, K_X^o and ε^o are the "true" values, and b is defined by equation (13). Using solubility parameters to estimate k_o and b (δ_{DA} was taken as the geometric mean of δ_{I_2} and δ_{BZ} for the benzene·I_2 complex), it was concluded that neglect of these effects could result in errors in K and ε as large as a factor of 2 in the case of the benzene·I_2 complex.

Other attempts to account for the effects of sizeable concentrations of the dissolved solutes have included the possibility that complexes other than the 1:1 adduct may form at large concentrations.[20,21] The consequences of multiple equilibria have been considered in some detail by Deranleau[21] who has shown that the Benesi-Hildebrand, Scott, or

Scatchard[22] ($\frac{A_{DA}}{\ell C_D C_A^o}$ vs. $\frac{A_{DA}}{\ell C_A^o}$) plots should in general give curved lines in the event of multiple equilibria. Deranleau presents extensive development of these methods with interpretation of the resulting slopes and intercepts in terms of equilibrium constants and extinction coefficients for various assumed species. However, such treatments must be based on the assumption that all the individual species obey Henry's law over the concentration range considered. For the weak complexes, the high donor concentrations employed makes this unlikely.[13] Therefore, any interpretation in terms of specific complexes alone, without consideration of activity effects on individual species at elevated concentrations, is probably an oversimplification.

The interpretation of the spectra of solutions of donor, acceptor, and complex at high concentrations may also be complicated by factors such as "contact charge-transfer" and the presence of numerous orientation isomers of the 1:1 complex.[20] Basically, these factors were proposed to explain the following observations. Mulliken noted that increases in K values which usually occur as the donor ionization potential decreases should be accompanied by an increase in the quantum mechanical dipole moment, oscillator strength of the charge-transfer transition, and thus the intensity of the charge-transfer band.[18] Benesi and Hildebrand's original work indicated that for the aromatic hydrocarbon·iodine complexes the reverse was true. In addition, these very weak complexes were found to have unexpectedly large extinction coefficients. In an attempt to explain these results, Orgel and Mulliken[20] proposed that there were two types of charge-transfer absorption; one associated with complexes which form when the components come together in an orientation favorable to

formation of a stable entity and another, which results during random encounters whenever a donor and acceptor are sufficiently close to one another, called "contact charge-transfer." The contact charge-transfer idea has been used to explain the ultraviolet absorbance of iodine in heptane-perfluoroheptane solutions. It has been observed that iodine dissolved in saturated hydrocarbons absorbs strongly in the ultraviolet at wavelengths as long as 260 mμ while iodine vapor shows very little absorption at wavelengths longer than 200 mμ. Evans[23] found that the spectra of iodine dissolved in perfluoroheptane was essentially identical with that observed in the vapor but when n-heptane is added to the system the absorbance at 260 mμ appears and increases linearly with the concentration of heptane added. A Benesi-Hildebrand plot of such data yields an extinction coefficient equal to infinity and an apparent equilibrium constant of zero.[20] Mulliken and Orgel concluded that this iodine·n-heptane absorbance is an example of pure contact charge-transfer while the iodine·aromatic hydrocarbon systems probably involve a mixture of both complex and contact absorption. For the contact charge-transfer case, the concentration of such contacts was given as

$$C_{cp} = \alpha(C_D^o - C_{DA})(C_A^o - C_{DA}) \qquad (14)$$

and the absorbance due to them by

$$A_{cp} = \ell\varepsilon_{cp} C_{cp} \qquad (15)$$

where C_{cp} refers to the concentration of contact pairs, α is a constant defined in terms of the number of sites for a donor molecule around the acceptor molecule under the conditions of loose thermal contact, and ε_{cp}

is the extinction coefficient for the contact pair. From the expression for the equilibrium constant and equation (14), it is possible to write

$$C_{cp} = (\alpha/K_c)\ C_{DA} \quad . \tag{16}$$

Now the absorbance at the charge-transfer band could be expressed as

$$A^{total} = A_{DA} + A_{cp} = \ell C_{DA}\ \varepsilon_{DA} + \ell C_{cp}\ \varepsilon_{cp} = \ell C_{DA}\ \varepsilon' \tag{17}$$

where

$$\varepsilon' = \varepsilon_{DA} + \frac{\varepsilon_{cp}}{K_c} \tag{18}$$

or defining $e = \frac{\varepsilon_{cp}}{\varepsilon_{DA}}$ where

$$\varepsilon' = \varepsilon_{DA}\ (1 + e/K_c) \quad . \tag{19}$$

According to this development, the Benesi-Hildebrand equation actually should be written as

$$\frac{\ell C_A^o}{A^{total}} = \frac{1}{K_c \varepsilon'} \left(\frac{1}{C_D^o}\right) + \frac{1}{\varepsilon'} \quad . \tag{20}$$

For the stronger complexes, the concentrations of the donor and acceptor may be kept at a minimum and thus the concentration and absorbance of the contact pairs are kept at a minimum. In this case the ε' is very nearly ε_{DA}. However, for the weak complexes it is necessary to use large concentrations of the donor or acceptor in order to obtain sufficient amounts of complex.[11] In this case the concentration of the contact pair will also be very large and the implication is that the extinction coefficient obtained in the usual treatments is given by the expression above for ε'. Unfortunately, there is no unambiguous way to separate the contact and charge-transfer absorptions. Mulliken and Orgel[20] chose,

more or less arbitrarily, values for the quantity e of 4 or 5 for the aromatic hydrocarbon·iodine complexes. For either of these values of e, the ϵ_{DA} values of these complexes agree with the theoretical expectations, in that they increase with increasing methylation or donor strength. On this basis, it is estimated that about 1/4 of the intensity of the charge-transfer band is due to complexes and 3/4 to contacts. Unfortunately, the force of these arguments is weakened by doubts as to the validity of spectrally determined values of K_C and ϵ.[11]

Mulliken and Orgel also considered the possibility that there exist various orientation isomers of the 1:1 complex.[20] In weak complexes such as those between the aromatic hydrocarbons and iodine, the geometry in the gas and solution phases may not be rigidly fixed.[24,25] The interpretation of spectra, which is complicated by these various orientation isomers of the 1:1 complex, would be difficult. The Benesi-Hildebrand method, if it is applicable at all to such systems, yields a value of K_C which is the sum of the formation constants of all the isomers of the 1:1 complex and a calculated value of ϵ_{DA} which is a weighted average of all the extinction coefficients of the various isomers.[20]

It has been proposed that certain of the individual isomers may contribute disproportionately to the absorbance.[20,24,27] This argument has been used to explain the observation that the values of the extinction coefficient for the charge-transfer bands of gaseous complexes are lower than the corresponding values in the condensed phase. In the gas phase, it is argued that most of the molecular arrangements which contribute to the stability of the 1:1 complex do not contribute

significantly to the intensity of the charge-transfer band.[25] However, in the case of complexes in solution, the values determined for K_c and ε may pertain more nearly to oriented complexes. Unfortunately, this argument is weakened somewhat by the doubts concerning the validity of these values for weak complexes. In this connection, Christian and Grundnes[27] have employed a unique method for studying weak complexes which is the gas phase analogy of the solubility method to be described in the present research. Their results indicate that dispersion forces can play an important role in stabilizing the weak molecular complexes of iodine. In fact, in the gas phase, it is suggested that the weak complex between benzene and iodine is stabilized by charge-transfer forces to the extent of only about 25%. This is in agreement with the conclusion of Atack and Rice[25] that the gaseous benzene·iodine complex is primarily a van der Waals complex, which exhibits little preference for a particular orientation.

The relative contributions of specific (e.g., charge-transfer) and non-specific (e.g., dispersion force) interactions in stabilizing weak molecular complexes in any medium is difficult to assess. The present method of studying complexes necessarily measures a combination of these effects. In spite of the difficulties in separating these effects, recent experimental[27] and theoretical[28] results indicate that the contribution of charge-transfer forces to the stabilization of weak complexes in the gas phase has been overestimated. Mulliken[5] has argued the effect of London dispersion forces approximately cancels out in inert solvents so that they may be approximately neglected, whereas they must be included for the vapor state complex. However, he does point out that

the degree of cancellation of van der Waals forces should not be exact, and should vary somewhat from case to case.

Solubility Methods

One of the limiting features in the conventional spectral studies of donor-acceptor interactions is the difficulty of controlling the concentrations of the various complexing species (vide supra). Christian et al. have described techniques for performing spectral and classical studies of liquid and vapor systems in which the activity of water has been maintained at a desired level by utilizing constant humidity sources, such as aqueous salt solutions or crystalline hydrates.[29] These methods have found wide application in solving the experimental problem of handling water at the low concentrations involved in the studies of hydrogen-bonded complexes of water in organic solvent systems of interest.[17] Physical measurements made on the water-solvent systems at constant water activity have been treated as blanks for measurements of properties of the ternary systems (water-polar solute-solvent) at the same water activity; changes in these properties are attributed entirely to the formation of discrete water-solute complexes. The similarities of problems encountered in studying iodine complexes and those arising in the investigations of complexes of water suggested the possibility that methods utilizing a constant iodine activity source might possess advantages over conventional techniques for investigating donor-acceptor interactions. Earlier research by Kortüm[30,31] had shown the feasibility of using solid iodine to control the activity of iodine in ternary (donor-iodine-organic solvent) systems, although the method described has not been widely applied in research on molecular complexes. In Kortüm's

method, the increase in the concentration of iodine at constant iodine activity upon the addition of very small amounts (about 1 mole %) of a donor, such as benzene, to the iodine-solvent system was attributed to the formation of a specific complex. The total concentrations (mole fraction units) of iodine ($X_{I_2}^{total}$) in a particular donor solution and in the solvent blank ($X_{I_2}^{o}$) were measured by titration. The mole fraction of the complex was then calculated from the difference ($X_{I_2}^{total} - X_{I_2}^{o} = X_{DI_2}$), the mole fraction of the free donor from ($X_D^{free} = X_D^{total} - X_{DI_2}$), and the mole fraction of the free iodine in all solutions was taken simply as $X_{I_2}^{o}$ (the mole fraction of the solvent blank). On this basis, the equilibrium constants of Table 2 were calculated. The equilibrium constants determined in this manner were constant (within experimental error) which was taken as indication of the validity of the assumption that only 1:1 complexes existed in the solutions. The existence of activity effects on the dissolved iodine due to the presence of the donor was recognized by Kortüm but since the donor concentrations were so low, such effects were generally assumed to be constant and small compared to the total effect being measured, and consequently they were neglected.

In view of the simplicity of the techniques described above, the development of a procedure which combined the advantages of both the spectral and constant activity methods has been undertaken. The polyiodides of inorganic and quaternary ammonium cations are employed as constant activity sources to control the concentrations of the complexing species and spectral techniques are used to determine these concentrations.

Literature Results

For purposes of later reference Tables 3 and 4 are included here.

TABLE 2

ASSOCIATION CONSTANTS FOR THE FORMATION OF SOME 1:1 COMPLEXES OF IODINE IN CYCLOHEXANE AT 25°C AS DETERMINED BY KORTÜM[30,31]

Donor	K_x^*	K_c (ℓ/mole)
Benzene	3.12	0.339
Toluene	4.40	0.479
Chlorobenzene	2.86	0.311
Dioxane	23.2	2.53

*Constants originally reported in mole fraction units. K_c was obtained from K_x using the relation:

$$K_c = K_x\left(\frac{M_1}{1000\ D_1}\right)$$

where M_1 and D_1 are the molecular weight and density of the solvent.

TABLE 3

ASSOCIATION CONSTANTS AND EXTINCTION COEFFICIENTS AT THE CHARGE-TRANSFER BAND FOR SOME 1:1 COMPLEXES OF IODINE AT 25°C

Donor	K (ℓ/mole)	λ (mμ)	ε ($\ell mole^{-1} cm^{-1}$)	Kε	Solvent	Ref.
Benzene	0.15[a]	292	16,400	2460	CCl_4	32
	0.155[a]	295	14,700	2280	CCl_4	33
	0.166[a]	296	16,700	2670	n-hexane	34
	0.212	290	13,550	2870	cyclohexane	35
	0.246	288	12,000	3000	n-heptane	36
Toluene	0.16[a]	302	16,700	2670	CCl_4	32
	0.293[a]	302	11,800	3460	n-hexane	34
	0.293	300	11,560	3390	cyclohexane	35
o-Xylene	0.27[a]	316	12,500	3380	CCl_4	32
	0.386[a]	318	10,600	4090	n-hexane	34
	0.407	320	9,950	4050	cyclohexane	35
m-Xylene	0.31[a]	318	12,500	3880	CCl_4	32
p-Xylene	0.31[a]	304	10,100	3130	CCl_4	32
Mesitylene	0.82[a]	332	8,850	7260	CCl_4	32
	0.579[a]	332	10,200	5910	CCl_4	33
	0.691[a]	333	9,900	6840	n-hexane	34
Diethyl ether[b]	1.3	250	5,480	7120	n-heptane	37
Pyridine	185	235	50,000	9.3×10^6	n-heptane	38
	157	---	------	------	n-heptane	39
	137	235	51,730	7.1×10^6	n-heptane	40

[a] Constants originally reported in mole fraction units; converted here to units of ℓ/mole.

[b] Results refer to an experimental temperature of 15°C.

TABLE 4

WAVELENGTHS AND EXTINCTION COEFFICIENTS OF THE BLUE SHIFTED IODINE BAND FOR SOME 1:1 COMPLEXES OF IODINE AT 25°C

Donor	λ^{bs} (mμ)	ε^{bs} ($\ell mole^{-1} cm^{-1}$)	Solvent	Reference
Benzene	500	-	n-hexane	34
	500	-	n-heptane	41
	500	1040	benzene	1
Toluene	497	-	n-hexane	34
	496	-	n-heptane	41
	497	1020	toluene	1
o-Xylene	495	-	n-hexane	34
	497	1060	o-xylene	1
p-Xylene	495	-	n-heptane	41
	495	1080	p-xylene	1
Mesitylene	490	-	n-hexane	34
	490	1190	mesitylene	1
Diethyl ether	462	950	n-heptane	37
	462	880	diethyl ether	1
Pyridine	422	1320	n-heptane	38

Table 3 lists the equilibrium constants and spectral properties of the charge-transfer band for various complexes of iodine. A comprehensive listing of properties for these and other complexes in various solvents is given by Briegleb.[3] Table 4 lists the wavelengths of maximum absorbance and corresponding extinction coefficients for the blue shifted iodine band and is essentially complete for the donors represented. The results in these tables were derived by use of the Benesi-Hildebrand or related techniques and, as such, are subject to the limitations previously discussed. Any inconsistencies are probably the results of the errors inherent in these techniques.

CHAPTER II

OBJECTIVES

The objective of this research was to develop and apply a new method to investigate the weak molecular complexes of iodine. The new method would utilize a constant iodine activity source to control the concentrations of the various complexing species and thereby avoid many of the problems inherent in the conventional spectral techniques for determining the properties of weak complexes. The results from the new method would be critically compared with those obtained by the more conventional techniques.

CHAPTER III

EXPERIMENTAL

Chemicals: Solvents and Donors

Heptane (Fisher, Spectral Quality) was predried over calcium sulfate and then stored over a drying agent (Linde 4A molecular sieve) in a three-foot glass column, or heptane (Fisher, Certified) was purified by standard techniques[42] and stored similarly. Pyridine (Baker, A.C.S.) was distilled from BaO and stored over KOH. All distillations were performed using a 30-plate Oldershaw column isolated from water vapor in the atmosphere. Diethyl ether (Malinckrodt, Anhydrous Reagent Grade) was distilled from calcium hydride and used immediately. Benzene (Eastman, Spectroquality), toluene (Matheson, Spectroquality), and m-xylene (Matheson, Spectroquality) did not discolor sulfuric acid; they were distilled from calcium sulfate, and the middle portion of the distillate was collected and stored over molecular sieves. P-xylene (Matheson, 99+mol %), o-xylene (Matheson, 99+mol %) and mesitylene (Matheson, Pract.) were scrubbed by successive washings with concentrated sulfuric acid until no dark coloration appeared in the acid layer. The organic layers were then washed with a sodium hydroxide solution and finally with distilled water. Excess water was removed with calcium chloride before distilling and storing as described above. Iodine

(Malinckrodt, "Resublimed" Reagent Grade) and tetramethylammonium iodide (Matheson, 99%) were stored in desiccator and used without further purification. Tetramethylammonium pentaiodide ($TMAI_5$) was prepared using the method of Chattaway and Hoyle.[43] The melting point (129°) and available iodine (71.6%), determined by thiosulfate titration, were in good agreement with the literature values.[42]

Instrumentation

A single-beam Beckman Model DU-2 spectrometer equipped with a temperature-regulated cell holder was used in the spectral measurements. Absorbances could be determined very accurately (±0.002) using this instrument; however, the procedure of obtaining spectral curves point-by-point was somewhat laborious. The temperature of the cell holder was controlled (±0.2°) by circulating water from an auxiliary thermostatted circulator (Haake). A separate refrigeration unit provided cooling for the Haake circulator when needed for experimental temperatures below ambient. The temperature of the cell solutions was calibrated by use of a small thermistor which could be suspended in the solution under operating conditions. The temperature was monitored using a Yellow Springs Instrument Company Model 425C Tele-Thermometer.

Spectral measurements were made in one of three pairs of matched cells (Beckman) with pathlengths of 0.1, 1.0 and 2.0 cm.; choice of the cell pathlength was dictated by the magnitude of the absorbance being measured. The 2.0 cm. cells were equipped with glass stoppers and standard silica windows and were used only in the visible region of the spectrum. The 0.1 and 1.0 cm. cells had far-ultraviolet windows and were used in both the ultraviolet and visible regions.

The constant temperature baths used in this study for equilibrations have been described elsewhere.[44]

Tetramethylammonium Polyiodides

Figure 3 shows the solid-vapor phase diagram for the tetramethylammonium iodide (TMAI)-iodine system at 25°C. The iodine activity, a_{I_2} is plotted against the ratio of the number of moles of I to the number of moles of tetramethylammonium cation (nI/n TMA). This diagram is the result of some excellent work performed in this laboratory by Stephen R. Roach. The iodine activities were determined by using a solubility method similar to that employed by Foote and Fleischer.[45] A weighed amount of pure TMAI was shaken for several days with a measured volume of a heptane solution of known iodine molarity; spectral determination of the iodine remaining in solution at equilibrium permitted calculation of the mole ratio of iodine to TMAI in the solid phase at a given solution concentration. The iodine activities in solution are based on a standard state of pure solid iodine. To a first approximation, a_{I_2} equals the ratio of the iodine concentration in solution to the limiting solubility of pure iodine in the hydrocarbon solvent at 25°C. Small activity coefficient corrections were made by employing solubility parameter theory.[19]

Solid $TMAI_5$, prepared by the method described by Chattaway and Hoyle,[43] is a convenient starting material for bringing systems to known iodine activities. In solution studies involving hydrocarbon solvents, the $TMAI_3/TMAI_5$ plateau is ideal for use in spectral experiments. The solid mixture $TMAI_3/TMAI_5$, equilibrated with the solvent heptane at 25°C, maintains an uncomplexed iodine concentration of 1.97×10^{-4} M. This is

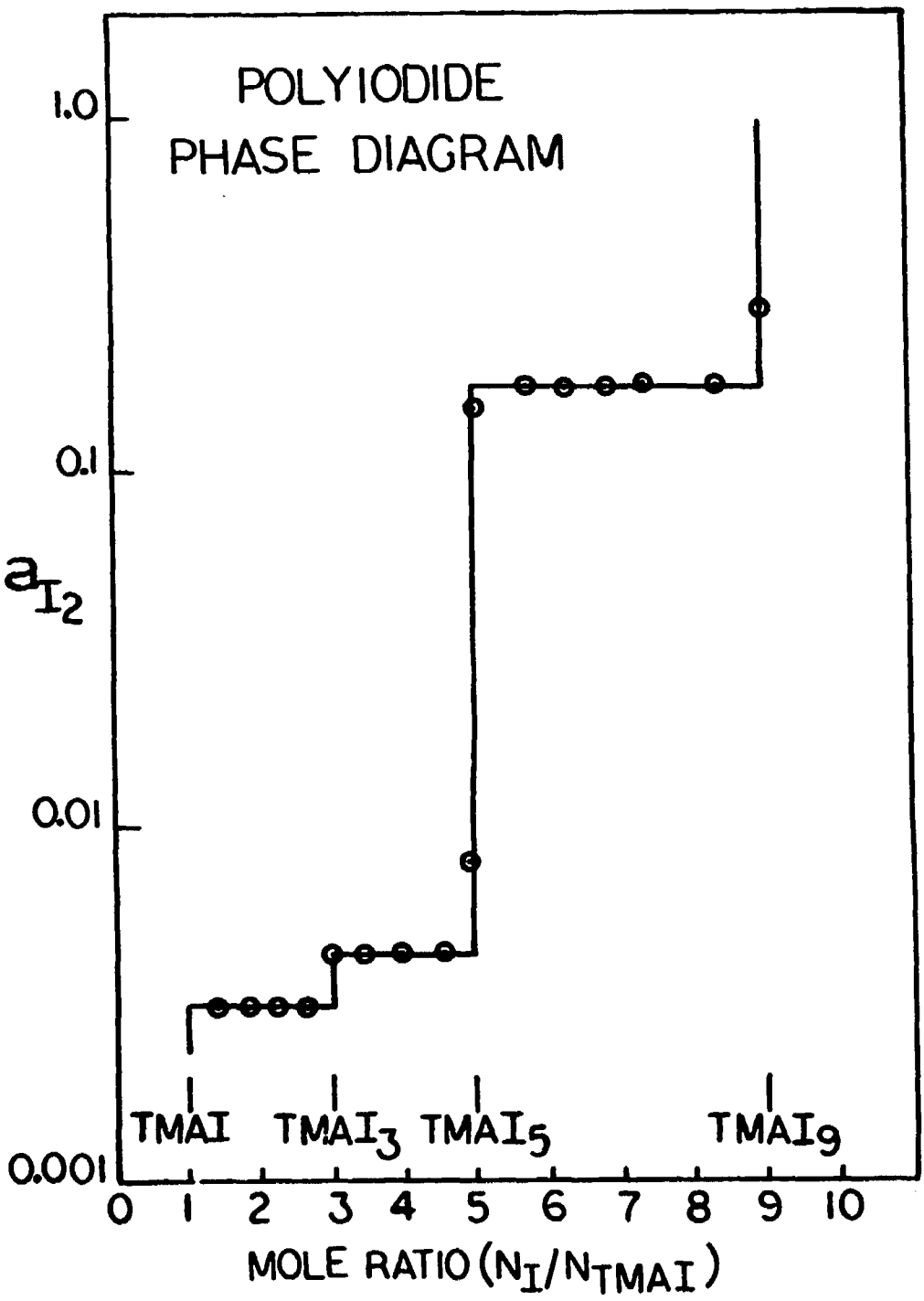

Figure 3. Solid-vapor Phase Diagram for the Tetramethylammonium Iodide-Iodine System at 25°C. The iodine activity a_{I_2} is plotted against the ratio of the number of moles of I to the number of moles of the tetramethylammonium cation in the solid mixtures.

an excellent starting concentration for studies of donor-iodine interactions using spectral techniques.

Technique

The experimental method for obtaining K_c and ϵ_{DA} is based on establishing the equilibrium

$$TMAI_5 \text{ (solid)} \rightleftarrows TMAI_3 \text{ (solid)} + I_2 \text{ (heptane)}$$

and observing changes in the iodine concentration and spectra which occur on addition of a donor to the heptane solutions. Equilibration of solid $TMAI_5$ with pure heptane or a heptane solution containing dissolved donor induces the dissolution of some iodine, producing an equivalent number of moles of solid $TMAI_3$. The resulting solid mixture of $TMAI_3$ and $TMAI_5$ is the constant activity source for iodine.

Mixtures of solvent/$TMAI_5$ and (donor + solvent)/$TMAI_5$ were prepared by placing approximately 0.5 grams of $TMAI_5$ in 150 cc screw cap bottles in contact with pure heptane or solutions of donor in heptane. Within the obvious plateau limits implied in the phase diagram, the spectra of the equilibrated solutions were independent of the amount of solid used. All donor/solvent solutions were prepared by the addition of either pure donor or stock solutions of the donor to volumetric flasks followed by dilution to the mark with heptane. Whenever possible such additions were accomplished by use of a calibrated micro-buret (Roger Gilmont Industries) but for very high concentrations of donor ordinary volumetric pipettes were used. The solutions were made at 25°C (except the ether solutions, which were made at 0.5°C) and the resultant concentrations calculated using the density data from Timmermans.[46] The

donor/heptane solutions were added to the bottles containing the $TMAI_5$ and the openings were quickly covered with sheets of polyethylene, which formed an air-tight seal when the cap was tightened. The bottles were then placed in a constant temperature bath (15 or 25° ± 0.05°C) and occasionally shaken to speed equilibration. The equilibration times were short, as is indicated by the rate data in Figure 4. The heptane blank and heptane plus donor solutions reach equilibrium in about 24 hours although all solutions were equilibrated for at least 48 hours to insure attainment of equilibrium. After equilibration, the polyethylene seals were punctured with the tip of a disposable pipette and the solutions removed and transferred directly to spectral cells for measurement. The spectra of the solutions were determined with pure heptane in the reference cell except when pyridine was the donor. In this case the high extinction coefficient (723 $\ell mole^{-1}cm^{-1}$ at 235 mμ) of pyridine in the vicinity of the charge-transfer band resulted in large donor absorption which was blanked by use of equal formal concentrations of pyridine in both sample and reference cells. This procedure was necessary only in the ultraviolet region since pyridine is transparent in the visible region. After sampling, the bottles were recapped and the samples preserved for subsequent measurement at the same or a different temperature. The spectral measurements were usually made at the same temperature as that employed during equilibration.

Measurements in the visible region were usually made using the 2.0 cm. cells. In the ultraviolet region the 1.0 and/or 0.1 cm. cells were employed. This procedure was necessary due to the higher intensities encountered in the latter region. As far as possible, the cell lengths

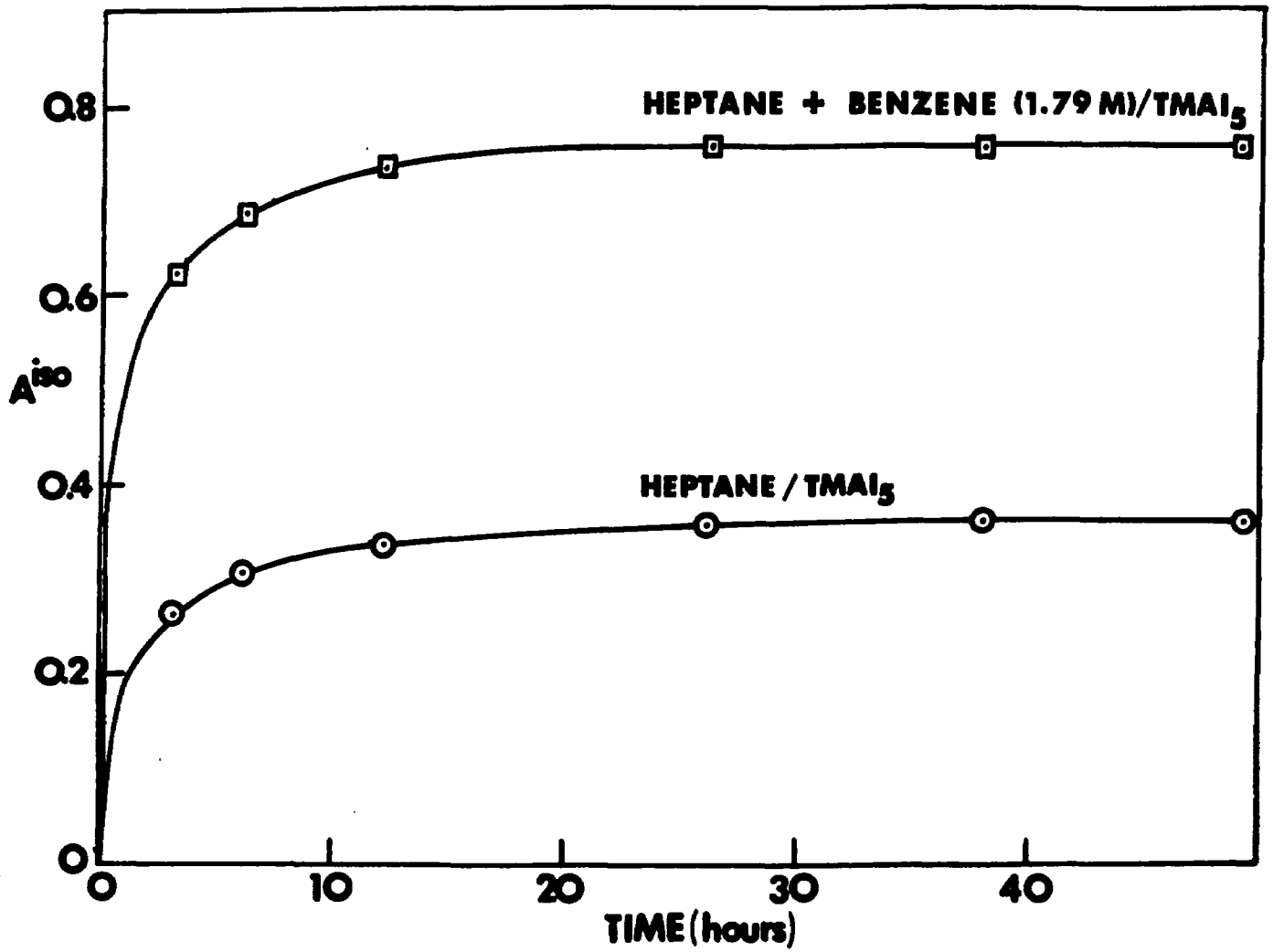

Figure 4. Absorbance at λ^{iso} of Solutions Equilibrated with $TMAI_5$ Plotted Against Time. The absorbance is proportional to the formal concentration of iodine in both the heptane blank and (heptane + donor) solution at this wavelength (cell pathlength, 2.0 cm.; temperature, 25°C).

were varied in such a way that the measured absorbances were never greater than 1.0. The resultant data were then normalized to one of the cells for comparison purposes.

Determination of Isosbestic Points

In order to obtain spectral data from which equilibrium constants and extinction coefficients could be calculated, it was necessary to determine accurate values for the wavelengths of isosbestic points (λ^{iso}) for the various systems. The following procedure was used to determine these wavelengths. Equal aliquots of a standard iodine solution and varying amounts of donor were added to heptane and diluted to a constant final volume with heptane. The subsequent spectral measurements made in the vicinity of the isosbestic point (2 mμ increments) yielded absorbance data at constant total concentration of iodine, from which the isosbestic points were determined to within ± 2 mμ (± 1 mμ in the pyridine and diethyl ether systems). The values of λ^{iso} obtained for the various systems were: benzene, 520 mμ; toluene, 518 mμ; o-xylene, 519 mμ; p-xylene, 518 mμ; m-xylene, 518 mμ; pyridine, 477 mμ; diethyl ether, 494 mμ; in good agreement with literature results.[1,37,38] The isosbestic points were stable for the systems involving the aromatic hydrocarbon donors even in solutions which were essentially pure donor. For the pyridine and diethyl ether systems, λ^{iso} was constant over the concentration range employed although not over the entire concentration range. It should be mentioned that a slight error in the determination of the isosbestic wavelength for the hydrocarbon donor systems will not lead to sizeable errors in determination of the iodine concentration in as much as the isosbestic wavelengths for these systems fall in the

relatively flat region of the iodine spectral curve, i.e., near 520 mμ. Errors in the isosbestic wavelength are somewhat more important in the ether and pyridine systems since the extinction coefficient varies more rapidly with wavelength in the vicinity of these isosbestic points.

Applications

In the polyiodide solubility method, the absorbance at the wavelength of the isosbestic point is directly proportional to the total concentration of iodine (free plus uncomplexed) and the increase in absorbance at this wavelength due to the presence of the donor is attributed to the formation of the complex. Since the extinction coefficient of the complex and of the uncomplexed iodine are equal at this wavelength, the concentration of the complex and K can be calculated directly. Figure 5 illustrates the processes occurring in the equilibrated solutions and the procedure used to obtain K from measurements on such solutions. The solid mixture ($TMAI_3$ + $TMAI_5$) maintains an uncomplexed iodine concentration of 1.97×10^{-4} M in both the heptane blank (solution I) and in the heptane plus donor solution (solution II). The presence of the donor (pyridine) in solution II induces the dissolution of additional iodine due to the formation of a complex. The concentration of the species were calculated from the absorbances at the isosbestic wavelength, using Beer's law and the known extinction coefficient of iodine at this point. The equilibrium constant was calculated to be 163 ℓ/mole at 25°. Figure 5 shows typical spectra obtained using the solubility method. The lower curve corresponds to heptane which has been equilibrated with the polyiodide mixture ($TMAI_3$ + $TMAI_5$) and the higher curves correspond to similar equilibrations but with increasing diethyl ether concentrations in the

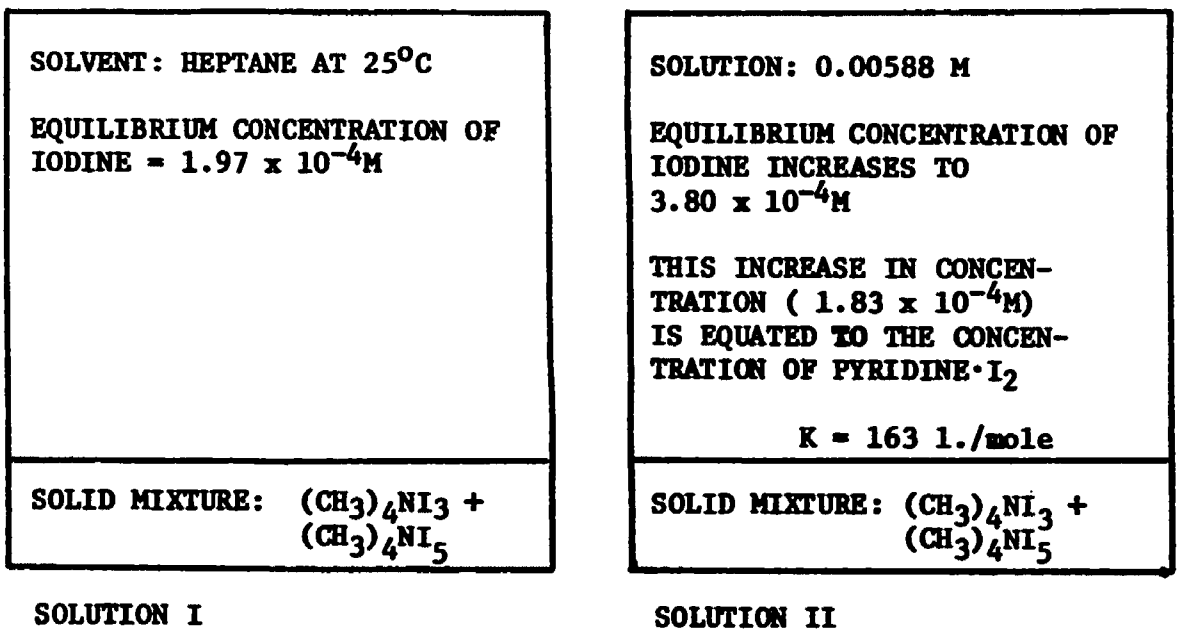

Figure 5. The Concentrations of the Uncomplexed and Complexed Iodine in the Polyiodide Solubility Method Solutions. Solution I is the heptane blank and Solution II is a (donor + heptane) mixture.

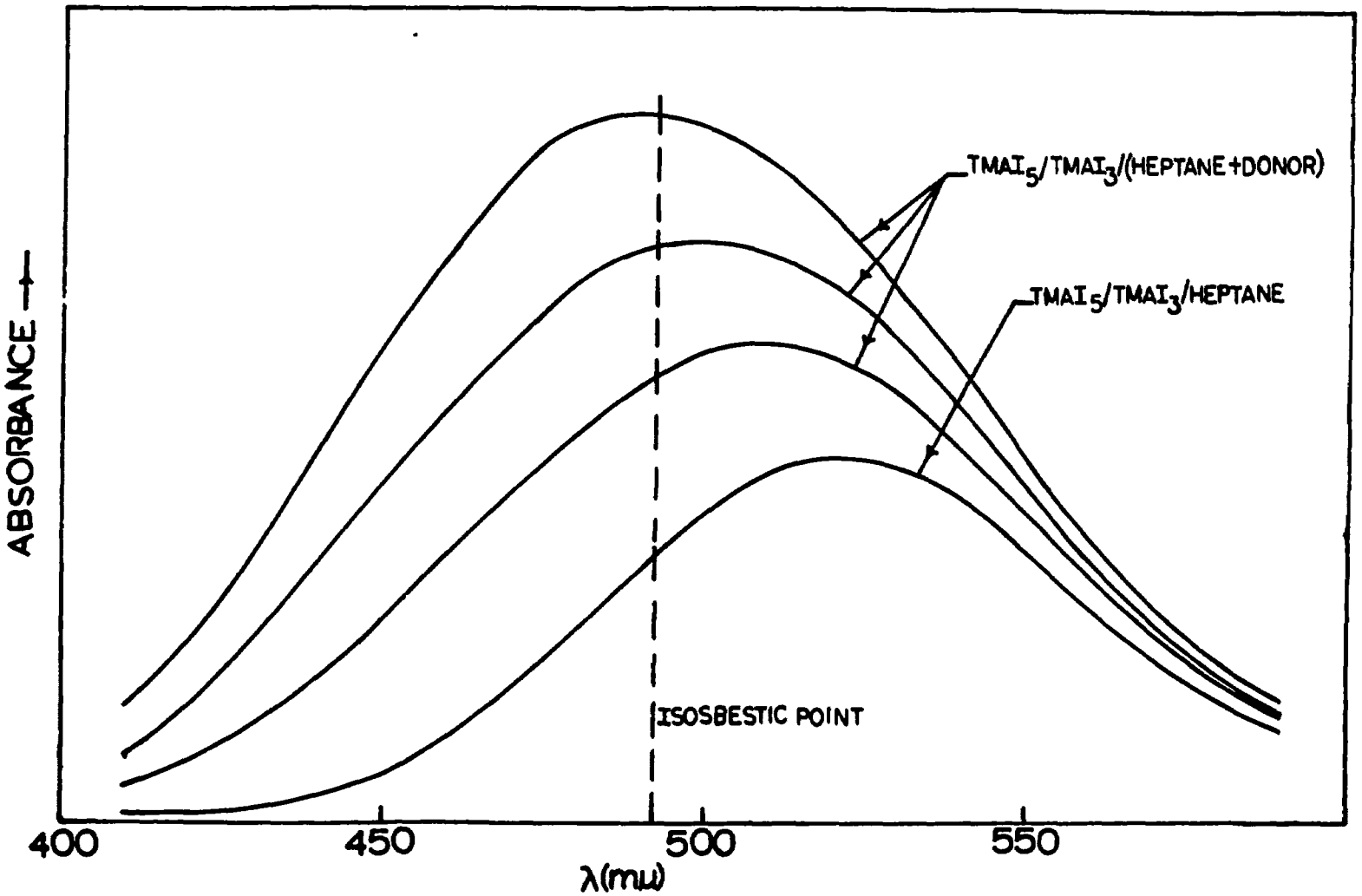

Figure 6. Typical Spectra Obtained with the Polyiodide Solubility Method. The lower curve corresponds to the heptane blank and the upper curves to increasing concentrations of diethyl ether in the heptane.

heptane at 15°C. The enhanced absorbance of these curves is attributed to an increase in the solubility of iodine due to the formation of a complex. The broken line represents the wavelength of the isosbestic point, where the difference in absorbance between a particular heptane plus donor solution and the heptane blank is proportional to the concentration of complex formed.

Variation of Properties with Temperature

It is worth noting that in studies of the variation of properties of a complex with temperature using the solubility method it is possible to equilibrate at any desired constant temperature, withdraw samples of the solution above the polyiodide mixture from the equilibrator vessels and determine the total iodine concentration of these solutions in a spectrometer thermostatted at another temperature. This procedure is possible since once a liquid sample is removed from the constant iodine activity source ($TMAI_5$) the total amount of iodine in the solution is fixed at least as long as the saturation concentration of iodine is not exceeded at the measurement temperature.

Thus, equilibrations can be performed at temperatures far removed from the ambient and samples analyzed at temperatures more convenient for spectral work. Simple corrections for volume changes with temperature allow calculation of the total iodine concentration at the equilibration temperature. This procedure is not possible in the conventional Benesi-Hildebrand techniques where the total iodine concentration is the same in all solutions and the spectral measurements are dependent on the concentration of the complex, which varies with the temperature. Similar problems are encountered in the polyiodide solubility method in the measurements

at the charge transfer band where the absorbance is a function of complex concentration which varies with temperature. As a result the equilibration and spectrometer temperatures must be the same when the charge-transfer band is under investigation.

This advantage of the solubility method was not fully exploited in the present research since temperature variations of the properties of the various complexes were not considered. Only in the case of the pyridine complex was such a study undertaken and then only to the extent of showing the feasibility of the method.

Limitation of the Polyiodide Solubility Method

A possible limitation of the applicability of the polyiodide solubility method is encountered when dissolution of quantities of the solid polyiodide in the form of ionic species occurs. This can be a problem when the solvent or donor have high dielectric constants. For example, the $TMAI_3$ compound is very slightly soluble as TMA^+ and I_3^- in the solvent dichloroethane[47] but not in the solvents such as heptane and toluene.[45] Since the triiodide ion has extinction coefficients of approximately 25,000 at 390 mμ and 45,800 at 292 mμ, dissolution of appreciable quantities of such species is easily detected.[47] There was some evidence of slight salt solubility at very high benzene concentrations (4 M). In fact, Foote and Fleischer[45] report that benzene does react with the solid $TMAI_5$ to form compounds of unknown stoichiometry, although careful analysis of the solid phase for toluene showed no indications of similar behavior. When pure benzene was added to a bottle containing $TMAI_5$, a very dark colored solution resulted which was not characteristic of solutions obtained by dissolving pure iodine in benzene.

Also, the solid phase ($TMAI_5$) apparently reacted with the benzene to form a black polymer-like substance which was presumably the compound reported by Foote and Fleischer.[45] Also, spectra of the benzene samples with benzene concentrations in excess of about 4M had broad shoulders on the low frequency side (~390 mμ) of the charge transfer band, which indicated the possible presence of traces of I_3^- and probably accounted for the odd coloration of these solutions. To check possible adsorption of the benzene by the solid phase, several solutions with varying amounts of $TMAI_5$ and the same concentration of benzene (1.79 M) were equilibrated and their absorbance at the isosbestic point determined. These solutions all had the same absorbance which indicated benzene adsorption was negligible at least for the less concentrated solutions. Moreover, the most likely soluble species involves I_3^-, and the low absorbances of the dilute solutions at around 390 mμ indicated that only very tiny amounts of I_3^- could be present in these solutions. Since the analysis of the data was restricted to the dilute solution region, it is not felt that the results for this complex were affected by the solubilization of polyiodide species. Problems with I_3^- appeared to be unique to the benzene system since similar behavior was not observed for the other donors.

Conventional Spectral Studies

Comparison of spectral and thermodynamic properties of a particular system derived from data obtained using both the polyiodide solubility method and the conventional spectral techniques was one of the major goals of the present research. Although most of the systems have been studied by conventional techniques, the reported spectral and

thermodynamic results for a given complex frequently vary from one laboratory to the next. This is presumably due to differences in the methods of data collection and treatment.[5] Thus, for reasonable comparisons it was necessary to perform conventional experiments of the Benesi-Hildebrand type on all the systems except pyridine. Such experiments involved measurements on solutions prepared exactly as those used in obtaining the isosbestic points. The measurements on these solutions were simply extended over the visible and ultraviolet spectral regions and the resultant data used to derive the desired spectral and thermodynamic properties.

CHAPTER IV

DATA TREATMENT

Benesi-Hildebrand Type Spectral Data

The numerical calculation of equilibrium constants for reactions of the type

$$\text{Donor (D)} + I_2\text{(A)} \rightleftarrows \text{Complex (DA)}$$

was based on the techniques of Sillén[48] for nonlinear least-squares analysis. Christian and Grundnes[10,49] adapted this technique to the analysis of spectral data to yield extinction coefficients and equilibrium constants for the 1:1 complex situation. The basic assumptions of their method are: (1) only the 1:1 complex exists in the solution (2) Beer's law and the other laws of dilute solution are valid over the concentration range studied. Under these assumptions, the following equations can be written

$$C_D^{\,o} = C_D + K_c C_A C_D \tag{1}$$

$$C_A^{\,o} = C_A + K_c C_A C_D \tag{2}$$

$$\frac{A}{1}^{\text{total}} - \varepsilon_A c_A - \varepsilon_D c_D = \frac{\Delta A}{\ell} = \varepsilon_{DA} K_c C_A C_D \tag{3}$$

where c_A and c_D represent concentrations of the species A and D (uncomplexed donor and acceptor), ε_A and ε_D are the known extinction coefficients of the species A and D, 1 is the pathlength of the cell, and

A^{total} is the measured absorbance. In the present application, ΔA is defined in a slightly different manner, i.e., it is the measured absorbance less the initial donor absorbance (A_D^o) and the initial acceptor absorbance (A_A^o). A_A^o is simply a measured constant for a particular set of solutions since all have the same initial iodine concentration and A_D^o is calculated by use of the known extinction coefficient and concentration of the donor. Data in Appendix II for the various complexes include the values of the absorbance, ΔA; initial concentrations of donor and acceptor, C_D^o and C_A^o ($C_D^o \approx C_D$ for the weak complexes); extinction coefficients of uncomplexed D and A, ε_D and ε_A; and the calculated values of the absorbance, ΔA(calc.) which were obtained by nonlinear least squares. Standard states of 1 ℓ/mole are used for all components. From absorbance versus concentration data, the method of Christian and Grundnes can be employed to derive equilibrium constants and extinction coefficients if allowance is made for the redefinition of ΔA. According to the present definition ΔA is given by

$$\Delta A = A^{total} - A_D^o - A_A^o \tag{4}$$

or

$$\Delta A = (A_{DA} + A_D^{free} + A_A^{free}) - A_D^o - A_A^o \ . \tag{5}$$

For weak complexes where $A_D^{free} \approx A_D^o$, equation (5) becomes

$$\frac{\Delta A}{\ell} = \varepsilon_{DA} K_c C_A C_D + \varepsilon_A C_A - \varepsilon_A C_A^o \tag{6}$$

upon inclusion of Beer's law and the relation for the concentration of the complex in terms of the equilibrium constant ($c_{DA} = c_A c_D K_c$). This equation can be further simplified to yield

$$\frac{\Delta A}{\ell} = (\varepsilon_{DA} - \varepsilon_A) K_c C_A C_D \tag{7}$$

which differs from equation (3) only by the inclusion of ε_A. From

equations (1), (2), and (7), two unknown constants, K_c and $(\epsilon_{DA} - \epsilon_A)$, are to be inferred from several sets of simultaneously measured values of ΔA, c_A^o and c_D^o. Equations (1) and (2) may be solved simultaneously (using an assumed value of K) to yield trial values of c_A and c_D corresponding to each pair of c_D^o, c_A^o values. Using these values of c_A and c_D, ΔA of equation (7) may be calculated for each set of measurements and by ordinary least squares analysis the best value of $(\epsilon_{DA} - \epsilon_A)$ may be calculated corresponding to the assumed value of K_c. The quantity

$$\Delta = \sum_{i=1}^{n} [\Delta A_i - (\epsilon_{DA} - \epsilon_A) K_c C_{Ai} C_{Di}]^2 \qquad (8)$$

is also computed for the entire collection of measurements, for a chosen value of K_c. By using an appropriate optimum seeking method,[50] Δ is minimized with respect to both K and $(\epsilon_{DA} - \epsilon_A)$, to yield the least-squares values of the parameters and the standard errors in them. As discussed previously, a sizeable percentage of the initial iodine should be complexed in the most concentrated donor solution in order to achieve good separation of K and ϵ by this method.[11] In the systems studied here this criterion was always considered; in the experimental determinations, the highest donor concentration was chosen such that approximately 50% of the iodine would be in the complexed form.

In this method, the position of the maximum of an observed spectral curve does not necessarily correspond to the maximum of the curve for the complex if either of the components absorbs in the region of the maximum for the complex. In order to obtain the position of the maximum in the complex spectrum, it is necessary to correct for the absorbance of uncomplexed donor and acceptor. The following procedure was used to

effect such corrections. If both the acceptor and donor absorb, the absorbance due only to the complex (A_{DA}) is given by

$$A_{DA} = A^{total} - A_D^{free} - A_A^{free} \tag{9}$$

For the weak complexes $c_D^o >> c_{DA}$ so that $c_D^o \simeq c_D$ which implies $A_D^o \simeq A_D^{free}$. Thus, the correction for uncomplexed donor is obtained directly from a blank containing only solvent and donor at the appropriate concentration. In practice, only the absorbance of a few donor/heptane blanks with a wide range of donor concentrations were measured. Since the solutions obey Beer's law (within experimental error), the extinction coefficient of the donor at a wavelength of interest could be obtained and then used to calculate the correction for donor absorbance at any concentration. The correction for uncomplexed iodine was obtained using the relation

$$A_A^{free} = \frac{A_A^o}{1 + Kc_D^o} . \tag{10}$$

This relation was derived from the previous expressions under the condition $c_D^o >> c_D$. The absorbance of the complex is then given by

$$A_{DA} = A^{total} - A_D^o - A_A^{free} . \tag{11}$$

For the complexes involving aromatic hydrocarbon donors, the correction for uncomplexed iodine is relatively small in the immediate vicinity of the charge-transfer band and the observed absorbance at various wavelengths, corrected only for uncomplexed donor absorbance, gave a good approximation to the maximum wavelength. The equilibrium constant was calculated at this wavelength, equation (10) was used to obtain the

free iodine correction at various wavelengths and the absorbance spectrum due to the complex alone was calculated. In the ultraviolet region, the new maximum position was never much different from that obtained by correcting for donor absorbance only. However, in the visible region, the corrections for uncomplexed iodine are relatively large and quite sensitive to the value of the equilibrium constant used in equation (10). Thus, the position of the maximum of the blue shifted band is also sensitive to the particular value determined for the equilibrium constant.[41,51] The conspicuous absence of literature values for the properties of the blue shifted band of the aromatic hydrocarbon complexes is probably a reflection of this difficulty. For the complexes studied here, A_D^o of equation (11) was zero in the visible region. Thus, determining the maximum wavelength and the corresponding intensity of the blue shifted band was accomplished by correcting only for the absorbance of free iodine and then plotting this corrected absorbance versus wavelength. The equilibrium constant for the 1:1 complex determined at the charge-transfer band was used in obtaining the correction for uncomplexed iodine. Figure 7 is a plot of the corrected absorbance versus wavelength for the p-xylene complex. The various curves correspond to various donor concentrations. The low initial iodine concentration and relatively small extinction coefficients in this region result in the small differences in absorbance plotted. Since the solutions were also used in the ultraviolet spectral region where the intensities of the charge-transfer band are very large, the low initial iodine concentration represents a compromise which allowed determinations in both spectral regions. The derived spectral properties

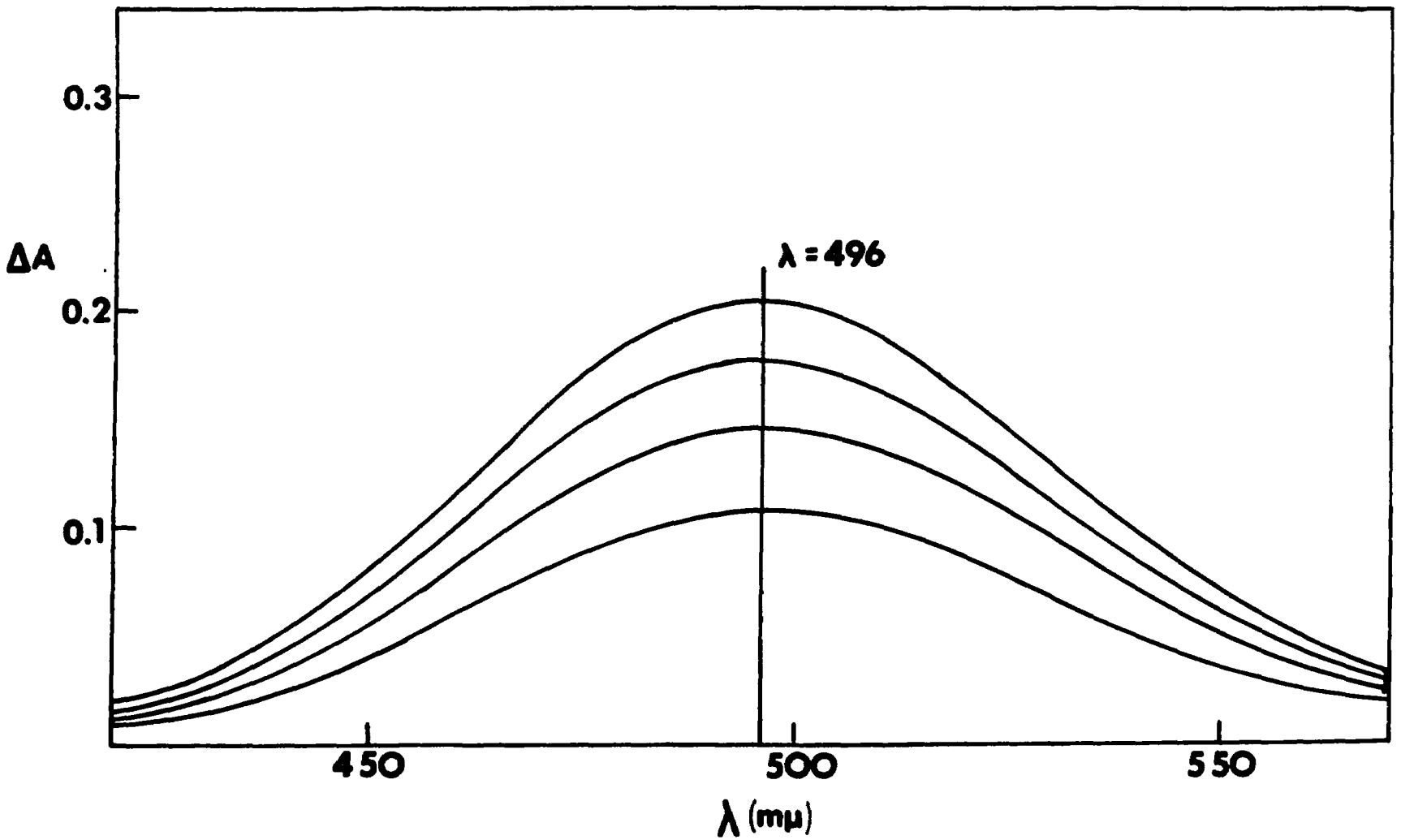

Figure 7. Blue Shifted Iodine Band for the p-Xylene·Iodine Complex as Determined with the Usual Spectral Technique. Various curves refer to increasing donor concentration in the range 0.646 to 1.614 M.

are determined from the plots of Figure 7. The wavelength of maximum absorbance was obtained by inspection to (±2mμ). The curves obtained in this manner are relatively broad due to the low initial iodine concentration and this results in a relatively high uncertainty in the value of the maximum of the peak, although not necessarily in the intensity. To calculate the intensity at the maximum it is necessary to know the concentration of the complex. The following procedure was used to calculate the concentration and intensity of the complex. First, the absorbance due to free iodine at 520 mμ was calculated using equation (10), then using Beer's law (the extinction coefficient of iodine at 520 mμ is 918 $\ell mole^{-1} cm^{-1}$)[5,52] the concentration of free iodine in a particular solution was calculated. This concentration was subtracted from the known initial iodine concentration to give the concentration of the complex. Then using the corrected absorbance at the blue shifted band maximum and Beer's law, the extinction coefficient of the complex was calculated. This procedure was followed for the four donor concentrations illustrated in Figure 7 and the reported extinction coefficient represents the average of four calculated values. Since only alternate solutions were scanned over the entire spectral range for each complex investigated, the reported extinction coefficients represent the average four or five determinations on each.

In addition to the peak maximum and intensity of the blue shifted iodine band, the oscillator strength f_{mn} for this electronic transition and the magnitude of the electronic transition dipole μ_{mn} were calculated. The oscillator strength is defined by

$$f = 4.318 \times 10^{-9} \int \epsilon_{\nu} d\nu$$

where ε_ν is the extinction coefficient at frequency ν and the integration is made over the entire absorption band that belongs to the particular transition.[5] To a first approximation, the integral is given by the product

$$f \simeq 4.32 \times 10^{-9} \varepsilon_{max} \Delta\nu_{1/2}$$

where ε_{max} is the extinction coefficient at λ_{max} and $\Delta\nu_{1/2}$ is the width in cm^{-1} of the band between the two frequencies at which $\varepsilon = (1/2)\varepsilon_{max}$. The transition dipole is given rigorously by

$$\mu_{mn} \text{ (debyes)} = 0.0958 \left(\frac{\int \varepsilon d\nu}{\bar{\nu}}\right)^{1/2}$$

where $\bar{\nu}$ is the average wave-number.[5] The approximate form of this equation is

$$\mu_{mn} \text{ (debyes)} \simeq 0.0958 \left(\frac{\varepsilon_{max} \Delta\nu_{1/2}}{\nu_{max}}\right)^{1/2}.$$

The approximate formulas were used in calculating f and μ for the transitions studied here. These quantities were not calculated for the charge-transfer band since the high frequency side of this band was usually obscured by very intense uncomplexed donor absorbance making the determination of $\Delta\nu_{1/2}$ difficult.[53] Use of donor in both the sample and reference beam would have made such determinations possible although this was not, in general, done here.

The various properties of the blue shifted band were determined using the techniques described above for all the complexes studied here except pyridine. For the pyridine complex, several good literature values[11] of the properties for this band existed and in view of the strength of this complex, the spectral parameters were considered accurate.

Solubility Method

The interpretation of results from the experiments based on the solubility method is reasonably simple, provided the assumption is made that each of the solute species individually obeys Henry's law in the limiting region of concentration and that non-specific donor-iodine interactions are either negligible or accounted for as part of the derived value for the equilibrium constant. The first assumption is also required in the Benesi-Hildebrand spectral methods, although it is commonly assumed the variations in the activity coefficients of the solute species will fortuitously cancel in the expressions for the derived equilibrium constants.[1,54] Concerning the second assumption, there have been attempts to divide the increased solubility of a solute in the presence of a donor into parts due to the specific donor-solute interactions and a part arising from the non-specific interactions.[15] There is no unambiguous way to separate these effects, although an attempt to accomplish such a separation using solubility parameter theory is given in Appendix I. The approach taken here is to report equilibrium constants which account for the entire enhancement of the solubility of the dissolved solute. This assumption considerably simplifies the interpretation of the solubility data and has commonly been employed in previous studies involving solubility techniques.[17,30]

At the wavelength of the isosbestic point (λ^{iso}) the absorbance of an equilibrated solution is directly proportional to the total concentration of iodine (free plus complexed) since the extinction coefficients of iodine and the complex are equal at this wavelength. The polyiodide ($TMAI_3 + TMAI_5$) constant activity source is assumed to maintain a constant uncomplexed iodine concentration ($C^{o}_{I_2}$) over the range of donor concentrations

employed. Thus, the difference between the absorbance of a donor/heptane solution and the heptane blank at the isosbestic point is proportional to the concentration of the complex which is formed. This difference may be expressed as

$$\Delta A^{iso} = \ell\, \varepsilon_A^{iso}\, C_{DA} \qquad (12)$$

where ε_A^{iso} is the extinction coefficient of iodine at λ^{iso}, ℓ is the cell pathlength, and C_{DA} is the concentration of the complex. Since ε_A^{iso} is known from either the literature or previous experiments, the concentration of the complex can be calculated directly. The concentration of the complex is also given as

$$C_{DA} = K_c C_A^{o} C_D \qquad (13)$$

where K_c is the equilibrium constant for the formation of the 1:1 complex. Substitution of this expression into equation (12) yields

$$\Delta A^{iso} = (\ell \varepsilon_A^{iso}\, C_A^{o})\, K_c C_D \qquad (14)$$

where the expression in parentheses is simply the absorbance (A^o) of iodine in the heptane blank at the λ^{iso}. Thus, equation (14) can be written as

$$\Delta A^{iso} = (A^{o}\, K_c)\, C_D \qquad (15)$$

where C_D is the equilibrium concentration of the free donor given by $C_D = C_D^{o} - C_{DA}$, C_D^{o} being the initial donor concentration. For the weak complexes (aromatic hydrocarbons and diethyl ether), C_D^{o} is always considerably greater than the concentration of the complex, so that the free donor concentration is virtually equal to C_D^{o}. However, in the case

of the strong pyridine complex, C_D must be calculated by correcting the initial pyridine concentration for the concentration of pyridine (C_{DA}) in the complexed form. Clearly, equation (15) implies that the relationship between ΔA^{iso} and C_D should be linear with slope (A^oK_c) and intercept 0. Figure 8 is a plot of the data for the pyridine complex and shows this linear relationship. The equilibrium constant is determined from the slope of this line using the relation

$$K_c = \frac{(\text{slope})}{A^o} \quad ;$$

the slope is determined by linear least squares analysis of the data. It should be noted that including additional terms to represent the dependence of ΔA^{iso} on higher powers of C_D did not significantly improve upon the RMSD of the linear fit (see Appendix III).

The extinction coefficient of the complex ϵ_{DA}^{ct} at the charge-transfer band can also be inferred directly from spectral measurements on the equilibrated solutions. For a particular solution, measurements were made of the absorbance at λ^{iso} and at the wavelength of the maximum of the charge transfer band λ^{ct}. At the charge-transfer band, the observed absorbance, corrected for the absorbance of the free donor and acceptor, is proportional to the concentration of the complex present in the solution. The correction for free donor is obtained by the same procedure employed in the Benesi-Hildebrand techniques. However, the correction for free iodine in all solutions is simply the measured absorbance of the blank at the wavelength of interest. The corrected absorbance at the charge-transfer band is given by

$$\Delta A^{ct} = \ell\, \epsilon_{DA}^{ct}\, C_{DA} \qquad (16)$$

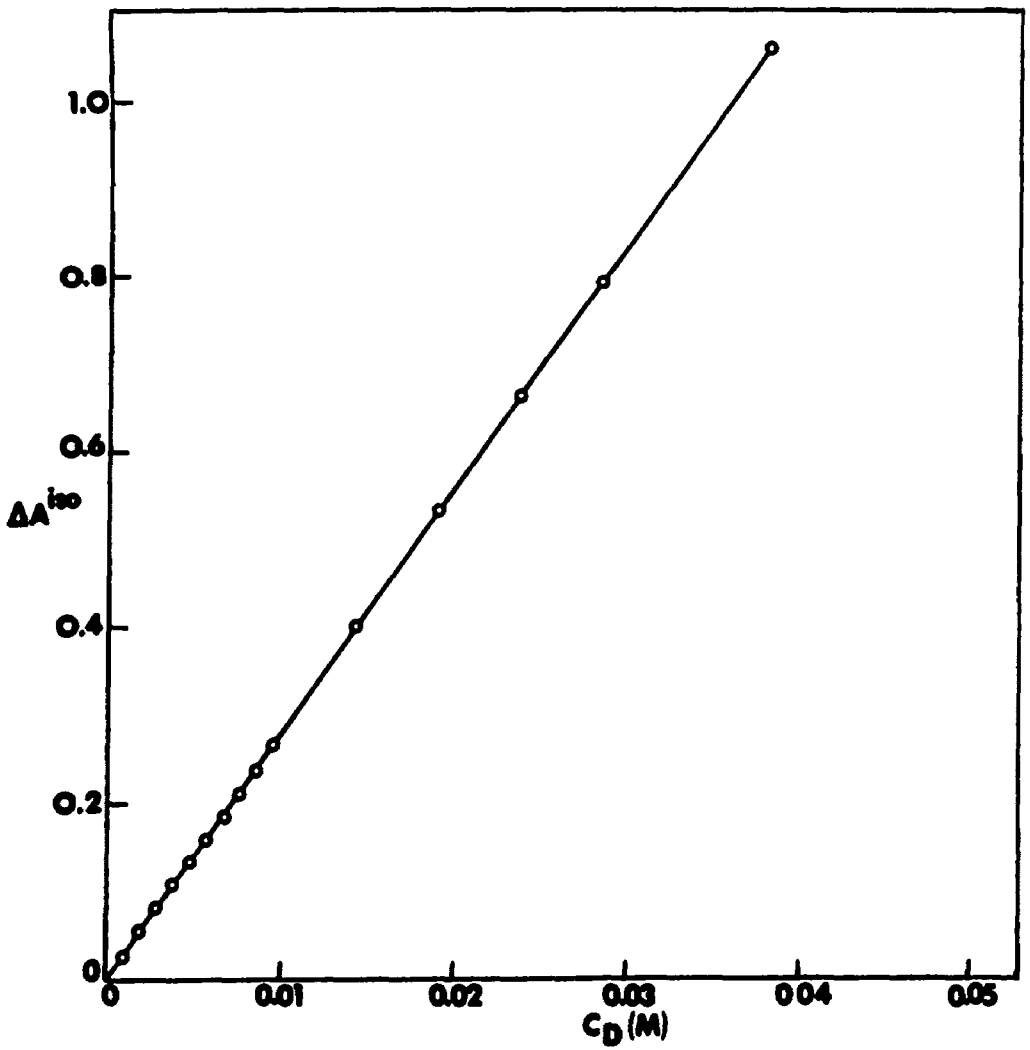

Figure 8. The Change in Absorbance at λ^{iso} Plotted as a Function of the Monomer Concentration of Pyridine (2.0 cm. Cell Pathlength).

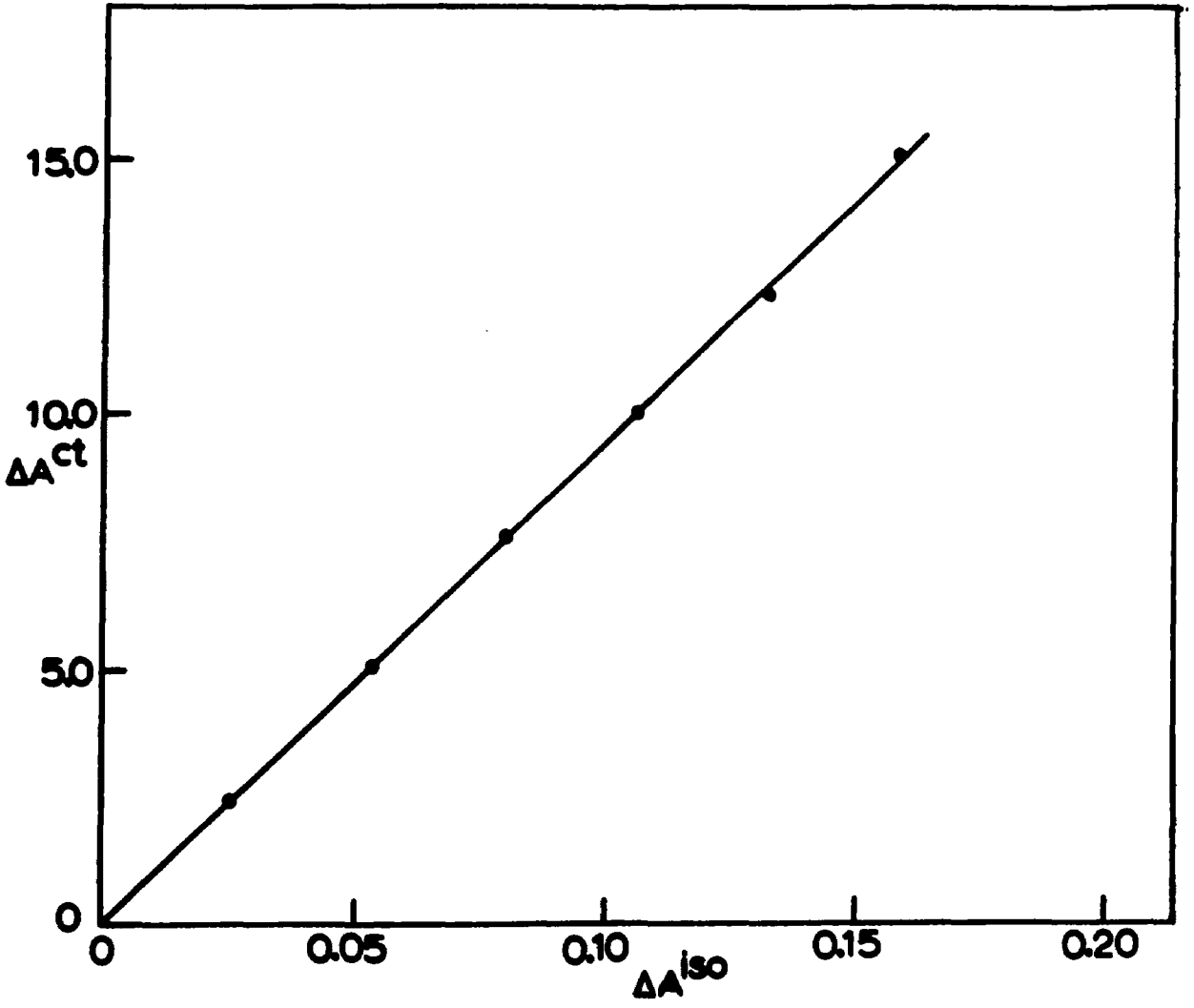

Figure 9. The Change in Absorbance at the Maximum of the Charge-Transfer Band Plotted as a Function of the Corresponding Change at λ^{iso} for the Pyridine·Iodine Complex (2.0 cm. Cell Pathlength).

and the ratio of the change in absorbance at the charge transfer band to the similar change at the isosbestic point is

$$\frac{\Delta A^{ct}}{\Delta A^{iso}} = \frac{\varepsilon_{DA}^{ct}}{\varepsilon_{A}^{iso}} \tag{17}$$

provided the data have been taken in common pathlength cells or normalized to the same. This equation implies that a plot of ΔA^{ct} against ΔA^{iso} should be linear with slope $\varepsilon_{DA}^{ct}/\varepsilon_{A}^{iso}$ and intercept 0. From the known extinction coefficient ε_{A}^{iso}, the extinction coefficient of the complex is calculated from

$$\varepsilon_{DA}^{ct} = (\text{slope})\ \varepsilon_{A}^{iso} \tag{18}$$

where the slope has been determined by least squares analysis of the data. Figure 9 is a plot of the data for the pyridine complex and is linear within experimental error. Fits involving higher order terms in ΔA^{iso} do not significantly improve upon the RMSD of the linear fit as demonstrated in Appendix III. Thus, in the solubility method K_c and ε_{DA}^{ct} are obtained directly in the separated form from measurements on dilute solutions at two wavelengths. This is the chief advantage of the solubility method over the Benesi-Hildebrand techniques.

The linear relationships observed for the pyridine complex were not observed for the weaker complexes. Figures 10 and 11 correspond to plots of ΔA^{iso} against C_D for the benzene and p-xylene complexes. These plots are characteristic of those obtained for weak complexes in that there is a slight but significant deviation from linearity at donor concentrations much in excess of 1M. This curvature may be attributed to either the formation of molecular complexes other

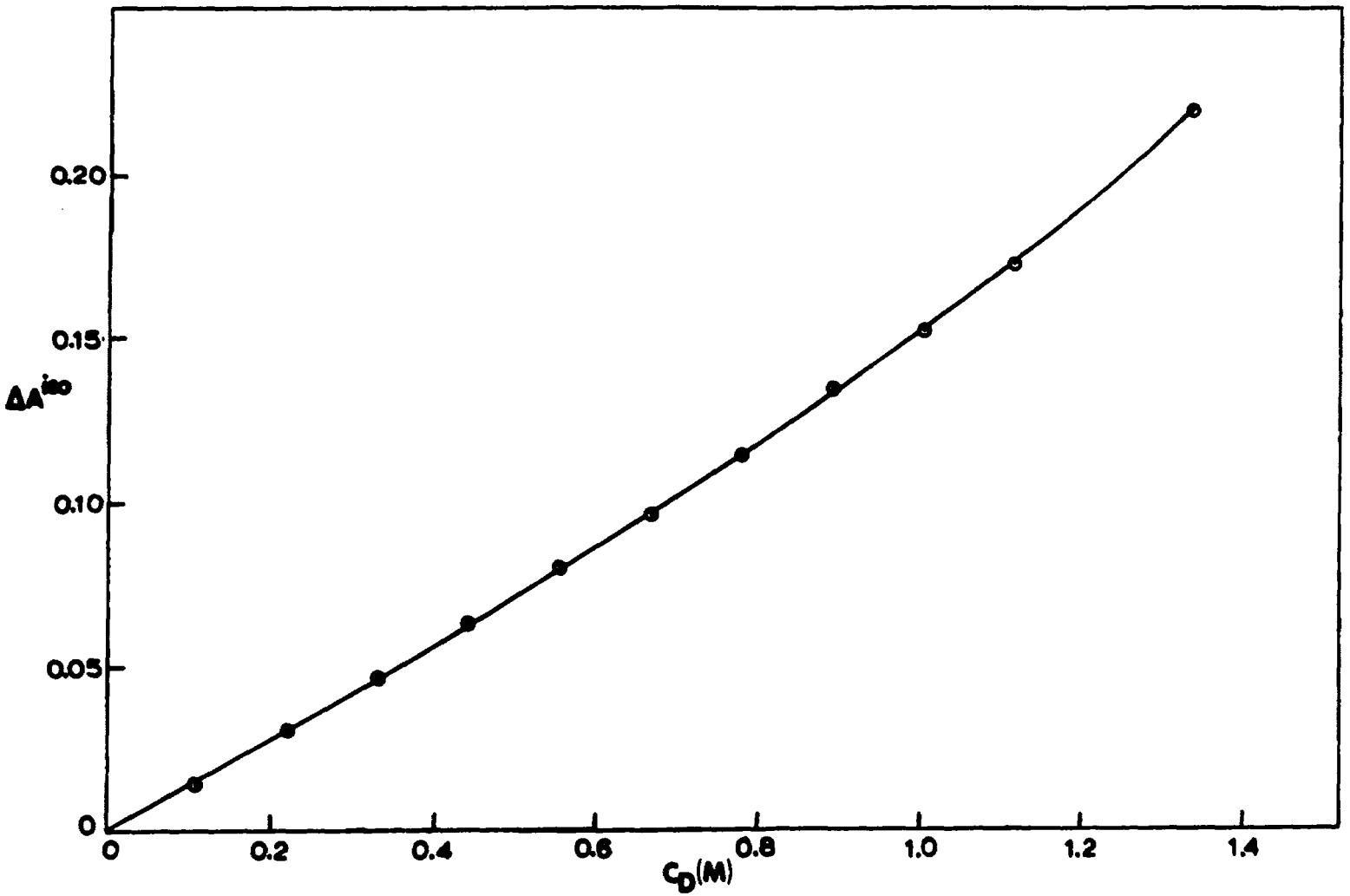

Figure 10. The Change in Absorbance at λ^{iso} Plotted as a Function of the Concentration of Benzene (2.0 cm. Cell Pathlength).

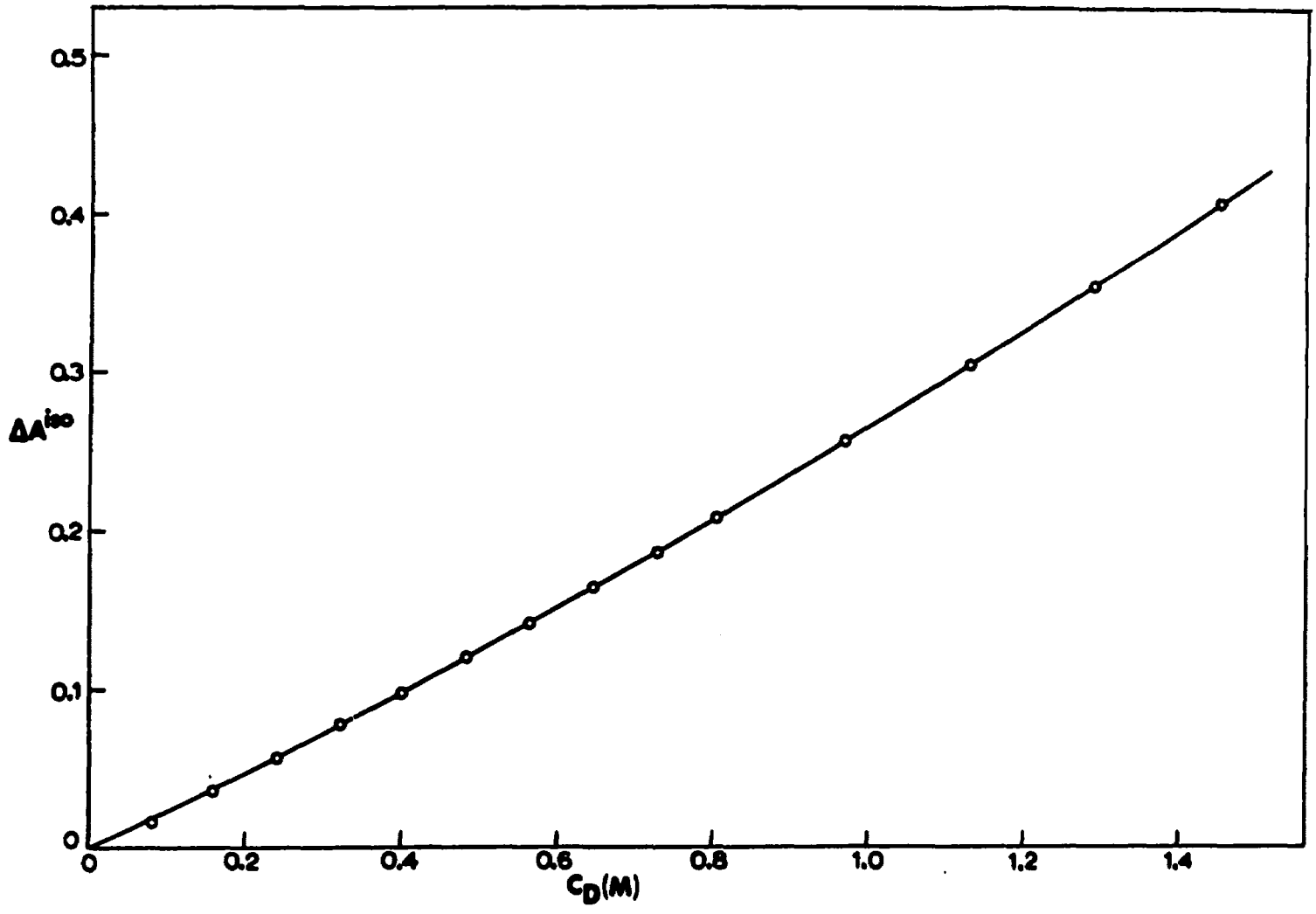

Figure 11. The Change in Absorbance at λ^{iso} Plotted as a Function of the Concentration of p-Xylene at (2.0 cm. Cell Pathlength).

than the 1:1 or to violation of the laws of dilute solution. In any event, for all the systems studied here it is possible to obtain a value of the limiting slopes of these curves and calculate K_c for the formation of the 1:1 complex. The procedure employed to obtain the limiting slope of these curves was to fit them by including with the linear concentration term of equation (15), a second-order correction term. The functional form of equation (15) thus becomes

$$\Delta A^{iso} = (A^o K_c)\ C_D + Q_1\ C_D^2\ . \qquad (19)$$

This equation is of the general form

$$Y = K_1\ X + K_2\ X^2 \qquad (20)$$

where Y and X are observables and K_1 and K_2 are unknown constants to be determined. Numerical linear least squares analysis of the data was used to determine the "best" unknown constants and their errors, by minimizing the RMSD in ΔA^{iso}. This program is described in detail elsewhere.[55] Inclusion of dependence on the concentration of the donor higher than second order did not significantly decrease the RMSD below the value obtained for fits involving only the linear and second order terms. This is demonstrated in Appendix III which includes the RMSD of various fits of ΔA^{iso} as a function of C_D. The data can be fit about equally well by including with the linear term a third order correction term. However, the limiting slope of such a fit is not significantly different from that involving the second order term. With this justification, the linear term of equation (19) can be used to calculate the 1:1 equilibrium constant since

$$\lim_{C_D \to 0} \frac{\alpha(\Delta A^{iso})}{\alpha C_D} = A^o K_c \ . \qquad (21)$$

Similar curvature at higher donor concentrations is observed in the ΔA^{ct} versus ΔA^{iso} plots. Typical examples of this behavior are shown in Figures 12 and 13 which display data for the donors benzene and p-xylene. These data were fit in the form

$$\Delta A^{ct} = \left(\frac{\varepsilon_{DA}^{ct}}{\varepsilon^{iso}}\right) \Delta A^{iso} + Q_2 \ (\Delta A^{iso})^2 \qquad (22)$$

using the same procedure described above. Exclusion of higher order terms of ΔA^{iso} was justified by examination of the RMSD values of various fits, as before, and the pertinent data in this region are also listed in Appendix III. The limiting slope of equation (22) is given by $(\varepsilon_{DA}^{ct}/\varepsilon_{A}^{iso})$ and this was used to calculate the 1:1 extinction coefficients, since ε_{A}^{iso} was known. Thus, the equilibrium constant and extinction coefficient for the 1:1 complex are obtained in the dilute solution region in the separated form. As the development in Appendix I demonstrates, the properties derived in this manner include all interactions between the donor and acceptor regardless of their origin.

It is possible to ignore the constants Q_1 and Q_2 of equations (19) and (22) without lessening the validity of the properties obtained from the limiting slopes of these curves. However, if all increases in the solubility of iodine are to be attributed to complex formation, Q_1 and Q_2 may be interpreted in terms of termolecular complexes much in the same manner used in other solubility techniques.[17] In the present interpretation, it is assumed that the most likely complex other than the 1:1 is a 2:1 complex involving two donor molecules and one acceptor. This assumption seems reasonable in view of the fact that the concentration

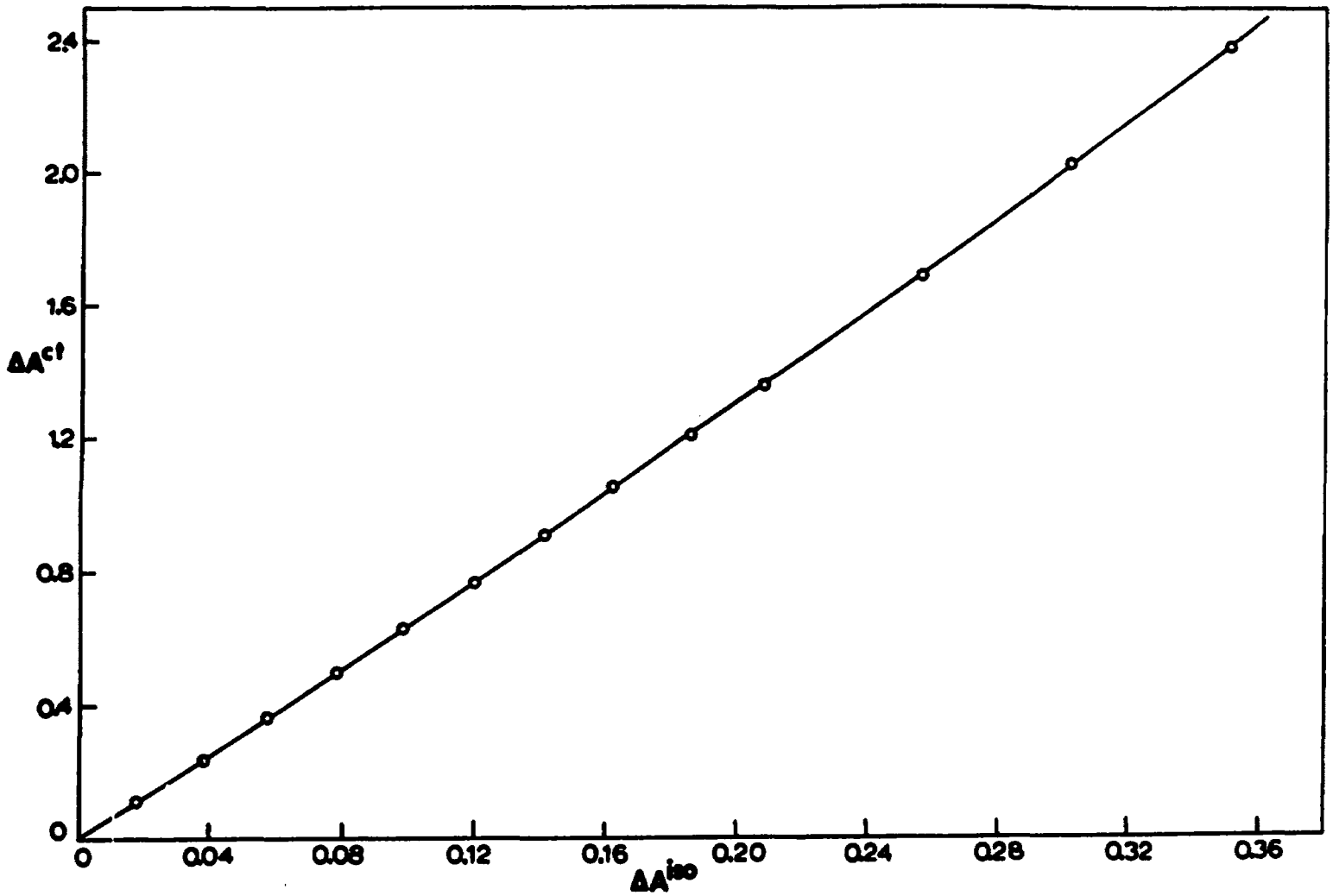

Figure 13. The Change in Absorbance at the Maximum of the Charge-Transfer Band Plotted Against the Corresponding Change at λ^{iso} for the p-Xylene·Iodine Complex (2.0 cm. Cell Pathlength).

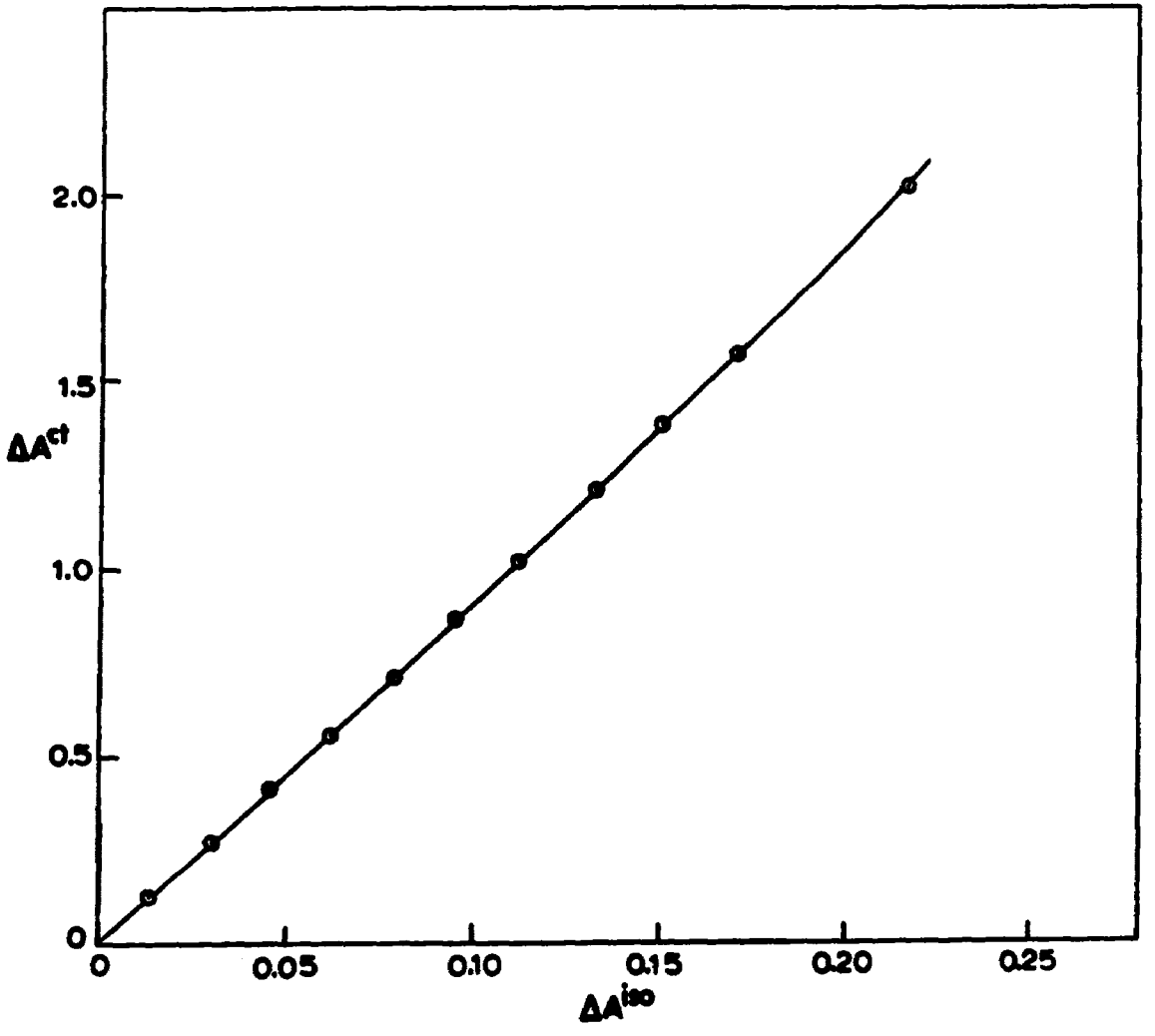

Figure 12. The Change in Absorbance at the Maximum of the Charge-Transfer Band Plotted Against the Corresponding Change at λ^{iso} for the Benzene·Iodine Complex (2.0 cm. Cell Pathlength).

of the donor is several orders of magnitude larger than that of the acceptor. Moreover, the crystal structure of the solid benzene-halogen complexes indicate that such an entity is possible.[87,88]

On this basis, the two equilibria involved are

$$D + A \rightleftarrows DA \quad ; \qquad K_{DA} = \frac{C_{DA}}{C_D C_A^{\,o}} \tag{23}$$

$$2D + A \rightleftarrows D_2A \quad ; \qquad K_{D_2A} = \frac{C_{D_2A}}{C_D^{\,2} C_A^{\,o}} \; . \tag{24}$$

The change in absorbance at λ^{iso} is now given by

$$\Delta A^{iso} = A_{DA} + A_{D_2A} \tag{25}$$

where A_{DA} is the absorbance due to the 1:1 complex and A_{D_2A} that is due to the 2:1 complex. Using Beer's law, equation (25) is expressed as

$$\Delta A^{iso} = \ell\, \varepsilon_{DA}^{iso}\, C_{DA} + \ell\, \varepsilon_{D_2A}^{iso}\, C_{D_2A} \tag{26}$$

where ε_{DA}^{iso} and $\varepsilon_{D_2A}^{iso}$ are the extinction coefficients of the 1:1 and 2:1 complexes at λ^{iso}. For the aromatic hydrocarbons, the isosbestic points were observed to be stable (i.e., independent of donor concentration) even in solutions which were essentially pure donor. This implies that the absorbance at λ^{iso} is still proportional to the total iodine concentration even at very large donor concentrations. This may be taken as indication that the extinction coefficients of the three species in the solution (iodine, 1:1 complex, 2:1 complex) are not much different at λ^{iso}. That is, evidently $\varepsilon_A^{iso} \simeq \varepsilon_{DA}^{iso} \simeq \varepsilon_{D_2A}^{iso}$ although this relation cannot be expected to be exact. On this basis little error should be involved in expressing equation (26) as

$$\Delta A^{iso} = \ell\, \varepsilon_A^{iso}\, C_{DA} + \ell\, \varepsilon_A^{iso}\, C_{D_2A} \quad . \tag{27}$$

where ε_A^{iso} has been substituted for the 1:1 and 2:1 extinction coefficients. The concentrations of the two complexes are given by

$$C_{DA} = K_{DA}\, C_A^{\,o}\, C_D \quad ; \quad C_{D_2A} = K_{D_2A}\, C_A^{\,o} C_D^{\,2} \quad . \tag{28}$$

and substituting these expressions with $C_A^{\,o}$ replaced by $\left(C_A^{\,o} = \frac{A^o}{\ell \varepsilon_A^{iso}}\right)$ into equation (27) yields

$$\Delta A^{iso} = (A^o K_{DA})\, C_D + (A^o K_{D_2A})\, C_D^{\,2} \quad . \tag{29}$$

Thus, the equilibrium constant of the 1:1 complex is obtained by dividing the linear C_D term of equation (29) by A^o and that of the 2:1 complex by dividing the second order term by A^o. Equation (29) gives the correct functional dependence on C_D as indicated by the "best" fits of the data. It should be noted that replacing the second order term by a corresponding third order term fits the data about equally well. However, of these two fits the one involving the second order term is chosen on the basis of the more reasonable physical model which results. Moreover, the model involving the 1:1 and 2:1 species receives some support from structural studies. In any event, the properties of the 1:1 complex are essentially unaltered from one fit to the other.

At the charge-transfer band, the change in absorbance can be written as

$$\Delta A^{ct} = \ell\, \varepsilon_{DA}^{ct}\, C_{DA} + \ell\, \varepsilon_{D_2A}^{ct}\, C_{D_2A} \tag{30}$$

where ε_{DA}^{ct} and $\varepsilon_{D_2A}^{ct}$ are the extinction coefficients of the 1:1 and 2:1

complexes at the maximum observed for the charge transfer-band. Substituting as above for the concentrations of the complexes yields

$$\Delta A^{ct} = \left(\frac{\varepsilon_{DA}^{ct} K_{DA} A^o}{\varepsilon_A^{iso}}\right) C_D + \left(\frac{\varepsilon_{D_2A}^{ct} K_{D_2A} A^o}{\varepsilon_A^{iso}}\right) C_D^2 \quad . \qquad (31)$$

Since the data at λ^{iso} and λ^{ct} were always normalized to a common cell pathlength, ℓ does not appear in this expression. From the coefficients of the least squares fit of ΔA^{ct} as a function of C_D, the extinction coefficients of the two species can be calculated since K_{DA} and K_{D_2A} are known from the measurements at the isosbestic point. However, this is not the functional dependence given by equation (22) where ΔA^{ct} was expressed as a function of ΔA^{iso}. To derive such dependence, equation (29) is solved for C_D in terms of ΔA^{iso} to yield

$$C_D = \left(\frac{1}{K_{DA} A^o}\right) \Delta A^{iso} - \left(\frac{K_{D_2A}}{K_{DA} (A^o)^2}\right) (\Delta A^{iso})^2 \qquad (32)$$

where the higher order terms in ΔA^{iso} have been truncated. Substituting this expression into equation (31) and again truncating the higher order terms in ΔA^{iso} results in the expression

$$\Delta A^{ct} = \left(\frac{\varepsilon_{DA}^{ct}}{\varepsilon_A^{iso}}\right) \Delta A^{iso} + \left(\varepsilon_{D_2A}^{ct} - \varepsilon_{DA}^{ct}\right) \left(\frac{K_{D_2A}}{\varepsilon_A^{iso} K_{DA}^2 A^o}\right) (\Delta A^{iso})^2 \qquad (33)$$

which has the expected limiting slope. Least squares analysis of the data in this form results in coefficients which can be used to obtain ε_{DA}^{ct} and $\varepsilon_{D_2A}^{ct}$. Equation (31) or (33) may be employed to derive the extinction coefficients of the two species, and in fact the results of the two methods of analysis agree to within experimental error. In view of this only the results from the ΔA^{ct}, ΔA^{iso} data will be reported.

In the solubility method, the blue shifted iodine band for a

particular complex is obtained directly, independent of the value determined for the equilibrium constant. To obtain this band it is only required that the heptane blank spectral curve be subtracted from the heptane/donor curves. This procedure corrects the heptane/donor curves for the absorbance of free iodine without reliance on a predetermined equilibrium constant. This procedure is considerably more convenient than that employed in the conventional techniques of the Benesi-Hildebrand type where the equilibrium constant must be known before the characteristics of the blue shifted band can be calculated.[51]

Figure 14 shows the blue shifted iodine band for the pyridine complex at several donor concentrations. Also, included is the spectrum of the heptane blank with its characteristic maximum at 520 mμ. The change in absorbance ΔA at a particular wavelength was obtained by subtracting from the observed absorbance of a donor/heptane solution the absorbance of the blank at that wavelength. No corrections for donor absorbance were necessary for the donors studied since they did not absorb in the visible spectrum. Also, the charge-transfer bands were well removed into the ultraviolet so that they did not significantly overlap the blue shifted band, at least at low donor concentrations. The curves with maxima near 422 mμ result from application of this procedure to the observed spectral curves for the pyridine system. As expected for stronger complexes, the maximum of the blue shifted band is in good agreement with literature values.[38] Similar curves for the blue shifted iodine band for the diethyl ether complex are shown in Figure 15. The broken line corresponds to the literature value for the maximum in these curves as determined by the conventional techniques.[37] The solid line

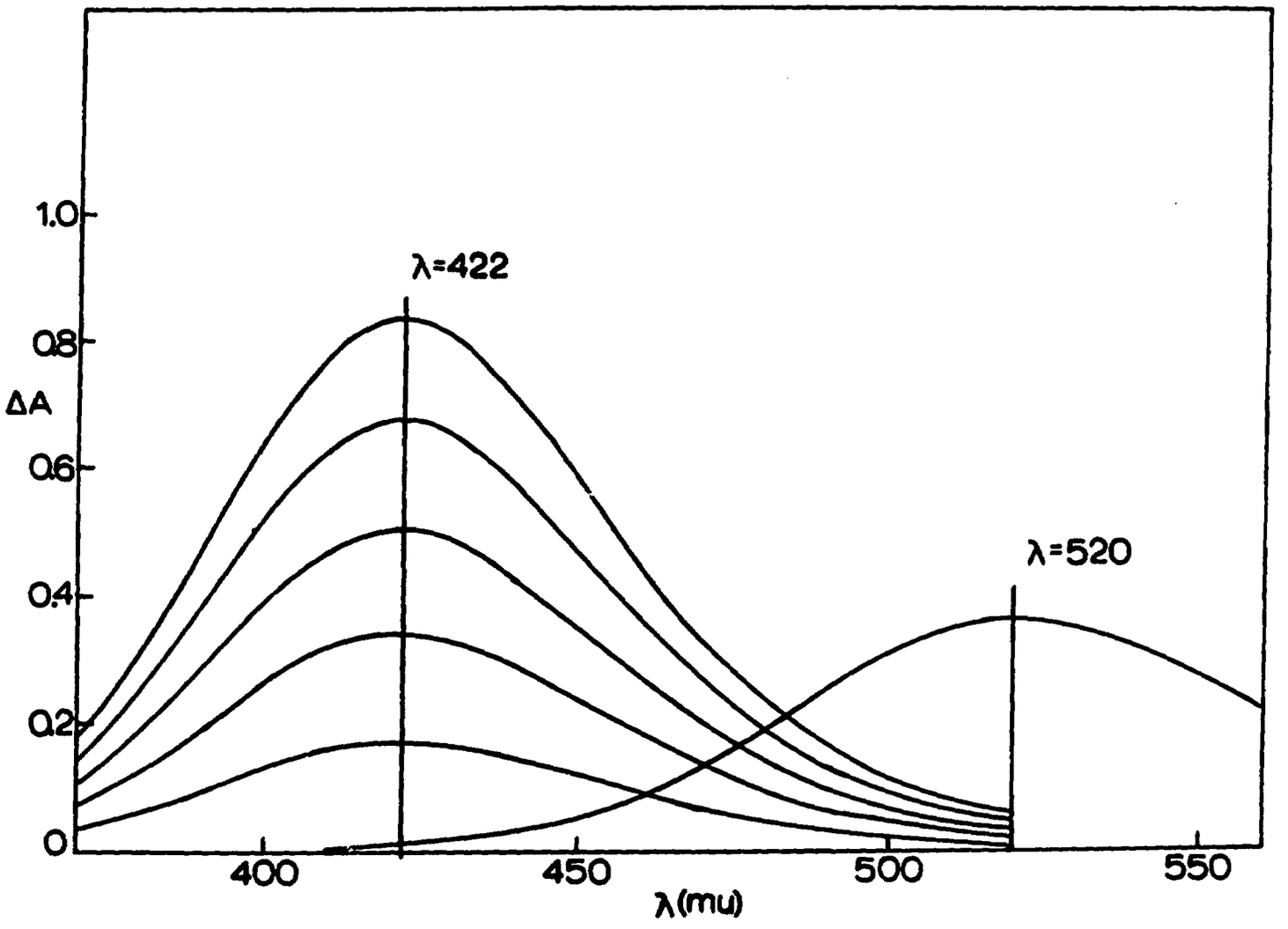

Figure 14. Blue Shifted Iodine Band for the Pyridine·Iodine Complex. The curve with maximum at 520 mμ corresponds to uncomplexed iodine spectrum (2.0 cm. cell pathlength).

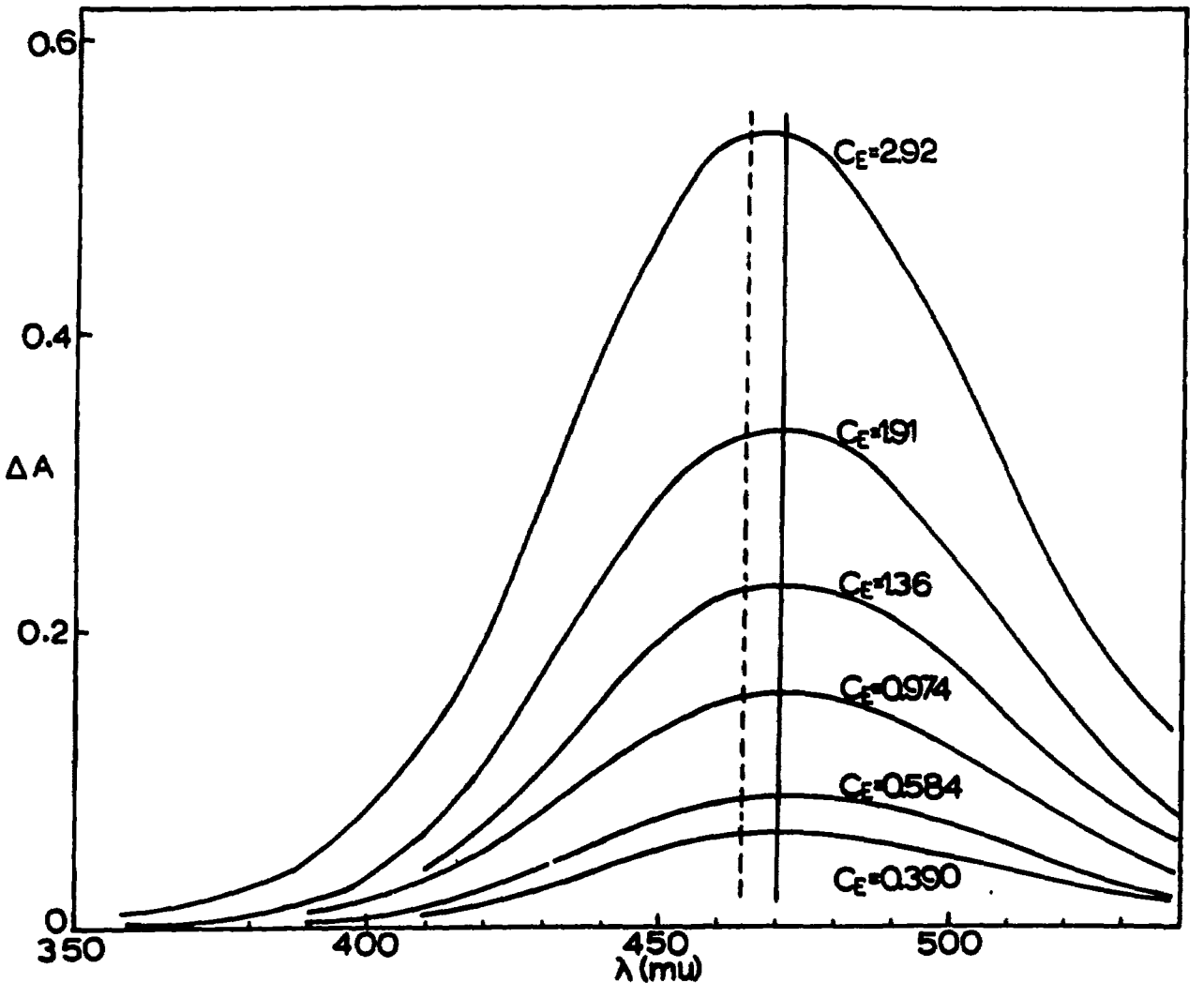

Figure 15. Blue Shifted Iodine Band for the Diethyl Ether·Iodine Complex at 15°C (2.0 cm. Cell Pathlength).

corresponds to the maximum (470 mμ) observed using the solubility method. As the concentration of the diethyl ether is increased much in excess of 1M, the maximum in these curves does appear to shift in the direction of the literature value and this is the subject of discussion in a later section. The blue shifted iodine band for the p-xylene complex is shown in Figure 16. The maximum in this case is located at 501 mμ which compares with a literature value of 495 mμ.[41] At donor concentrations much in excess of about 1.5 M, the charge-transfer band does begin to overlap the blue shifted band and this results in an increasing half-band width of the curves at high donor concentrations. Consequently, the blue shifted iodine bands for the aromatic hydrocarbon donor curves were usually studied at donor concentrations less than 1.5 M.

The extinction coefficient (ϵ^{bs}) at the wavelength of the blue shifted band maximum (λ^{bs}) can be calculated using the relation

$$\epsilon_{cx}^{bs} = \frac{\Delta A^{bs}}{\ell C_{cx}} \qquad (34)$$

where ΔA^{bs} is the observed absorbance corrected for uncomplexed iodine and C_{cx} is the total concentration of complex (1:1 plus 2:1) as determined at the isosbestic point. This calculation results in an extinction coefficient which is a weighted average of those for the 1:1 and 2:1 complexes. To obtain the separated coefficients, the limiting slope of a plot of ΔA^{bs} against C_D should be used in the same manner employed to obtain the extinction coefficients at the charge transfer band. As demonstrated in Figure 17 for the p-xylene complex, such plots show curvature at the higher donor concentrations. However, a corresponding plot of ΔA^{bs} against ΔA^{iso} is linear within experimental error. This is taken

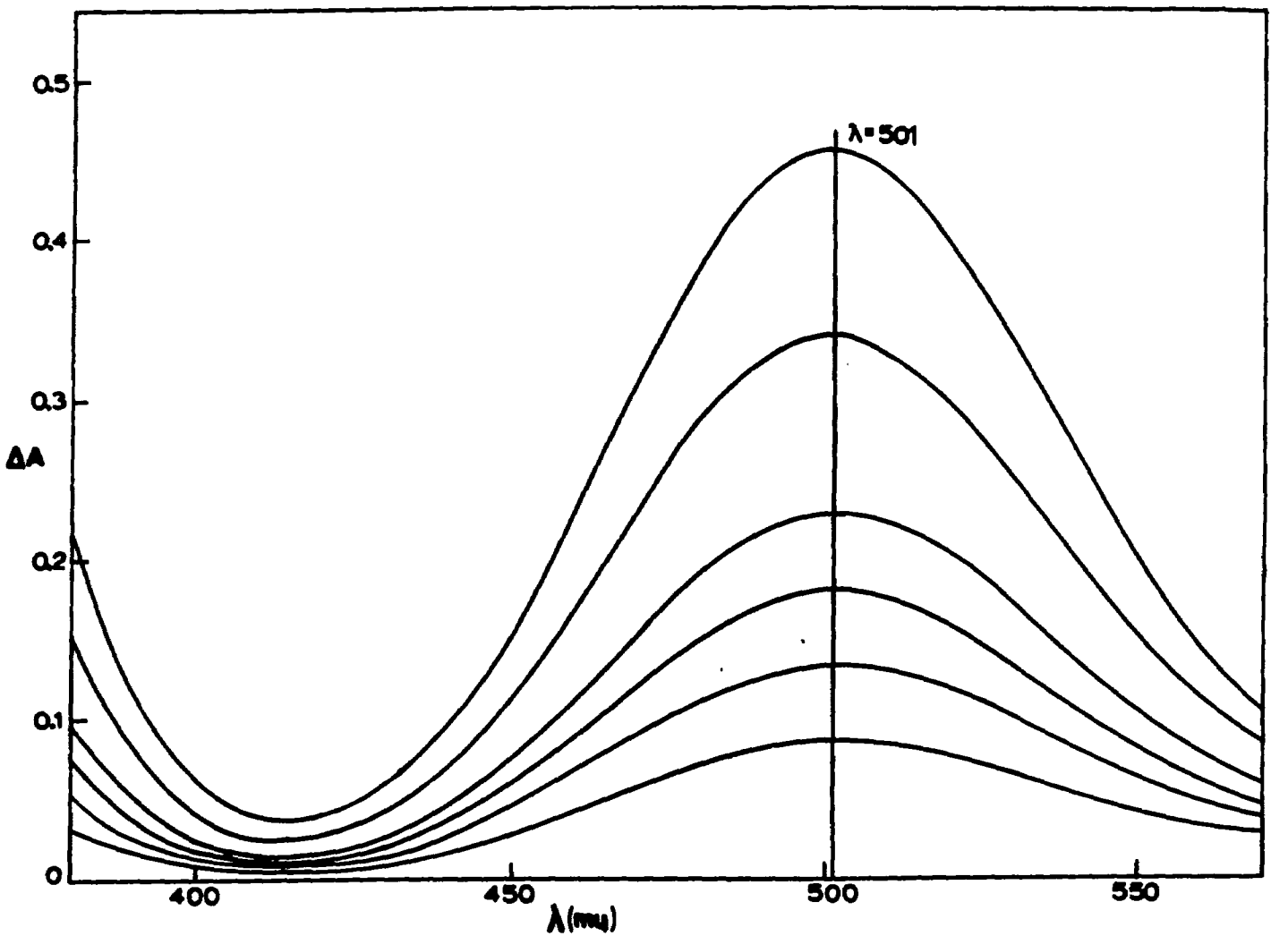

Figure 16. Blue Shifted Iodine Band for the p-Xylene·Iodine Complex (2.0 cm. Cell Pathlength).

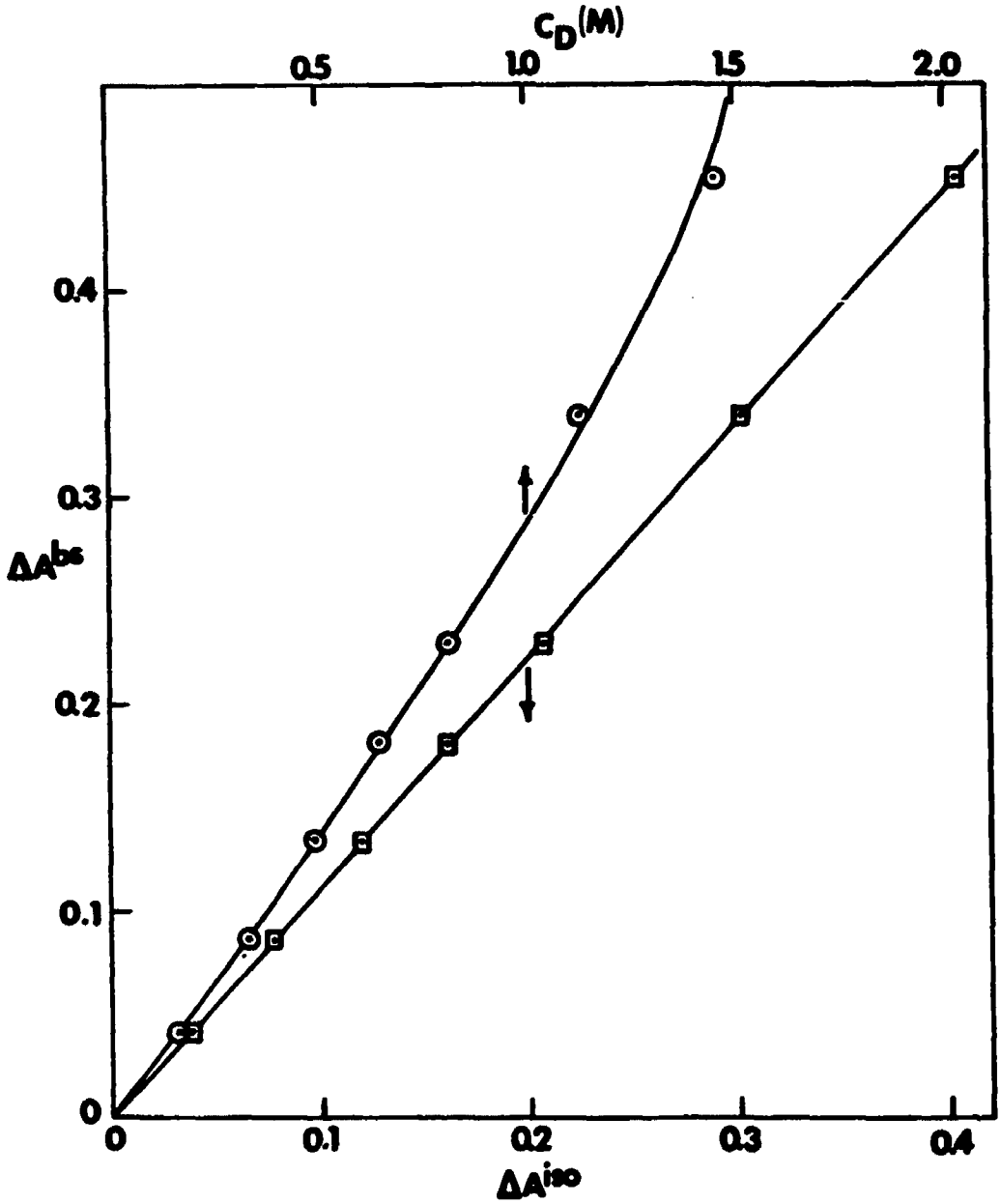

Figure 17. Change in Absorbance at λ^{bs} Versus the Corresponding Change at λ^{iso} and the Concentration of p-Xylene (2.0 cm. Cell Pathlength).

as an indication that the 1:1 and 2:1 extinction coefficients are not much different at λ^{bs}. The absorbance at λ^{bs} is given by

$$\Delta A^{bs} = A_{DA} + A_{D_2A}$$

or

$$\Delta A^{bs} = \ell\varepsilon_{DA}\, C_{DA} + \ell\varepsilon_{D_2A}\, C_{D_2A} \quad .$$

If ε_{DA} is not much different from ε_{D_2A} then to a first approximation

$$\Delta A^{bs} = \ell\varepsilon_{DA}\, (C_{DA} + C_{D_2A})$$

or

$$\Delta A^{bs} = \ell\varepsilon_{DA}\, C_{Cx} \qquad (35)$$

since $C_{Cx} = (C_{DA} + C_{D_2A})$. The concentration of the complex as calculated at the isosbestic point ($C_{Cx} = \frac{\Delta A^{iso}}{\ell\varepsilon_A^{iso}}$) can be substituted into equation (35) to give

$$\Delta A^{bs} = \left(\frac{\varepsilon_{DA}}{\varepsilon_A^{iso}}\right) \Delta A^{iso} \quad . \qquad (36)$$

In this manner the assumption that ε_{DA} and ε_{D_2A} are not much different at λ^{bs} is shown to be reasonable since equation (36) predicts the linear dependence which is experimentally observed. Thus, the extinction coefficient obtained from equation (34) should give a good approximation to ε_{DA}. Even in the most concentrated donor solution, the weighted average obtained for ε_{Cx} can contain only a 3 to 4% contribution from the 2:1 complex.

The procedure employed to obtain ε_{DA}^{bs} for a given complex was simply to average the extinction coefficients obtained from equation (34) at the various donor concentrations. Usually, five to seven determinations

were used in the averaging procedure; the small number of points resulted from the experimental procedure employed in which only alternate solutions were scanned over the entire visible spectrum. The other derived properties were obtained from spectral curves like those presented for the p-xylene complex using the approximate formulas discussed earlier. The peak maximum and half-band widths were calculated by averaging the results from the various curves. There was little variation of the values used to obtain a particular average as long as the donor concentrations were less than about 1.5 M. This further reinforces the conclusion that complexes other than the 1:1 contribute little to the blue shifted band at the lower donor concentrations.

CHAPTER V

CONCLUSIONS AND DISCUSSION

The presentation and discussion of the results of this study are divided into five major sections. In the first section the equilibrium constants and extinction coefficients at the maximum of the charge-transfer band for the 1:1 complexes will be discussed. The interpretation of the results from the polyiodide solubility experiments in terms of termolecular complexes will be given in the second section. The third section will present the results obtained for the properties of the blue shifted iodine bands. A brief discussion of the relative importance of specific and non-specific interactions in stabilizing weak molecular complexes will be presented and a short summary will conclude this chapter. Through each of these sections emphasis will be placed on comparisons of the results derived from the solubility experiments with the corresponding results derived from the conventional experiments of the Benesi-Hildebrand type.

Extinction Coefficients and Equilibrium Constants for the 1:1 Complexes

The extinction coefficients at the charge-transfer band and equilibrium constants for the 1:1 complexes are summarized in Table 5. Included in this table are the results and standard errors obtained

TABLE 5

EQUILIBRIUM CONSTANTS AND EXTINCTION COEFFICIENTS AT THE CHARGE-TRANSFER BAND FOR THE 1:1 COMPLEXES OF IODINE AT 25°C

	Polyiodide Solubility Method			Conventional Spectral Method		
Donor	K_c (ℓ/mole)	ε_{DA}^{ct} ($\ell mole^{-1}cm^{-1}$)	$K_c\varepsilon_{DA}^{ct}$	K_c (ℓ/mole)	ε_{DA}^{ct} ($\ell mole^{-1}cm^{-1}$)	$K_c\varepsilon_{DA}^{ct}$
Benzene	0.356(7)	8080(80)	2880(90)	0.203(7)	14200(300)	2880(160)
Toluene	0.500(6)	6900(60)	3450(70)	0.315(5)	10700(90)	3370(80)
o-Xylene	0.641(9)	6520(60)	4190(100)	0.423(7)	9680(90)	4100(110)
p-Xylene	0.642(6)	5710(50)	3660(70)	0.411(6)	8860(70)	3640(80)
m-Xylene	0.698(6)	6550(50)	4570(70)	0.539(20)	8990(160)	4850(27)
Diethyl ether*	1.44(6)	5720(130)	8230(520)	1.23(5) 1.3[a]	5560(90) 5480[a]	6840(390) 7120[a]
Pyridine	163(2)	41400(500)	$(6.8\pm0.2)\times10^6$	185[b] 157[c] 137[d]	50000[b] ----- 51730[d]	9.3×10^6[b] 7.1×10^6[d]

*Results for the diethyl ether complex refer to 15°C.

[a]Ref. 37; [b]Ref. 38; [c]Ref. 39; [d]Ref. 40.

with the polyiodide solubility method and the results and standard errors from the present research and from the literature which were inferred solely from conventional experiments of the Benesi-Hildebrand type. The equilibrium constants obtained with the polyiodide solubility method may be compared with those obtained by Kortüm (Table 2). The agreement between the two sets of results for the benzene and toluene systems is reasonably good in view of the different solvents and constant activity sources employed. In Kortüm's method[30,31] the use of pure iodine as a constant activity source results in relatively large iodine concentrations and this has been the basis of criticism of this technique.[56] Unfortunately, Kortüm made no comprehensive spectral investigations in conjunction with his solubility studies as has been done in the present research. Thus, the equilibrium constants are the only basis for comparison of the present results with those of Kortüm.

The results obtained with the conventional spectral method can be compared to the corresponding literature results listed in Table 3. In general, the agreement between the present results and those from the literature is satisfactory in view of the uncertainty in the properties determined in this manner.

More significant are comparisons of properties determined by the polyiodide solubility techniques with those obtained with the conventional spectral methods. As seen in Table 5, the reported values of the product $K_c \varepsilon_{DA}^{ct}$ are reasonably consistent for a given complex, whether determined by the solubility method or by the conventional spectral techniques. However, for the weaker complexes (aromatic hydrocarbon donor·iodine) the solubility method yields much larger values of K_c and correspondingly

reduced values of ϵ_{DA}^{ct}. Results for the ether system show less discrepancy, although K_c determined by the solubility method is somewhat greater than that determined by the conventional method. In the case of the moderately strong pyridine complex, both K_c and ϵ_{DA}^{ct} are reasonably consistent from one method to the other.

These observations point out both the similarities and differences in the two methods. First, the agreement between the products $K_c\epsilon_{DA}^{ct}$ for a given complex results because they are determined in the limit of infinite dilution with both techniques. Thus, it might be anticipated that such products are determined with a reasonable degree of accuracy in either method. Second, the disagreement between the separated K and ϵ values (for the weak complexes) evidently arises because of the different techniques employed in separating the respective products. It should be recalled that in the case of weak complexes separation can be accomplished in the conventional technique only by increasing the donor concentration to a level far removed from the dilute solution region.[11] However, in the solubility method both K_c and ϵ_{DA}^{ct} are obtained directly in the separated form from measurements restricted to the dilute solution region. As the strength of the complexes increases through the weak aromatic hydrocarbon·iodine complexes to the moderately strong pyridine complex, the range of donor concentrations necessary to separate $K_c\epsilon_{DA}^{ct}$ by the conventional method becomes smaller. For example, for the pyridine·iodine complex it is possible to achieve a high percent complexation of the acceptor in the dilute solution region (less than 0.05 M pyridine) and thus separate the product without increasing the donor concentration beyond this region.[38] Thus, the separated components obtained from

either method agree satisfactorily for this complex, but not for the weaker complexes. It should be noted that determination of the extinction coefficient for the charge-transfer band of the pyridine complex is experimentally difficult regardless of the method employed.[40] This probably accounts for the disagreement between the value obtained by the solubility method and the corresponding value reported in the literature.

The important results obtained for the extinction coefficients of the complexes at the charge-transfer band are reported in Table 6. Also included are the wavelength λ^{ct} of maximum absorbance of the charge-transfer band and the corresponding extinction coefficients of iodine dissolved in the pure donors. As mentioned in Chapter I, Mulliken's theory[18] predicts that the extinction coefficient should increase as the donor strength increases through a series of similar donors like the aromatic hydrocarbons. It is evident from Table II that this trend was not observed in the extinction coefficients determined by the conventional method. In fact, a rather drastic reversal of the predicted trend is found. This trend was originally reported by Benesi and Hildebrand[32] and it has been the basis of much speculation.[5] In view of this, the extinction coefficients determined by the solubility method are of particular interest and are considered in some detail in the following discussions.

The results from the solubility method also show a slight decrease in intensity with increasing donor strength through the series of aromatic hydrocarbon·iodine complexes. However, the decrease is not so drastic as that observed in the constants obtained with the conventional spectral methods and thus the new results are not as difficult

TABLE 6

EXTINCTION COEFFICIENTS AT THE CHARGE-TRANSFER BAND FOR THE 1:1 COMPLEXES OF IODINE

Donor	Polyiodide Solubility Method		Conventional Spectral Method		In Pure Donor	
	λ^{ct} (mμ)	ε^{ct}_{DA} ($\ell mole^{-1}cm^{-1}$)	λ^{ct} (mμ)	ε^{ct} ($\ell mole^{-1}cm^{-1}$)	λ^{ct} (mμ)	ε^{ct} ($\ell mole^{-1}cm^{-1}$)
Benzene	288	8080	289	14200	297	9770[1]
Toluene	300	6900	300	10700	306	8400[1]
o-Xylene	313	6520	314	9680	319	8400[1]
p-Xylene	303	5710	302	8860	315	7400[1]
m-Xylene	314	6550	314	8890		
Diethyl ether	250	5720	250	5560		
Pyridine	235	41,400	235	50,000[38]		

to rationalize with Mulliken's theory. The concept of contact charge-transfer[20] and the other common rationalizations[2-6] may still be invoked to account for the slight decrease which is observed in these results. However, such effects appear to be far less important than indicated by the results from the conventional experiments. Considering the fact that all of the aromatic hydrocarbons have similar donor strengths, it is tempting to predict a priori that the charge-transfer band intensities should not be very different within the series of hydrocarbon complexes studied here. The results obtained with the solubility method imply a much smaller range for these intensities, which is more in accord with this expectation.

The extinction coefficients of iodine dissolved in the pure donors were obtained by simply dissolving iodine in the pure donor and using the absorbance at λ^{ct} to calculate the reported extinction coefficient.[1] For a given complex, the extinction coefficient determined in this manner is smaller than the corresponding value determined with the conventional method but larger than that determined with the solubility method. In both cases, there are rationalizations to explain the observed differences. However, the same explanations obviously cannot be used in both cases and in fact, the discussion which follows illustrates the basic differences in viewpoint of the two methods.

It seems reasonable to expect that iodine molecules dissolved to the extent of approximately 10^{-4}M in pure benzene are surrounded by an environment of benzene molecules. Although there is no unambiguous way to know how many of the iodine molecules are involved in specific complexes and how many are merely solvated in some non-specific sense,

it seems likely that all the iodine molecules interact with benzene in one of these ways. Therefore, the extinction coefficient determined with the solubility method will include the contribution of both of these interactions to the extinction coefficient. In fact, the extinction coefficient of iodine dissolved in pure donor where the non-specific interactions between donor and acceptor are at a maximum might be viewed as an upper limit on the extinction coefficient determined with the solubility method. The results listed in Table 6 are consistent with this view.

For a particular system, the extinction coefficient determined for iodine dissolved in pure donor is somewhat greater than that determined for the complex with the solubility method. If it is assumed that ternolecular complexes (donor·I-I·donor) exist, then the extinction coefficient of iodine in the pure donor should represent some weighted average of the extinction coefficients of the assumed species. This weighted average is anticipated to be greater than the extinction coefficient of the isolated 1:1 complex whenever the extinction coefficient of the 2:1 complex is greater than that of the 1:1 complex. Since interpretations of the solubility data in terms of multiple complexes (Table 7) leads to derived values of the extinction coefficient of the 2:1 complex which are greater than those indicated for the 1:1 complex, the difference in the extinction coefficients obtained by these two techniques can be explained on this basis. On the other hand, an alternative explanation in terms of solvent effects would simply imply that the extinction coefficient of the 1:1 complex surrounded by benzene molecules is somehow different from the corresponding value for the complex surrounded by heptane molecules. For example, the non-specific

TABLE 7

EXTINCTION COEFFICIENTS AT λ^{ct} AND EQUILIBRIUM CONSTANTS FOR THE 1:1 AND 2:1 COMPLEXES OF IODINE (POLYIODIDE SOLUBILITY METHOD)

Donor	K_{DA} (ℓ/mole)	K_{D_2A} ($ℓ^2$/$mole^2$)	K_{D_2A}/K_{DA}	ε_{DA} ($ℓmole^{-1}cm^{-1}$)	ε_{D_2A} ($ℓmole^{-1}cm^{-1}$)
Benzene	0.356(7)	0.063(3)	0.18	8080(80)	9350(270)
Toluene	0.500(6)	0.066(3)	0.13	6900(60)	8130(470)
o-Xylene	0.641(9)	0.100(6)	0.16	6520(60)	8900(650)
p-Xylene	0.642(6)	0.092(3)	0.14	5710(50)	7730(320)
m-Xylene	0.698(6)	0.078(4)	0.11	6550(40)	13700(1300)
Diethyl ether	1.44(6)	0.130(13)	0.09	5720(130)	8700(1200)

contribution to the extinction coefficient in pure benzene may be greater than that in heptane. In any event, the solvent effect on the extinction coefficient is difficult to predict so that the magnitude of this effect is essentially unknown.[36] In all probability, the observed difference between the coefficient determined in pure donor and that determined with the solubility method is the result of some combination of both the specific and non-specific effects.

The approach which has been employed to explain the difference between the extinction coefficient obtained with the conventional method and that obtained by dissolving iodine in the pure donor is deceptively simple.[2] The reasonable assumption is made that the iodine molecules dissolved in pure benzene are not all involved in specific complexes. Thus, the extinction coefficient of iodine determined in the pure donor is expected to be less than that of the 1:1 complex dissolved in another solvent. Since it is assumed that the extinction coefficient determined with the conventional method is somehow devoid of any non-specific contribution, a correction for the amount of uncomplexed iodine present must be made. Using the 1:1 equilibrium constant in some "inert" solvent such as heptane, the amount of complex present is estimated and the extinction coefficient recalculated on this basis. Such "corrected" extinction coefficients are usually within 20 to 30% of the values obtained with the conventional technique.[2] This agreement is commonly taken as justification for the procedure.[2,5] However, Christian and Tucker[13] have discussed the dangers involved in such an approach. Basically, the problem lies in using the 1:1 equilibrium constant determined in some inert solvent to correct for the uncomplexed iodine in a different medium. Ideally, such an equilibrium constant refers to the formation

of the complex in the dilute solution region where the limiting laws (Henry's law, Beer's law, etc.) are obeyed. To use such a constant over the entire donor concentration range, as is done above, requires the assumption that these laws are obeyed over the entire concentration range, which seems at best doubtful. Actually, in usual spectral studies of weak complexes it is not possible to determine the equilibrium constant in the dilute solution region. This point was discussed in some detail in Chapters I and IV. Thus, agreement between the two extinction coefficients seems to be fortuitous and although the correction procedure appears self-consistent, it does not necessarily give accurate values of the extinction coefficients.

Termolecular Complexes

As indicated in Chapter IV, the curvature in the various plots of the solubility data may be interpreted in terms of multiple complex formation. The most likely complex in addition to the 1:1 was proposed to be a 2:1 complex involving two donors and one acceptor. Here again the derived equilibrium constants include both the specific and non-specific effects on solubility in essentially unknown proportions. However, the situation for the 2:1 complex is somewhat different from that of the 1:1 complex in that determination of the properties for the former necessarily involves increasing the donor concentration to a level high enough to produce significant curvature in the various plots. This necessitates use of donor concentrations up to about 1.5M in most of the systems considered. This procedure is similar to that required in conventional method for determining the properties of the 1:1 complex and, as such, is subject to the same criticism directed at the conventional

method.[2-6] Consequently, any conclusions based on the results for the 2:1 complex are probably subject to some question. In view of this, only a brief discussion of the results in Table 7 is presented.

The equilibrium constants of Table 7 refer to the following reactions:

(1) $D + A \rightleftarrows DA$

and (2) $2D + A \rightleftarrows D_2A$.

For a given donor, the equilibrium constant for the first reaction (K_{DA}) is always considerably larger than that for the second reaction (K_{D_2A}). There is in general a slight decrease in the ratio (K_{D_2A}/K_{DA}) as K_{DA} increases; however, in view of the experimental error, the significance of this trend is difficult to assess.

It is interesting to note that the relation

(3) $K_{D_2A} = K_{DA}^2 /4$

gives a good approximation to the 2:1 equilibrium constant for most of the systems. This relation was derived from considerations of the reaction dynamics involved in the formation of a 2:1 complex from the 1:1 complex in a sequential manner. Ling and Christian[57] applied this technique in their studies of the formation of multiple complexes of the hydrogen bonding type; however, it is just as applicable in the present situation. The derivation of this relation involved the assumption that the acceptor has two sites, either of which may be used to form a complex bond. In the present case, these would correspond to the two iodine atoms of the acceptor. These two sites were considered equivalent and independent. That is, the formation of the 1:1 complex does not interfere with the subsequent formation of the 2:1 complex. The following reactions were

then considered:

$$(4)\quad D + A \underset{k_2}{\overset{k_1}{\rightleftharpoons}} DA$$

$$(5)\quad D + DA \underset{2k_2}{\overset{k_1/2}{\rightleftharpoons}} DAD$$

where the various rate constants are given. As implied in these reactions, it was assumed that the forward rate constant for reaction (5) was given by $k_1/2$ and the reverse rate constant by $2k_2$. The subsequent development of equation (3) easily followed. Using equation (3) and the predetermined values of K_{DA}, the corresponding values of K_{D_2A} can be calculated. Such results agree reasonably well with the observed values of K_{D_2A} for most of the systems. However, for the benzene·iodine complex, this procedure underestimates the observed value of K_{D_2A} by about a factor of 2 and for the diethyl ether complex by about a factor of 4. Evidently, the assumptions are not particularly good for these two systems. However, if the result for the benzene·iodine complex is ignored, then, at least for the aromatic hydrocarbon·iodine series, the sequential complex formation scheme appears plausible.

Unfortunately, for a given complex, the extinction coefficients of the two species bear no simple relation to one another. The extinction coefficient of the 2:1 complex is always greater than that of the corresponding 1:1 complex although neither the differences nor the individual coefficients follow a discernible trend. The extinction coefficients were determined at the observed wavelength of maximum absorbance in the charge-transfer band. Using arguments similar to those proposed

for the blue shifted iodine band in Chapter IV, this wavelength probably corresponds closely to the maximum for the 1:1 complex. However, this may or may not be true for the 2:1 complex. If the maximum for the 2:1 complex does not fall near that of the 1:1 complex, then the extinction coefficient for the 2:1 complex would not necessarily bear any straightforward relation to the corresponding 1:1 coefficient and variations of the 2:1 extinction coefficients through a series would likewise show no particular trend. The main point here is that the extinction coefficient at the maximum of the band is the one of most theoretical significance.

Blue Shifted Iodine Band

As discussed in Chapter IV, an appealing feature of the solubility method is that the spectra of the blue shifted iodine bands are obtained directly by difference, independent of the value determined for the equilibrium constant. This procedure is contrasted with that employed in the conventional method where prior knowledge of the equilibrium constant is required to obtain information about the blue shifted band.[41,51] Both of these techniques were employed in the present research to obtain the spectra and properties of these bands. The spectral properties obtained with the solubility method are summarized in Table 8 and those derived using the conventional method in Table 9.

For the pyridine complex, the reported values of the spectral properties of this band agree, whether determined by the solubility method or by the conventional method. However, for the weaker complexes, the solubility method yields smaller blue shifts of the position of this band (relative to iodine in heptane alone) and correspondingly smaller values

for their extinction coefficients. The half-band widths are usually larger while the oscillator strengths and transition dipoles are smaller.

As determined by the conventional method, the derived spectral properties of the blue shifted band are dependent on the value determined for the equilibrium constant. If this constant is inaccurate, then so are the derived properties. Thus, in light of previous discussions, it is not too surprising that the results for the moderately strong pyridine complex agree from one method to the other while those for the weaker complexes do not. Tamres and Brat[51] have considered the errors in the derived properties of the blue shifted band which result from the use of an inaccurate equilibrium constant. From their results and the discussions in Chapter IV, it can be seen that if the equilibrium constant determined by the conventional method is too low, as is indicated by the results from the solubility method, then for a given complex the calculated blue shift and extinction coefficient will be overestimated. This would account for the differences in the properties of this band which are obtained for the weak complexes from one method to the other.

The results given in Tables 8 and 9 provide some interesting comparisons of the properties which are observed with the two methods. As the donor strength increases through a series of similar donors Mulliken's theory predicts that there should be an increasing blue shift of the position of this band and a corresponding increase in its intensity.[58] However, the results obtained with the conventional method (Table 9) are not consistent with this prediction. The position and intensity of the blue shifted band varies little through the aromatic hydrocarbon donor series, although the donor strengths are sufficiently different

TABLE 8

CHARACTERISTICS OF THE BLUE SHIFTED IODINE BAND AND DERIVED SPECTRAL CONSTANTS FOR THE 1:1 COMPLEXES OF IODINE (POLYIODIDE SOLUBILITY METHOD)

Donor	K (ℓ/mole)	λ^{bs} (mμ)	ε^{bs} ($\ell mole^{-1}cm^{-1}$)	f_{mn}	μ_{mn} (debyes)	$\Delta\nu_{\frac{1}{2}}$ (cm^{-1})
n-Heptane	---	520	918	0.0124	1.18	3220
Benzene	0.356	504	984	0.0142	1.24	3320
Toluene	0.500	502	1020	0.0143	1.24	3240
o-Xylene	0.641	501	1030	0.0153	1.28	3450
p-Xylene	0.642	501	1030	0.0153	1.28	3460
m-Xylene	0.698	499	1060	0.0158	1.29	3430
Diethyl ether	1.44	470	852	0.0144	1.20	3910
Pyridine	163	422	1370	0.0252	1.50	4250

TABLE 9

CHARACTERISTICS OF THE BLUE SHIFTED IODINE BAND AND DERIVED SPECTRAL CONSTANTS FOR THE IODINE COMPLEXES (CONVENTIONAL SPECTRAL METHOD)

Donor	K_c (ℓ/mole)	λ^{bs} (mμ)	ε^{bs} ($\ell mole^{-1} cm^{-1}$)	f_{mn}	μ_{mn} (debyes)	$\Delta\nu_{\frac{1}{2}}$ (cm^{-1})
n-Heptane	---	520	918	0.0124	1.18	3220
Benzene	0.203	498	1150	0.0162	1.30	3260
Toluene	0.315	496	1120	0.0154	1.27	3170
o-Xylene	0.423	496	1130	0.0162	1.31	3320
p-Xylene	0.411	496	1210	0.0175	1.36	3350
m-Xylene	0.539	496	1160	0.0169	1.34	3380
Diethyl ether*	1.23 1.3[a]	469 462[a]	890 950[a]	0.0143	1.19	3710
Pyridine	185[b]	422[b]	1320[b]	0.024[b]	1.48[b]	4300[b]

*Experimental temperature 15°C; all others 25°C.

[a]Ref. 37; [b]Ref. 38.

that more variation might reasonably be expected. In contrast, the properties determined by the solubility method (Table 8) show quite different behavior. Here there is an increasing shift to higher frequencies of the position of the maximum in the blue shifted band as the equilibrium constant increases. This trend for the aromatic hydrocarbons is fairly distinct although because of the weakness of the complexes, the shifts are not very large. Somewhat more impressive is the smooth increase in the intensity of the bands with increasing equilibrium constant through this series. Figure 18 is a plot of the extinction coefficient at the band maximum versus the equilibrium constant for these donors and is presented here to illustrate the smoothness of this trend. Included on the ordinate of this plot is the extinction coefficient of iodine dissolved in heptane alone. The line appears to extrapolate to a value near this extinction coefficient. This behavior is opposed to the erratic trend observed by application of the conventional techniques and is in better agreement with Mulliken's theory.[5] Since the donor orbitals involved in complex formation through this series are not expected to be very different, the progression of equilibrium constants and extinction coefficients through this series evidently is caused by variation in donor strengths. This increases with increasing methyl substitution on the ring. On this basis, the smooth trends of the spectral properties of the aromatic hydrocarbon iodine complexes observed with the solubility method are intuitively very pleasing.

From benzene through pyridine, the observed overall trends in the spectral properties are also in the predicted direction, although the extinction coefficient of the diethyl ether complex seems anomalously low.

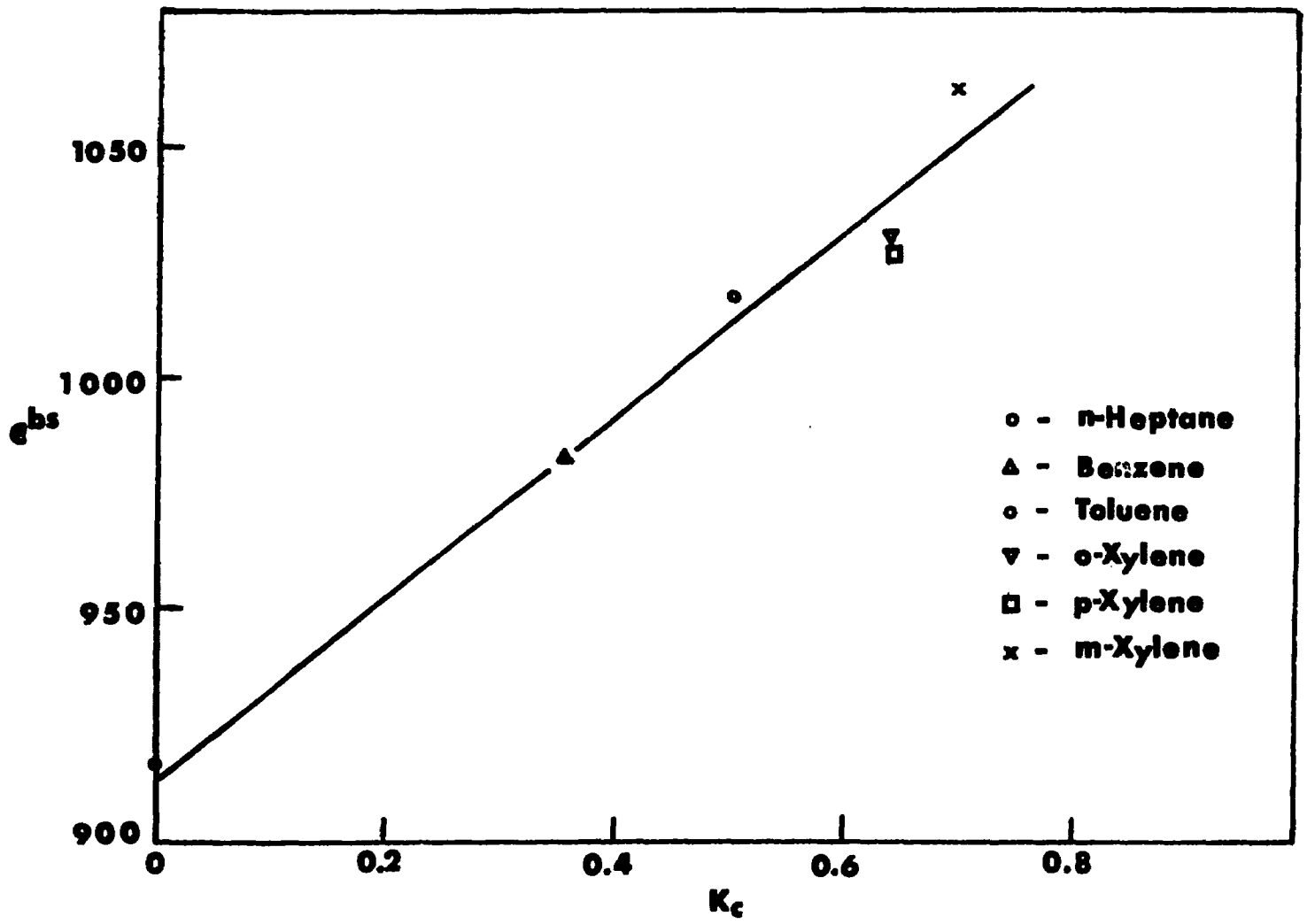

Figure 18. Intensity at λ^{bs} Versus the Equilibrium Constant for the Various Iodine Complexes.

This behavior for the ether complex is observed regardless of the method used and there is no ready explanation of this behavior in terms of Mulliken's theory.[58] As implied previously, comparisons of the general properties of charge-transfer complexes appear to show reasonable trends only within a series of similar donors, i.e., donors in which the donating orbitals are of a similar nature.[18] The oscillator strengths, transitions dipoles, and half-band widths obtained from the solubility data are also quite reasonable and the trends are in the general direction predicted by Mulliken although the half-band width for the benzene system seems somewhat large.

The extinction coefficients at λ^{bs} for iodine dissolved in the pure donors (Table 4) may be compared with the corresponding results of the present research. The extinction coefficients determined in the pure donors are quite close to those determined with the solubility method. This is consistent with the assumption made in Chapter IV that the extinction coefficients of the 1:1 and 2:1 complexes are not much different in the vicinity of λ^{bs}. The argument here is similar to that employed at the charge-transfer band.

Application of the Solubility Method to Study the Thermal Dependence of the Observed Properties

Employing the solubility method, the equilibrium constant for the pyridine·iodine complex was determined at two different temperatures (15 and 25°C). The equilibrium constant for the 1:1 complex at 25°C is 163 ± 2 ℓ/mole and at 15°C it is 275 ± 6 ℓ/mole. These values lead to an estimation of ΔH^{o} for the formation of this complex of 8.6 kcal./mole. This value is in good agreement with corresponding literature values.[38,59]

Basically, this study was undertaken to demonstrate the convenience and feasibility of studying the thermal dependence of the various properties with the solubility method. Obviously, this technique was not exploited to the full extent possible in the present research. In addition to the thermodynamic properties, the variation of the various spectral properties with temperature could have been determined with similar convenience. This would be a worthwhile project since thermal variation of the spectral properties of weak complexes in solution has not been extensively studied. At lower temperatures where the specific effects become more pronounced, it may be possible to obtain a better estimate of the relative contribution of the specific and non-specific effects.

Mesitylene·Iodine Complex

The results for the mesitylene complex were not included in the comparisons discussed here because of serious difficulties encountered in the studies of this system. The conventional studies of the Benesi-Hildebrand type indicated that some irreversible process occurred in this system which removed iodine from the system; half of the initial iodine was lost in approximately 2 to 4 hours. Evidently, this process involved some photochemical reaction since determinations in the dark did not demonstrate this behavior. Since this behavior has not been reported in the literature at this experimental temperature[60,61] and since only the solutions which contained donor showed this behavior, it was supposed that the donor being employed contained some impurity. Numerous attempts were made to remove this impurity employing the usual techniques, however none of these attempts were successful. No attempts to characterize

either the supposed impurity or the irreversible reaction were made. This time-dependent decay of the iodine is not particularly critical in the conventional method since such studies can be performed relatively quickly, but such an effect would have unknown consequences in the solubility method with its extended equilibration times. Eventually, the determinations on this system were performed in the dark where the process evidently did not occur. The results of this study are presented in Table 10. The effect of any impurity on these results is essentially unknown. It is interesting to note that these results do not conflict with any of the basic conclusions of this research. In fact, the conclusions derived from the previous solubility results are reinforced by the results in Table 10. The equilibrium constant and the extinction coefficient at λ^{ct} are quite consistent with those for the other aromatic hydrocarbon donors and the point (K_c, ε^{bs}) for the blue shifted band falls almost in the expected position (Figure 18).

General

Throughout this study, there have been numerous references to the fact that the properties obtained with the polyiodide solubility method include both the specific and non-specific effects on the solubility of iodine. Appendix I presents an attempt to apply Hildebrand and Scott's solubility parameter theory to estimate the relative contributions of the two effects to the equilibrium constants determined with the solubility method. However, given the limitations of solubility parameter theory, it was concluded that this treatment provides at best only a first approximation of these effects. Part of the problem lies in the subtle nature of the specific effect in weak complexes like

TABLE 10

SPECTRAL AND THERMODYNAMIC PROPERTIES OF THE

MESITYLENE·IODINE COMPLEX

Polyiodide Solubility Method

$$K_{DA}(\ell/mole) = 0.967(5) \quad ; \quad K_{D_2A}(\ell^2/mole^2) = 0.116(6)$$

$$\lambda^{ct}(m\mu) = 327; \ \varepsilon_{DA}(\ell mole^{-1}cm^{-1}) = 7730(50); \ \varepsilon_{D_2A}(\ell mole^{-1}cm^{-1}) = 11200(1100)$$

$$K_{DA} \ \varepsilon_{DA} = 7480(90)$$

$$\lambda^{bs}(m\mu) = 495; \ \varepsilon^{bs}(\ell mole^{-1}cm^{-1}) = 1110$$

$$\Delta\nu_{\frac{1}{2}}(cm^{-1}) = 3470; \ f = 1.69; \ \mu_{mn} = 1.32 \ D$$

Conventional Spectral Method

$$K(\ell/mole) = 0.748(0.018)$$

$$\lambda^{ct}(m\mu) = 327; \ \varepsilon^{ct}_{DA}(\ell mole^{-1}cm^{-1}) = 10,110(140)$$

$$K_c \ \varepsilon^{ct}_{DA} = 7560(300)$$

---

those involving the aromatic hydrocarbon donors. In these cases, it is estimated that the non-specific interactions of the donor and acceptor are about the same order of magnitude as the corresponding specific interactions. Indeed, Christian and Grundnes[27] have shown that in the vapor phase charge-transfer forces may not be the major forces stabilizing the weak complexes of iodine. Similar views have been proposed previously by O. K. Rice.[24,25] The situation in solution is probably somewhat more favorable to the specific effect since the environment of solvent molecules may serve to stabilize the specific complex to some extent[25] and, as Mulliken has argued, the dispersion forces probably cancel out to some degree in solution.[54] For the stronger complexes the situation is much simpler, since the large specific effect of complex formation probably overshadows the smaller non-specific effects.

The conventional experiments of the Benesi-Hildebrand type also measure some combination of these effects although it has been commonly assumed that through some fortuitous cancellation, the results of this method are relatively free from such effects.[1,54] Actually, it has been argued here that the situation is considerably worse in this method than in the solubility method because of the excessive donor concentrations which are required in the former. However, the problems of measuring the properties of weak complexes are not entirely avoided by use of the solubility method since the derived properties do include both a specific and non-specific contribution. As shown in Appendix I, it is possible to derive an expression which clearly shows the activity effect on the derived equilibrium constant. This is a definite improvement over the procedures which have been employed in the past to study weak

complexes and until a method is devised which unambiguously separates these two effects, it is felt that the solubility method is the most reasonable alternative. In fact, the reasonable trends of the spectral and thermodynamic properties obtained with this method might be taken as indication that the total effect is after all the one of most direct theoretical significance.

Summary

A new method for studying the weak complexes of iodine has been developed which involves the use of tetramethylammonium polyiodides as constant activity sources for iodine. The charge-transfer complexes of iodine with aromatic hydrocarbons, diethyl ether, and pyridine as donors have been studied by this technique. In addition, conventional experiments of the Benesi-Hildebrand type have also been employed to study these complexes. The results from these two methods have been critically compared.

The polyiodide solubility method avoids many of the difficulties inherent in the conventional spectral techniques for determining K and ϵ for weak molecular complexes. The new method permits the determination of the spectra and concentration of iodine complexes directly by the difference between the observed spectral curve and that of a blank. Since only one parameter is determined in the limiting region of concentration, there is no necessity of increasing the donor concentration to a level high enough to force a large percent of the acceptor molecules into the complexed form. Problems introduced by variations of the activity and extinction coefficients with concentration are thus kept at a minimum.

The results obtained with the solubility method are chemically and physically very reasonable. The following three facts make it an appealing substitute for the conventional spectral methods 1) there is no drastic decrease in the intensity of the charge-transfer band with increasing donor strength in the aromatic hydrocarbon series 2) both the intensity and wavelength of the blue-shifted iodine band vary smoothly and monotonically as the equilibrium constant increases and 3) the solubility and conventional techniques yield similar results for the strong complexes for which it is possible to achieve a high percent complexation of the acceptor in the dilute solution region.

The contributions of non-specific interactions to the results obtained from both methods are discussed. Hildebrand and Scott's solubility parameter theory is employed in an attempt to estimate such contributions to the equilibrium constants determined with the solubility method. Finally, since the results obtained with the new method are so reasonable, it is proposed that the total effect (specific plus non-specific) on solubility is the one of most fundamental significance.

II. CRYSTAL AND MOLECULAR STRUCTURE OF THE CHARGE-TRANSFER COMPLEX BETWEEN TRIMETHYLAMINE AND SULFUR DIOXIDE

CHAPTER VI

INTRODUCTION

Although the crystal and molecular structures of donor-acceptor (DA) type complexes have been widely investigated for a variety of donors and acceptors, almost no attention has been given to such complexes which involve sulfur dioxide (SO_2) as the acceptor. Since solid complexes of this type have long been known,[64] this seems somewhat surprising. In the belief that a complete understanding of the nature of these complexes is impossible in the absence of crystallographic data, a program of research to investigate the crystal structures of these complexes has been initiated.

The complex selected for initial investigation was that formed between trimethylamine(TMA) and sulfur dioxide(SO_2). This complex had a minimum number of atomic parameters to determine and its existence in the solid state had been reported.[65] The convenient rule of thumb which is used as a guide in the selection of a heavy atom

$$\frac{\Sigma Z^2_{heavy}}{\Sigma(Z^2_{light})} \simeq 1 \qquad (Z = \text{atomic number})$$

indicated that the heavy atom method could be used in this determination.[66] Also, the dielectric properties,[67] infrared[68] and ultraviolet spectra,[49] and energetics[49] of this complex were known. These properties would be useful in any subsequent theoretical interpretations.

A brief review of the literature follows. Studies of the general properties of the amine·SO_2 complexes are presented. Also, the structures of solid DA complexes, determined using crystallographic techniques, are briefly reviewed.

General Properties of Amine·SO_2 Complexes

Most of the early studies in this area involved determination of the properties of the solid adducts of SO_2 with various amines. A review of this work is given by Byrd.[64] The solid adduct TMA·SO_2 was investigated by Burg[65] who reported the thermodynamic constants for the reaction

$$(CH_3)_3N\ (g) + SO_2\ (g) \rightleftarrows (CH_3)N{\cdot}SO_2\ (s)$$

for which he reported

$$\Delta F^{o} = 28.95 - 0.0704\ T.$$

In these calculations it was assumed that the vapor above the solid compound consisted almost entirely of the dissociated components. Similar studies for the complexes of other amines are numerous.[64]

Moede and Curran[67] studied the dielectric properties for mixtures of amines with SO_2 in benzene. They determined a dipole moment of 4.95 D for the TMA·SO_2 complex compared to moments of 1.6 D for SO_2 and 0.86 D for TMA. Assuming the angle between the N-S bond and the SO_2 moment vectors to be 55° and that the moments of the components were increased by approximately 0.2 D in the complex, they calculated a moment of 2.7 D

for the N-S bond. They suggested that this rather low value for the N-S bond moment, compared to 4.2 D for the N-O bond in amine oxides, was due to resonance of the molecule between two structures

$$R_3N{-}{-}{-}{-}SO_2 \rightleftarrows R_3N^+{-}{-}SO_2^- \ .$$

That is, resonance between a dipole-dipole bond and a purely covalent bond in which the electrons are equally shared. The assumption was made that the dipole-dipole structure made a significant contribution to the stability of the complex and thus reduced the N-S bond moment appreciably below the N-O moment in amine oxides, since the latter had practically no dipole-dipole character. In Mulliken's later formulation,[18] this was equivalent to assuming the "no-bond" (no electron transfer) structure made a significant contribution to the ground state wavefunction. Similar calculations were performed for the complexes of triethylamine, tri-n-butylamine and pyridine with SO_2.

The infrared and Raman spectra of the complexes of amines with SO_2 have several features in common. In particular, Hata[68] found that the frequencies of the symmetric (ν_1) and asymmetric (ν_3) S-O stretching vibrations were considerably shifted to lower wave numbers compared with free SO_2. The shifts in the stretching vibrations were attributed to the transfer of an electron from the nonbonding orbital of the amine to some empty antibonding orbital of the sulfur resulting in a weaking of the S-O bond. For the TMA·SO_2 complex, the infrared spectrum of the crystalline complex gave values of 1090 cm^{-1}, 1210 cm^{-1} and 555 cm^{-1} for ν_1, ν_3 and ν_2, respectively. These values may be compared with 1144 cm^{-1} (ν_1), 1324 cm^{-1} (ν_3), and 523 cm^{-1} (ν_2) for crystalline SO_2.[69] It is

interesting to note that the O-S-O deformation vibration (ν_2) of "complexed" SO_2 is shifted to higher wave numbers whereas the stretching vibrations are shifted to lower values. Also, new bands appeared which were assigned to the N-S stretching vibration of the complex. This band was located at 186 cm^{-1} for the $TMA \cdot SO_2$ complex in benzene. Included in this study were the complexes of dimethylamine, trimethylamine, N,N-dimethylaniline, and N,N-diethylaniline with SO_2. The infrared spectra of the complexes of pyridine and benzoid amines with SO_2 have also been investigated.[70]

Relatively little thermodynamic work has been done on amine complexes with SO_2 in solution and even less is known about gas phase complexes. Moede and Curran[67] listed some thermodynamic properties of the complexes listed previously; sulfur dioxide complexes with aromatics,[71-73] olefins,[72] amines[74] and simple alcohols[75] in various solvents have also been investigated. The small number of these investigations is probably due to the experimental difficulties involved in handling sulfur dioxide quantitatively. The most comprehensive investigation of this type is that of Christian and Grundnes[49] who studied the ultraviolet spectra and thermodynamic properties of the reaction

$$TMA + SO_2 \rightleftarrows TMA \cdot SO_2$$

in both the gas phase and in heptane. The values of the equilibrium constants and enthalpies of formation for this reaction were

Gas Phase $\quad K_c^{298} = 340$ ℓ/mole

$\Delta H^o = -9.7$ Kcal/mole

Solution (Heptane) $K_c^{298} = 2550$ ℓ/mole

$\Delta H^o = -11.0$ Kcal/mole

These values indicated that the interaction between TMA and SO_2 was a relatively strong one. The increase in both the equilibrium constant and $-\Delta H^o$ for the molecular complex formation reaction as the medium was changed from gas to non-polar solvent was opposite that observed in the few charge-transfer systems for which such data were reported. This effect was attributed to stronger interaction of the complex (due to its large dipole) with the solvent than the two separated components.[67] The prominent spectral feature (Figure 19) was the charge-transfer band of the complex which had a maximum absorbance at 276 mμ in gas and 273 mμ in heptane. The figure shows the gas phase spectra for the individual components, the spectrum for the complex plus components (upper curve) and that for the complex alone. The observed blue shift of the complex band (from 276 mμ in gas to 273 mμ in heptane to 258 mμ in dichloromethane) was opposite to that commonly observed on transfer of a charge-transfer complex from the gas phase to solution. Using Mulliken's formulation, this effect was described as a solvent effect in which the solvent increased the contribution of the dative structure to the ground state wave function on transfer from gas to solution leading to the observed blue shift.

Crystal and Molecular Structures of Donor-Acceptor Complexes

Since several excellent review articles concerning the structures of DA complexes appear in the literature,[4,5,76,77] a comprehensive

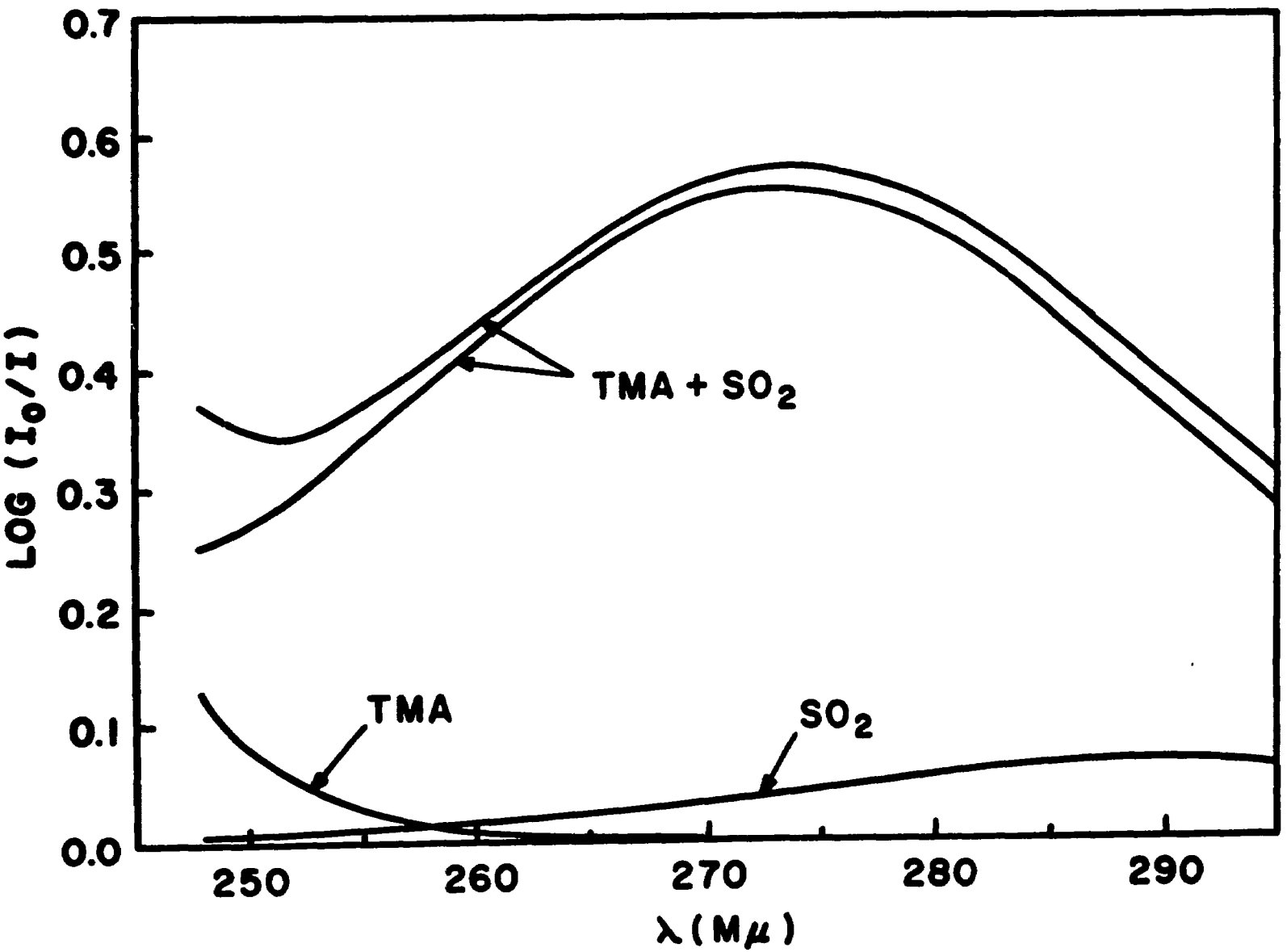

Figure 19. Gas Phase Spectra of the TMA·SO_2 Complex, After Reference 49.

review of this subject is not justified here. However, a discussion of some of the important features of these structures should prove instructive.

Numerous crystallographic determinations have been made on complexes of n-donors (compounds containing lone pair electrons) with halogen or inter-halogen acceptors.[77] The intermolecular charge-transfer bond is formed by partial donation of an electron from the nonbonding lone-pair orbital of the donor to some empty orbital of the acceptor. In some cases this results in structures consisting of infinite chains or sheets of alternating donor and acceptor molecules (Figure 20(A)). The structures of these complexes have several features in common: 1) The complexes with diatomic halogen acceptors have a linear orientation of the halogen molecule with the donor atom (Figure 20(B)). 2) The charge-transfer bond length is intermediate between the van der Waals distance and a normal single bond between the atoms. 3) There is a significant lengthening of the halogen-halogen bond length. Table 36 summarizes some of the crystallographic data on these complexes.

In the weak complexes of π-donors and halogen acceptors of which the classic examples are the complexes of benzene with bromine or chlorine (Table 36, Figure 21), the donor-acceptor distance is shorter than the corresponding van der Waals distance, but this shortening is considerably less than that for the n-donors. There is no significant lengthening of the halogen-halogen bond.

The π-donor and π-acceptor complexes are formed from stacks of alternate donor and acceptor molecules.[76] Most of these complexes involve aromatic hydrocarbons (with or without attached electron donating

Figure 20

(A) Structure of the Dioxane·Bromine Complex, After Reference 84

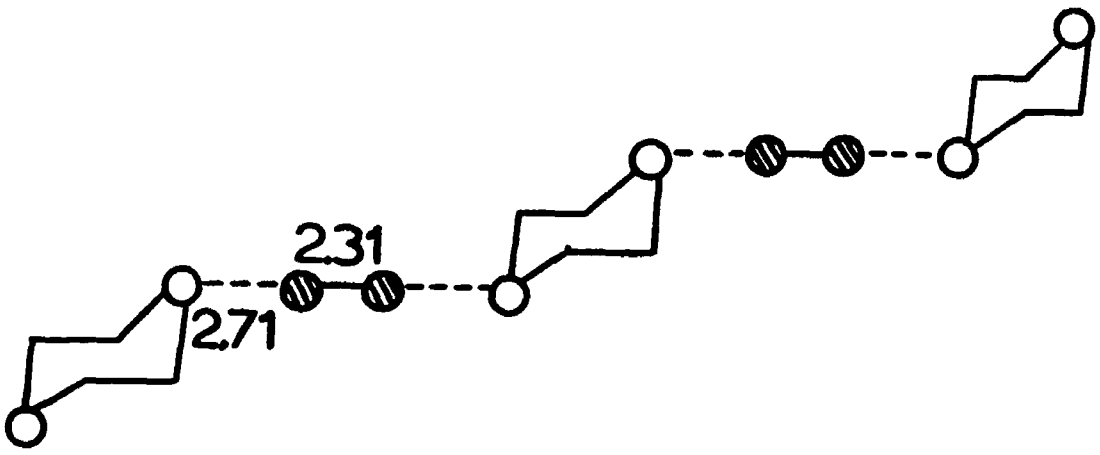

(B) Structure of the Trimethylamine·Iodine Complex, After Reference 78

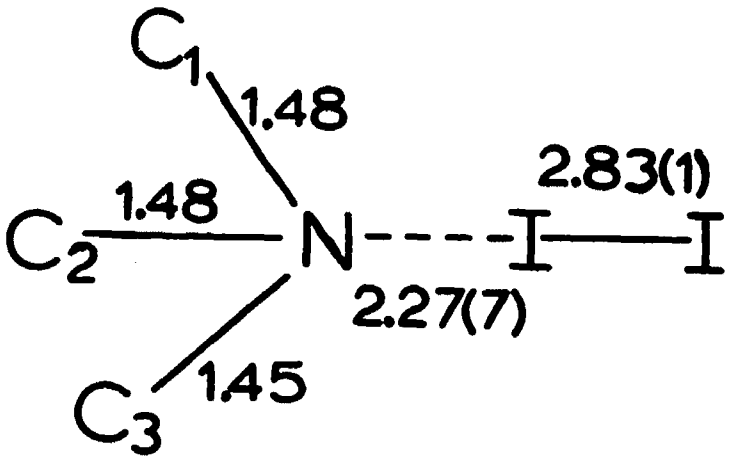

Angles: C_1-N-C_2 (114°), $C_{1(2)}$-N-C_3 (108°), I_1-N-$C_{1(2)}$ (107°), I_1-N-C_3 (114°), N-I_1-I_2 (179°).

Figure 21. The Structure of the Benzene.Bromine Complex, After Reference 87. The structure consists of infinite stacks of alternating donor and acceptor molecules. The Br-Br bond coincides with the six-fold axis of the benzene molecule.

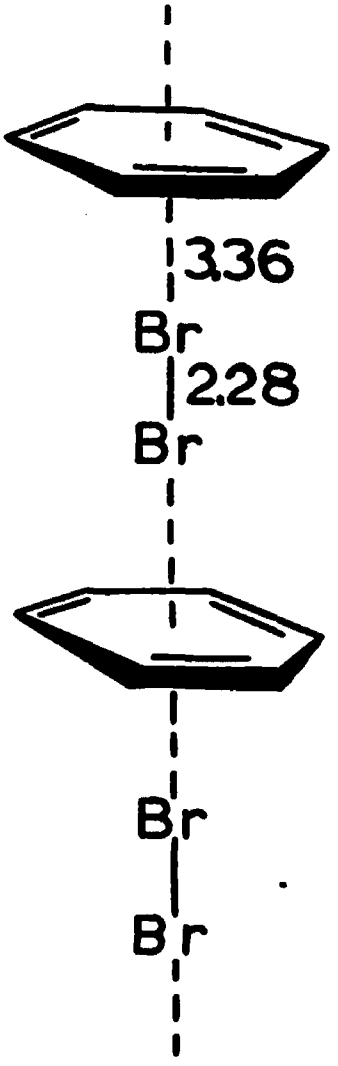

TABLE 36

STRUCTURAL PARAMETERS FOR VARIOUS CHARGE-TRANSFER (CT) COMPLEXES

Complex	CT Bond	CT Bond Length	Sum of Covalent Radii	Sum of van der Waals Radii	Complexed Acceptor Bond Length	Free Acceptor Bond Length	Reference
Trimethylamine·I_2	N-I	2.27Å	2.03	3.65Å	2.83Å	2.67Å	78
Trimethylamine·ICl	N-I	2.30	2.03	3.65	2.52	2.32	79
Pyridine·I_2	N-I	2.16	2.03	3.65	2.74	2.67	80
3-Picoline·I_2	N-I	2.31	2.03	3.65	2.83	2.67	81
Pyridine.IBr	N-I	2.26	2.03	3.65	2.66	2.47	82
Acetonitrile·Br_2	N-Br	2.84	1.84	3.45	2.33	2.28	83
1,4-Dioxan·Br_2	O-Br	2.71	1.80	3.35	2.31	2.28	84
Acetone·Br_2	O-Br	2.82	1.80	3.35	2.28	2.28	85
Dibenzyl Sulphide·I_2	S-I	2.78	2.37	4.00	2.82	2.67	86
Benzene·Br_2	Bz-Br	3.36		3.65	2.28	2.28	87
Benzene·Cl_2	Bz-Cl	3.28		3.50	1.99	1.99	88
p-Xylene·CBr_4	Bz-Br	3.34		3.65	1.93	2.28	89

substituents) combined with aromatic or ethylenic hydrocarbons (with electron withdrawing substituents). The separation of the donor and acceptor within a given stack is usually less than the corresponding van der Waals distance. However, measurements on a variety of complexes have shown that the average separation within a stack is only slightly dependent on the particular DA pair. All such distances which have been determined fall within the range 3.2-3.4 A^{o}.[76] Foster[4] has suggested that maximum charge-transfer interaction in these complexes should be realized when the planes of the two components are parallel, one directly above the other, if the bonding is through the delocalized π-orbitals of both components. That many of these complexes violate this principle is probably a reflection of the weak nature of this type of bonding. In the weaker complexes, the crystal structures can become a compromise between molecular orientation most favorable to π-overlap, hydrogen bonding interactions, and molecular packing. For example, in the N,N,N',N'-tetramethyl-p-phenylenediamine complexes of chloranil or bromanil,[90] the charge-transfer forces overwhelm any other lattice forces which might lead to alternative orientations and the maximum overlap principle appeared to hold. Whereas, the p-benzoquinone complex of p-chlorophenol involves intermolecular hydrogen bond interactions in addition to charge-transfer forces and it was suggested that the observed configuration might be a result of compromise between the two.[91]

Although there are no reported crystal structures involving SO_2 analogous to those discussed above, there are structures in which SO_2 was used as a ligand in coordination complexes of transition metals.

Vogt, et al.,[92] have determined the structure of the complex $(RuCl(NH_3)_4(SO_2))Cl$. In this complex the Ru central atom is at the center of a slightly distorted octahedron, the Ru-S distance is 2.072(3)A^o, and the Ru-SO_2 fragment is planar. A quite different situation was reported for the complex $IrCl(CO)(SO_2)(P-(C_6H_5)_3)_2$[93] where the coordination geometry was that of a tetragonal pyramid with CO, Cl, and trans P atoms in the base and the S of the SO_2 at the apex (Figure 22). The striking features of this complex were the long Ir-S bond (2.49(1)A^o) and the angle (32°) between the Ir-S bond and the normal to the SO_2 plane. The different orientations of the SO_2 molecules in these two complexes has been rationalized in terms of the different roles played by the SO_2 molecule.[94] In the bond between Ru and the sulfur dioxide ligand, it was assumed that sulfur dioxide functioned as a Lewis base donating electrons to the central atom. The planar configuration of the Ru-SO_2 fragment suggested that a hybridized sp^2 orbital on sulfur was used. In the Ir-complex no empty metal orbitals were readily available to accept electrons, and SO_2 acted as a Lewis acid accepting electrons from the central atom. The approximate tetrahydral arrangement around sulfur suggested that a hybridized sp^3 orbital of sulfur was used in forming this complex.

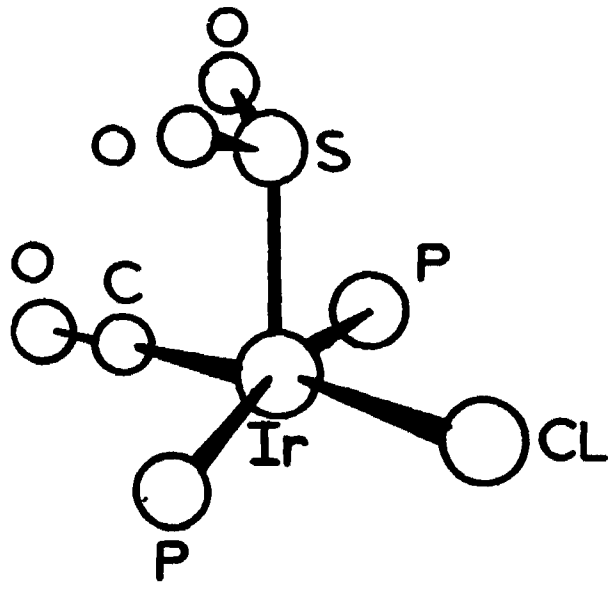

Figure 22. The Coordination around Ir in IrCl(CO)$(SO_2)(P(C_6H_5)_3)_2$, After Reference 35.

CHAPTER VII

CRYSTAL AND MOLECULAR STRUCTURE OF TRIMETHYLAMINE·SULFUR DIOXIDE

Experimental

Crystals of the donor-acceptor complex between trimethylamine and sulfur dioxide were prepared by vapor phase reaction of the components. The reaction was carried out in the following manner. The trimethylamine (Matheson, 99.0% purity) in dry heptane was placed in vapor contact with sulfur dioxide (Matheson, 99.98% purity) in heptane as in Figure 23. Large amounts of a white, flocculent material formed in the connecting tube within a few hours. Since this product is very sensitive to moisture, all work has to be performed in a nitrogen dry box. The initial product was transferred into glass vials with tightly fitting screw cap lids and stored at approximately 5°C in a refrigerator. In about two days clear, well-defined crystals sublimed onto the walls of the glass vials. These crystals were transferred to thin walled lithium glass capillaries. The open end of the capillaries was temporarily sealed with a commercial sealing compound (Apiezon Q) before removal from the dry box. The capillaries were then removed from the dry box and permanently sealed with a small flame. During this collection procedure, the crystals had an annoying tendency to lose their crystalline faces and reappear as a drop within the capillary.

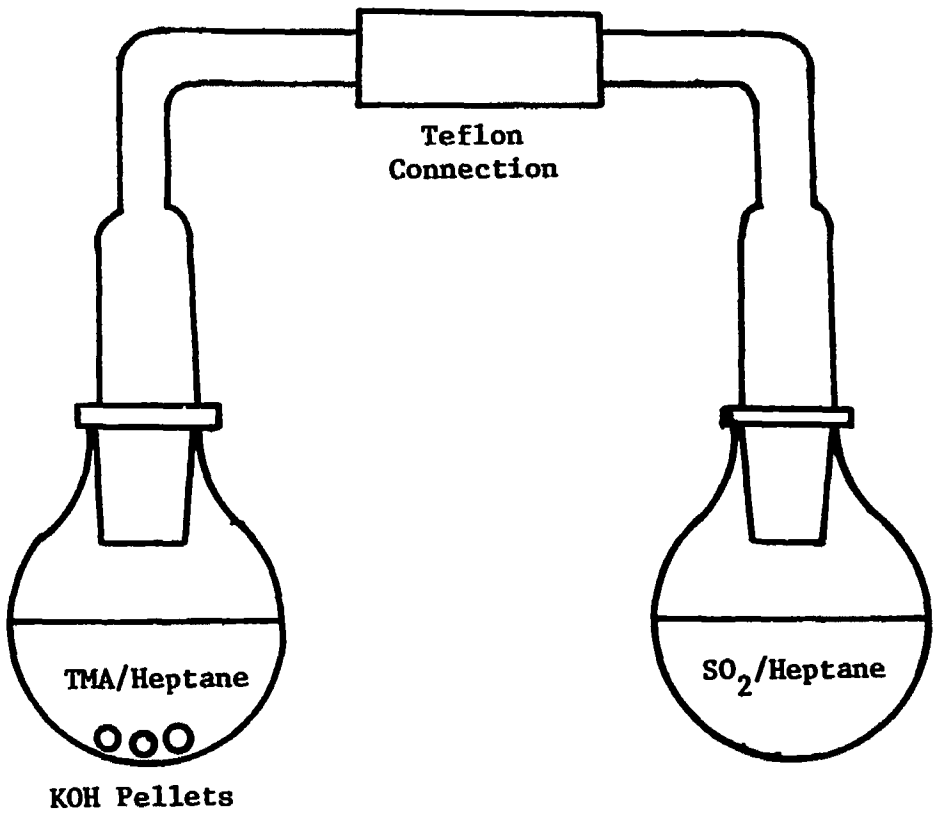

Figure 23. Apparatus Used to Obtain the Initial TMA·SO_2 Crystals.

However, with some patience a well-formed crystal was obtained. The capillary containing the crystal was secured to the goniometer with clay and x-ray examination begun.

It should be noted that a method for obtaining excellent crystals of TMA·SO_2 and other amine·SO_2 complexes was later discovered. In this method the initial product is simply transferred to the capillaries which are then sealed as above. The capillaries are then partially suspended in a cold bath (0^oC) in such a way that the portion of the capillary containing the crystal is at room temperature and the empty portion is at the lower temperature. In this way, resublimed crystals of excellent quality can easily be obtained.

The X-RD5 G.E. diffractometer was used for the space group determination and collection of the integrated intensity data. Cu-Kα radiation was used in both cases. The space group was determined by plotting the reflections found in the okℓ, hoℓ and hko planes. The plots revealed systematic extinctions for the hoℓ plane when ℓ was odd and for oko when k was odd. The only space group consistent with these extinctions was $P2_1/c$. It was determined unambiguously.

The cell dimensions were refined by the method of least squares using forty-one general reflections. The density determined by the flotation method was consistent with the assumption of four complexes in the unit cell. The preliminary crystal data are shown in Table 37. The agreement of the observed and calculated densities was probably fortuitous since experimental difficulties made the error in D_{obs} large.

A crystal of dimensions (0.26 x 0.31 x 0.35 mm) and mosaic of 0.5^o was selected as the data crystal. The theta-two theta scan

TABLE 37

CRYSTAL DATA FOR TMA·SO_2

Space Group $P2_{1/c}$

No. of Molecules 4

Cell Dimensions:

a = 5.906(0.006)

b = 10.912(0.006)

c = 10.557(0.015)

β = 108.83(0.11)

Density (Determined in heptane/CCl_4 mixture)

obs. = 1.29 g/cc

calc. = 1.27 g/cc

Vol. = 643.9

F(000) = 264

Reciprocal Cell Dimensions

a^* = 0.1789(0.0002)

b^* = 0.09164(0.00005)

c^* = 0.1001(0.0001)

β^* = 71.17(0.11)

vol^* = 0.001553

technique with a take-off angle of 3° was used in the data collection process. Of the 1209 reflections with two theta less than 140°, 900 had intensities distinguishable from background radiation.

Absorption corrections given by the expression

$$I = I_{o}\int e^{-\mu t}d\nu \quad (\mu = 34.20cm^{-1})$$

were applied to the observed intensity data. The evaluation of the integral was accomplished by use of the computer program written by Dr. Philip Shapiro which involves a three-dimensional numerical integration using the method of Gauss.[95]

Lorentz and polarization corrections were made on the intensities by multiplying them by the factor

$$L.P. = \frac{2 \sin 2\theta}{1 + \cos^{2}2\theta} .$$

Determination and Refinement of Structure

A sharpened Patterson synthesis was calculated for one-fourth of the unit cell. The map was sharpened by multiplying $|F|^{2}$ by the function[96]

$$M(s) = \left(\frac{\Sigma Z_{i}}{\Sigma f_{i}}\right)^{2} \quad \text{where}$$

ΣZ_{i} = sum of atomic numbers

Σf_{i} = sum of the scattering factors at $\sin\theta/\lambda$ of the amplitude which is modified.

Sections were calculated along the c-axis having points fixed approximately 0.2Å apart. The space group $P2_{1}/c$ has the equivalent positions

X, Y, Z

-X, -Y, -Z

-X, ½ + Y, ½ - Z

X, ½ - Y, ½ + Z.

The Patterson map had the symmetry of P2/m and the positions for any vector (U, V, W) are

U V W

-U -V -W

-U V -W

U -V W.

The equivalent positions of $P2_1/c$ were used to generate the vectors between symmetry related atoms. The coordinates of these vectors correspond to the Harker line, Harker plane and general position in the Patterson map.[118] These equations were given by

U	V	W	Type	
0	½-2Y	½	Harker Line	(1)
-2X	½	½-2Z	Harker Plane	(2)
2X	2Y	2Z	General Position	(3)

The Patterson was then inspected along the Harker line and in the Harker plane for large peaks which could correspond to vectors between sulfur atoms. Such peaks were located at

U	V	W	Relative Height	
0	0	½	1024	(4)
5.4/24	½	15.8/50	516	(5)
18.8/24	½	9.4/50	451	(6)

The relative peak height is given by the relation ($Z_1 \times Z_2$) where Z_1 and Z_2 are the atomic numbers of the atoms considered. The relative peak heights are qualitative since sharpening and thermal motion of the atoms alter their values from ideal. The deviation of the observed heights for the Harker plane peaks (5 and 6) is a result of two heavy-heavy atom vectors being coincident. That is, the vectors between one pair of screw-related atoms fall on top of those of the other pair and a doubling of the relative peak height occurs. The same rationale is also true for the Harker line peak (4), obtained from glide-related atoms. This doubling of relative heights is always observed in the space group $P2_1/c$. However, this accounts for approximately only half of the observed height of the Harker line peak. The reason for the anomalously large height of this peak became apparent when the Y-coordinate of the heavy atom was obtained. In the usual manner, vector (4) was assigned to the Harker line (1) and the value of $Y = \frac{1}{4}$ was obtained for the sulfur heavy atom coordinate. This value indicated that the sulfur atom lay in the glide plane in real space and thus the mirror plane in vector space. Furthermore, this value results in all four of the heavy-heavy atom vectors becoming coincident. In this event the relative height of this peak is predicted to be approximately $4 \times Z_s^2$ as observed. Another consequence of this psuedo special position of the sulfur atom was that the general position (3) lay in the Harker plane. This resulted in the two observed Harker plane peaks (5,6) instead of the usual one. There was no way to know which of these peaks corresponded to the general position and which to the Harker plane peak. The assignments were made by trial and error. First, vector (5) was assigned to

the Harker plane peak (2) and the sulfur atom position which resulted was

$$-2.7/24,\ \tfrac{1}{4},\ 4.6/50. \qquad (7)$$

Then, vector (6) was assigned to the general position and the sulfur position which resulted was

$$2.7/24,\ \tfrac{1}{4},\ 7.9/50. \qquad (8)$$

Similar assignments using vector (6) resulted in positions which differ from those above only by shifts of $\frac{1}{2}$ or $-\frac{1}{2}$ in X and consequently are not different solutions. Thus, the Patterson map in this case had a two-fold ambiguity and yielded two different sets of equivalent positions for the sulfur atom (Table 38) only one of which can be correct.

To eliminate this ambiguity, it was necessary to solve the Patterson using first one solution then the other. Since the position of the sulfur atom was assumed to be unique, it was expected that one of the solutions would lead to a sensible structure while the other would not.

The following general procedure was used in solving the Patterson. First, one set of the equivalent sulfur atom positions (Solution 1 or 2) was selected and then some vector (U, V, W) located in the map. This vector was assumed to be that between some light atom and the sulfur atom. Due to the symmetry of the Patterson, this vector could represent one of the four equivalent vectors of P2/m. The heavy atom position (X, Y, Z) was then added to each of these vectors to give four possible positions for the light atom. These positions in

TABLE 38

HEAVY ATOM SOLUTIONS FOR THE TMA·SO_2 STRUCTURE

SOLUTION 1:

Assignment: (5.4/24 1/2 15.8/50) to
(-2X 1/2 1/2-2Z)

Equivalent Positions for the Four Sulfur Atoms in the Unit Cell:

X	Y	Z
-2.7/24	1/4	4.6/50
2.7	3/4	-4.6
2.7	3/4	20.4
-2.7	1/4	29.6

SOLUTION 2:

Assignment: (5.4/24 1/2 15.8/50) to
(2X 1/2 2Z)

Equivalent Positions of the Sulfur Atom in the Unit Cell:

X	Y	Z
2.7/24	1/4	7.9/50
-2.7	3/4	-7.9
-2.7	3/4	17.1
2.7	1/4	32.9

general notation were

$$\begin{array}{ccc} U + X & V + Y & W + Z \\ -U + \bar{X} & -V + Y & -W + Z \\ -U + Z & V + Y & -W + Z \\ U + X & -V + Y & W + Z. \end{array}$$

If one of these positions was indeed correct, then the map had to contain three other vectors which were formed between that light atom position and the other three heavy atom positions in real space. Thus, it was necessary to form four vectors for each of the four possible light atom positions and then check these vector positions for existence in the map. The four vectors for each possible light atom position were

(a)	U	V	W	(9)
(b)	U + 2X	V + 2Y	W + 2Z	
(c)	U + 2X	V - ½	W + 2Z - ½	
(d)	U	V + 2Y - ½	W - ½	
(a)	-U	-V	-W	(10)
(b)	-U + 2X	-V + 2Y	-W + 2Z	
(c)	-U + 2X	-V - ½	-W + 2Z - ½	
(d)	-U	-V + 2Y - ½	-W - ½	
(a)	-U	V	-W	(11)
(b)	-U + 2X	V + Y + 1	-W + 2Z	
(c)	-U + 2X	V - ½	-W + 2Z - ½	
(d)	-U	V + 2Y - ½	-W - ½	

(a)	U	-V	W	(12)
(b)	U + 2X	-V + 2Y	W + 2Z	
(c)	U + 2X	-U - ½	W + 2Z - ½	
(d)	U	-V + 2Y - ½	W - ½	

Since the Y-coordinate of the sulfur atom was ¼, the light atom positions 9 and 12 generated the same set of vectors, likewise 10 and 11 generated the same set. This was easily seen by substituting Y = ¼ into the various vector equations and using the symmetry of P2/m. This implied that each vector (U, V, W) in the Patterson would result in two positions for the light atom. In the course of solving for light atom positions, it quickly became apparent that these two possible positions were in fact related by a simple mirror operation through a false mirror plane located at Y = ¼ in real space. Two models of the molecule were being obtained, one of which was the mirror image of the other. Inspection of the three-dimensional model revealed that these two molecules are in the same relative relation to the symmetry elements of the space group. This implied that the two solutions were the same and differed only in the choice of origin. The proof that such was the case involved calculations of structure factors for both models. The structure factor expressions in simplified form were obtained from the International Tables[97] and were given as

$$K + L = 2n$$

$$A = 4 \cos 2\pi (hx + \ell z) \cos 2 \pi kY; \quad B = 0$$

$$K + L = 2n + 1$$

$$A = -4 \sin 2\pi(hx + \ell z) \sin 2 \pi kY; \quad B = 0$$

If it were assumed that the coordinates for an atom in one image were (X, Y, Z), then the coordinates of its mirror image were (X, ½-Y, Z). Substituting the mirror image coordinates into the structure factor expression and denoting the resulting expression as A', the relation between A and A' for both K + L = 2n and K + L = 2n + 1 was shown to be $A' = (-1)^K A$. The structure factors for the two mirror images differed only by a change of sign for all reflections with odd K, but there were no changes in their absolute values. This was exactly as expected for a simple origin shift. Therefore, the only precaution necessary was to be consistent in building on either one image or the other but not both simultaneously. The particular choice was arbitrary.

The equivalent positions of the sulfur atom were initially chosen as those listed as solution 1 (Table 38). The procedure outlined above was then used to obtain various light atom positions which were plotted on a three-dimensional coordinate system. These atomic positions quickly led to impossibly short bond lengths of the intramolecular and intermolecular types. In addition, no recognizable skeleton for the model ever developed and these were numerous light atom vectors in the Patterson which would not check any light atom position. This was expected to be the case for the false solution.

When the equivalent positions of the sulfur atom were chosen as those listed in solution 2 (Table 38), a reasonable trial structure was rapidly obtained.

Refinement of the Structure

The trial structure was refined by the block diagonal least-squares method.[98] In these computations, the structure factors corre-

sponding to the trial structure are calculated, the positions, thermal parameters and overall scale are refined, and the standard deviations are estimated. The quantity which is minimized is given by

$$R = \Sigma w(k|F_o| - |F_c|)^2$$

where k is the overall scale and w is the weight assigned to each reflection. The value of w is determined by the conditions

$$\sqrt{w} = |kF_o|/P_1 \quad \text{if} \quad |kF_o| \leq P_1, \text{ or}$$

$$\sqrt{w} = P_1/|kF_o| \quad \text{if} \quad |kF_o| > P_1$$

where P_1 = 13 electrons. This weighting scheme is based on the nature of the counting statistics of the instrument. Since very weak or very strong intensities are determined with less accuracy than those of intermediate size, the extreme intensities are given smaller weights. Ideally P_1 corresponds to the most accurately determined intensity.

The intensity of an unobserved reflection was assigned a value which was a fixed fraction of the background radiation for that reflection. The fraction was obtained by dividing one-half the minimum observable intensity (5 counts) by the average background (75 counts). In the refinement, such reflections were included in the least squares portion if $|F_c| > 2|F_c|$. Observed reflections were omitted from the refinement according to the criteria described by Nicholas and van der Helm.[99] In this scheme, a reflection is rejected on the basis of its relation to $|F_{min}|$, the amplitude of the minimum observable intensity. The probability for rejection becomes smaller as $|F_o|$ becomes larger.

Initial refinements using isotropic temperature factors and atomic scattering factor curves from the International Tables[97] resulted in an R-index $\left(\frac{\Sigma||k\,F_o| - |F_c||}{\Sigma|kF_o|}\right)$ of 0.23. Particularly noticeable at this point in the refinement were the large isotropic temperature factors of the two oxygens (8.3,9.7) of the SO_2 component. A difference Fourier[100] in which only the fragment $((CH_3)_3N{\cdot}S)$ was included did not result in new positions for the oxygen atoms. However, the diffuse nature of the peaks which were assigned to these atoms indicated the possibility of large anisotropic thermal motion. Subsequent refinements employing anisotropic temperature factors decreased the R-value to 0.15. At this point a difference Fourier was used to locate the hydrogen atoms. The distances and angles of these atoms with respect to the carbon atom to which they were attached indicated their positions were reasonable. The hydrogen atom positions were included in subsequent structure factor calculations but were not refined. Final refinements with all atoms (except hydrogens) refined anisotropically resulted in an R-value of 0.127. The refinement was terminated when the shifts in the parameters were less than or equal to one-third of the standard deviations.

The coordinates of the atoms and anisotropic temperature factors with the corresponding standard deviations are given in Tables 39 and 40. Table 41 gives the final observed and calculated structure factors.

A final difference Fourier was calculated to check the validity of the model and to gain some insight to the residual error. The fourier contained one particularly noticeable peak (1.1 $e/\text{Å}^3$) located at (0.141, 0.210, 0.064) which corresponds to a position in the complex which is approximately on the center of the line connecting the two oxygen atoms.

TABLE 39

FRACTIONAL ATOMIC PARAMETERS FOR TMA·SO_2*

Atom	X	Y	Z
S	0.1060(3)	0.2478(2)	0.1560(2)
O_1	0.2522(8)	0.3311(4)	0.1174(5)
O_2	-0.0623(8)	0.1878(5)	0.0561(6)
N	0.3406(6)	0.1072(3)	0.2374(3)
C_1	0.2112(10)	0.0135(5)	0.2837(6)
C_2	0.5455(10)	0.1556(6)	0.3440(6)
C_3	0.4253(10)	0.0567(6)	0.1298(5)
$H_1(C_1)$	0.079	-0.030	0.217
$H_2(C_1)$	0.139	0.070	0.340
$H_3(C_1)$	0.313	-0.050	0.340
$H_4(C_2)$	0.642	0.215	0.313
$H_5(C_2)$	0.675	0.075	0.390
$H_6(C_2)$	0.504	0.180	0.433
$H_7(C_3)$	0.542	0.126	0.102
$H_8(C_3)$	0.272	0.033	0.050
$H_9(C_3)$	0.528	-0.035	0.161

*Standard deviations are given in parentheses.

TABLE 40

THERMAL PARAMETERS FOR TMA·SO_2

Anisotropic Temperature Factors x10^4

$\exp-(h^2b_{11} + k^2b_{22} + {}^2b_{33} + k\,b_{23} + h\,b_{13} + hkb_{12})$

Atom	b_{11}	b_{22}	b_{33}	b_{23}	b_{13}	b_{12}
S	461(5)	110(1)	259(3)	105(4)	177(6)	137(7)
O_1	731(23)	111(4)	304(9)	160(10)	213(22)	-46(18)
O_2	646(23)	189(6)	318(10)	90(13)	-377(24)	-56(20)
N	270(13)	75(3)	87(5)	-6(7)	98(12)	-39(12)
C_1	533(26)	102(6)	214(10)	103(12)	270(27)	-55(21)
C_2	488(27)	161(8)	169(9)	-38(14)	33(24)	-132(26)
C_3	578(27)	156(7)	113(8)	-14(12)	221(24)	93(25)

	B^*_{iso}
H (C_1)	7.16
H (C_1)	7.16
H (C_1)	7.16
H (C_2)	8.48
H (C_2)	8.48
H (C_2)	8.48
H (C_3)	7.79
H (C_3)	7.79
H (C_3)	7.79

*B_{iso} for the hydrogen atoms was obtained by adding 2.0 to the B_{iso} value of the atom to which the hydrogen was attached.

TABLE 41

LIST OF OBSERVED AND CALCULATED STRUCTURE FACTORS FOR TMA·SO_2

USING FINAL PARAMETERS FOR ALL ATOMS



TABLE 42

PEAK HEIGHTS OF HYDROGEN ATOMS IN DIFFERENCE FOURIER*

Atom	$e/\AA^3$
$H_1(C_1)$	0.59
$H_2(C_1)$	0.46
$H_3(C_1)$	0.38
$H_4(C_2)$	0.43
$H_5(C_2)$	0.27
$H_6(C_2)$	0.39
$H_7(C_3)$	0.42
$H_8(C_3)$	0.32
$H_9(C_3)$	0.32

*Peak heights refer to values fround in the difference Fourier at R = 0.15 and prior to inclusion of hydrogen atoms in refinement.

In addition, there were numerous smaller positive and negative peaks ($<0.4e/\AA^3$) which were concentrated in the vicinity of the SO_2 component. It seems quite possible that these peaks result from the large thermal motion of this fragment at the experimental temperature. Evidently, the conventional expressions for anisotropic thermal motion are inadequate to describe the large thermal motions in this structure.[101]

As indicated in Table 43, the intermolecular distances in this structure are reasonable. This may be taken as further indication of the validity of the structure. The distances are compatible with the van der Waals interactions they represent. It is interesting to note that one of the oxygens is involved in seven contacts less than 4.0 Å while the other is involved in only three. There is no hydrogen bonding in this structure. The packing of the molecules within the unit cell is shown in Figure 24.

TABLE 43

VAN DER WAAL'S CONTACTS LESS THAN 4.0Å

Atom X	Atom Y	Distance
S	C_1(-X,½+Y,½-Z)	3.619
S	C_2(x-1,½-Y,Z-½)	3.985
O_1	N(1-x,½+y,½-Z)	3.851
O_1	C_1(-X,½+Y,½-Z)	3.793
O_1	C_1(1-x,½_y,½-Z)	3.600
O_1	C_1(X,½-Y,Z-½)	3.846
O_1	C_2(1-X,½+y,½-Z)	3.717
O_1	C_2(X,½-Y,Z-½)	3.818
O_1	C_3(1-X,½+y,½-Z)	3.679
O_2	C_2(X-1,Y,Z)	3.889
O_2	C_2(X-1,½-Y,Z-½)	3.155
O_2	C_3(-X,-Y,-Z)	3.585
C_3	C_3(1-X,-Y,-Z)	3.374

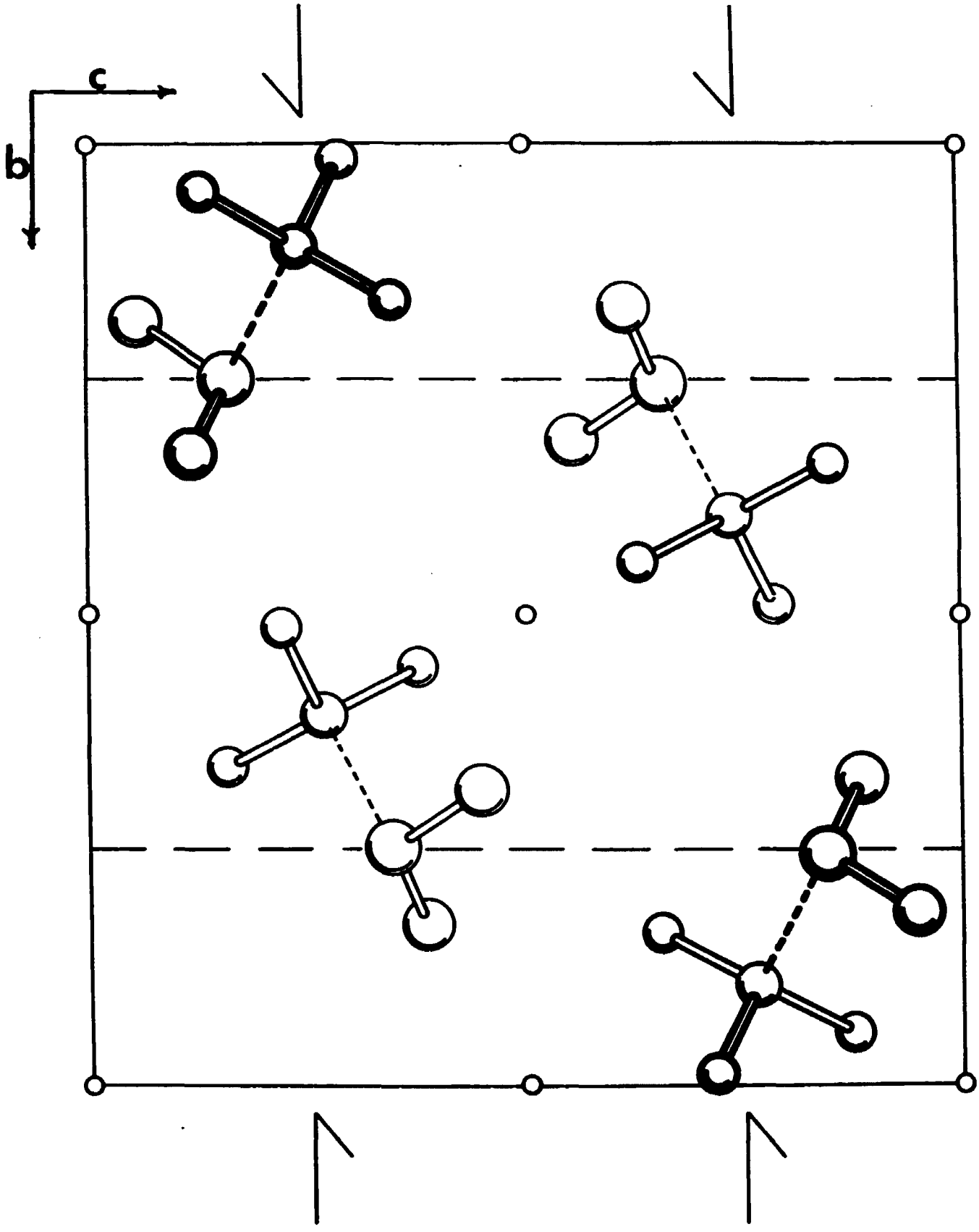

Figure 24. Packing of the TMA·SO_2 Complex in the Unit Cell. Projection onto the "bc" plane.

CHAPTER VIII

DISCUSSION OF THE STRUCTURE

Interesting features of the structure are the charge-transfer (N-S) bond length (2.06 Å, Figure 25), the angle (22.4°) between the normal to the SO_2 plane and the N-S bond, and the approximate C_m symmetry of the complex (Figure 26). The N-S bond length is intermediate between the normal van der Waals' contact and the predicted N-S single bond distance as expected for complexes of the charge-transfer type, e.g., $TMA \cdot I_2$ (Table 44). The angle between the N-S bond and the normal to the SO_2 plane verifies the assumptions of Christian and Grundnes[49] and Moede and Curran[67] of a non-zero value for this angle. In later discussions it is convenient to discuss the angle between the N-S bond and the bisector of the O-S-O angle. Under exact C_m symmetry this angle is simply 90° plus the angle between the N-S bond and the normal to the SO_2 plane. In the present structure, this angle is 112.2°. As implied, the complex has approximate C_m symmetry (Figure 27); however, due to the uncertainties in this structure, significance of the deviations from this symmetry is not known. Figure 26 also indicates that the three-fold axis of the amine may be taken as directed at the sulfur of the SO_2 within the limits of this determination. Coordination through the sulfur is consistent with the results found for the metal complexes involving SO_2 as a ligand[94] and with the assumption that the highest unfilled orbital

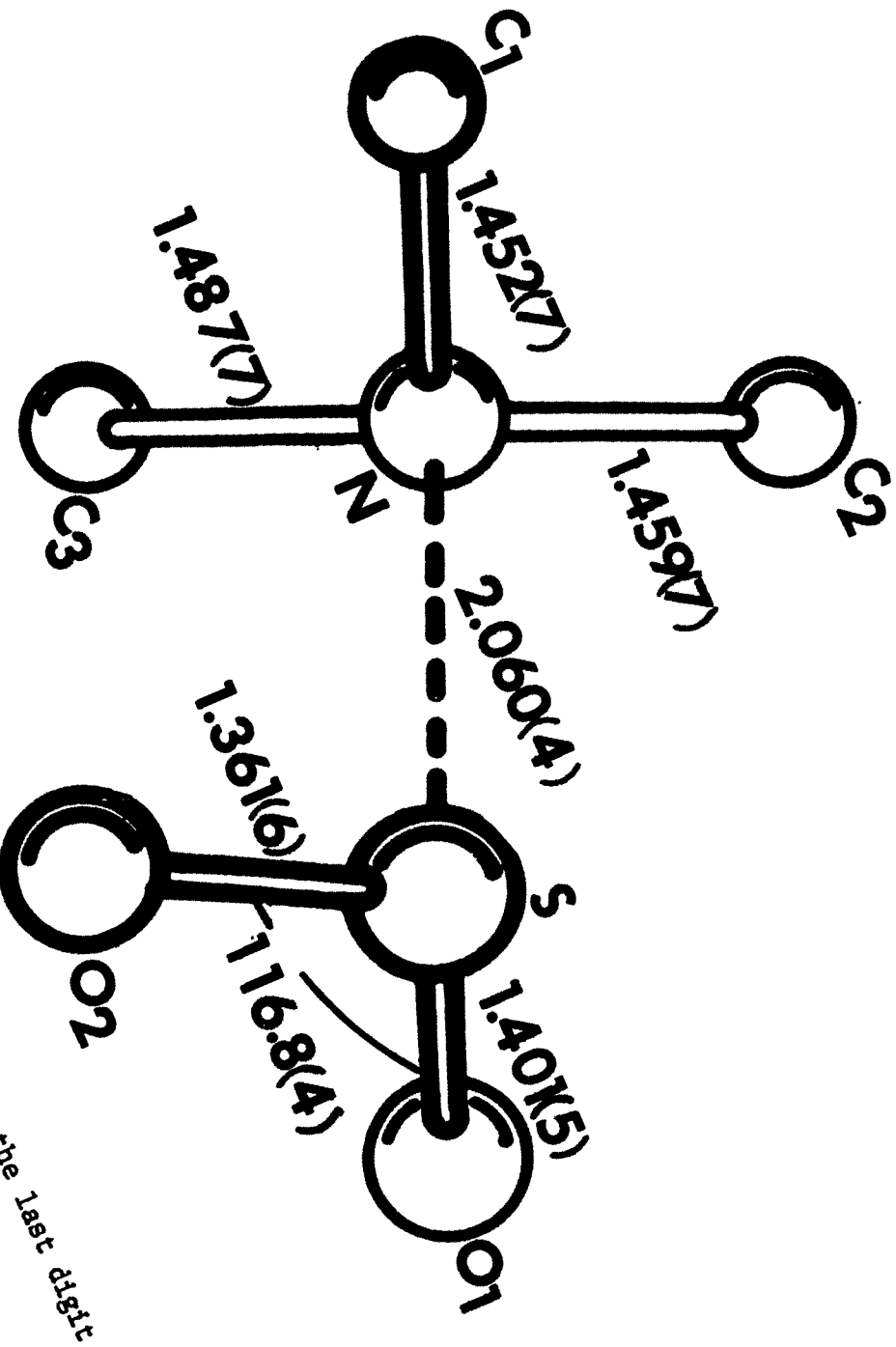

Figure 25. Bond Distances. Standard deviations for the last digit are given in parenthesis.

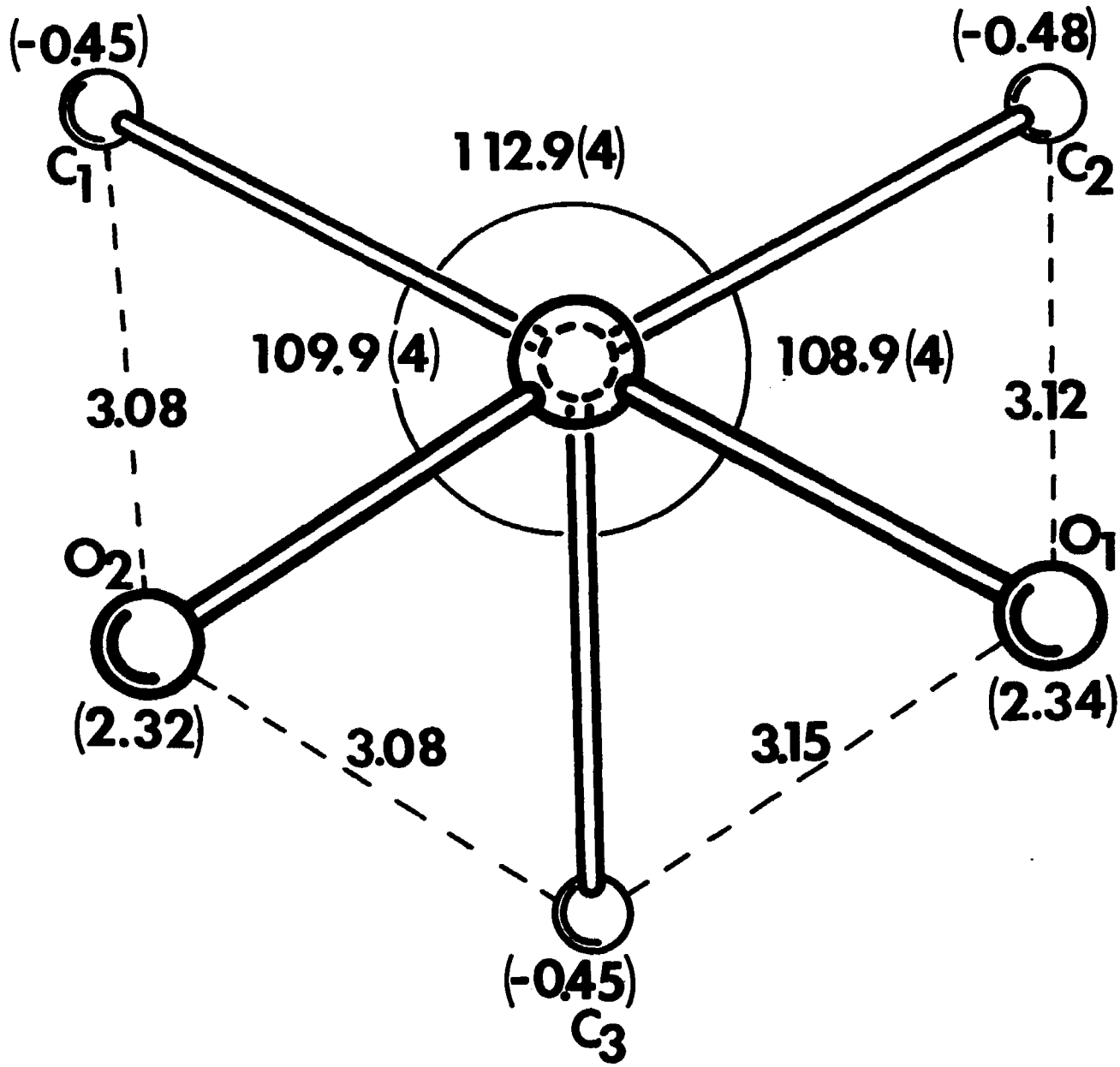

Figure 26. Projection of the Structure down the N-S Bond. The distances in parentheses indicate heights above and below the plane in Å. The heights of N and S are 0 and 2.060 Å, respectively.

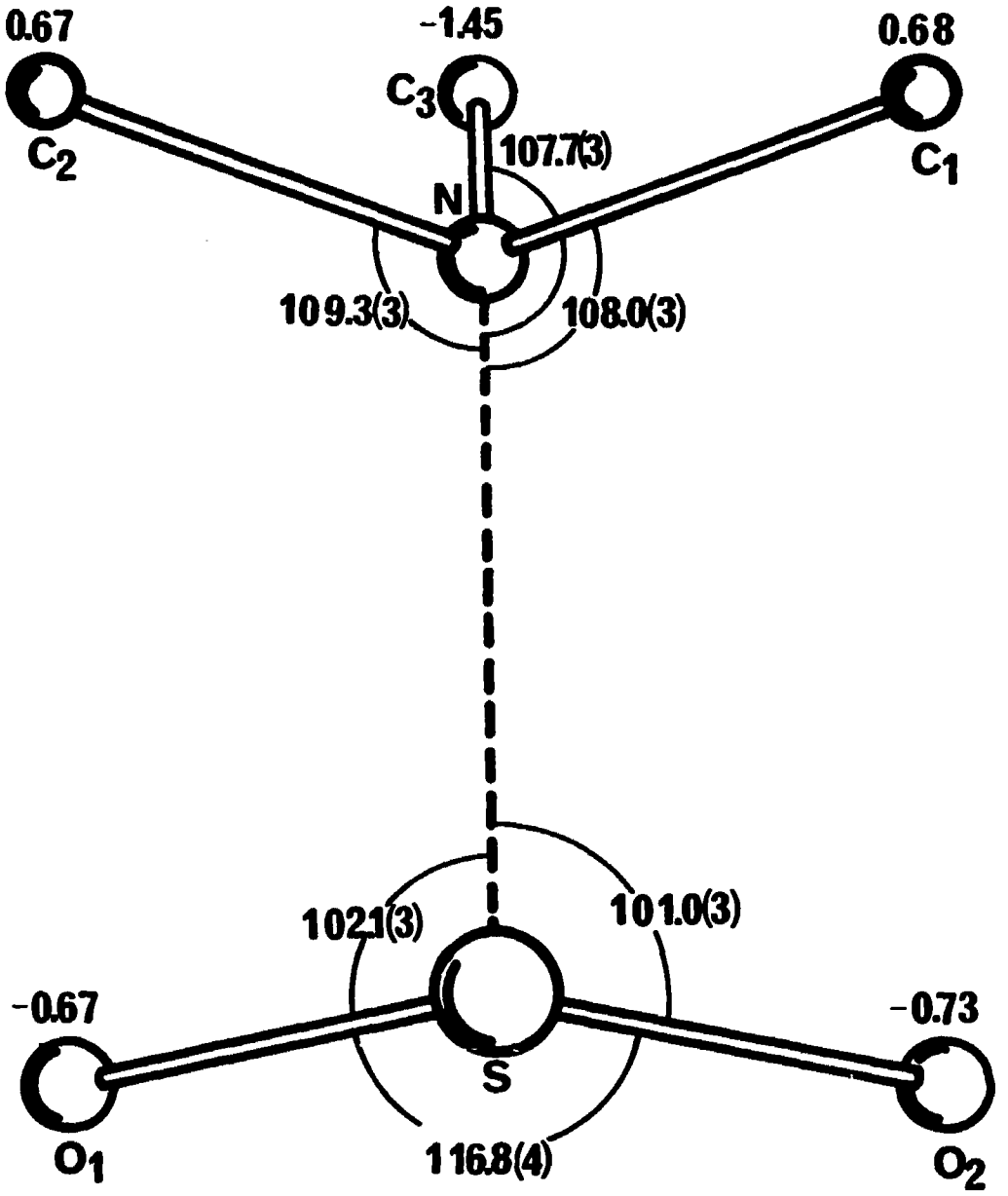

Figure 27. Bond Angles. A projection of the structure along the N·S bond. The N and S are both in the plane of the figure and the heights of the other atoms above and below the plane are listed.

TABLE 44

CHARGE TRANSFER BOND DISTANCES

	(N·S) Distance (Å)
$(CH_3)_3N \cdot SO_2$	2.060
Single Bond (Sulfamic Acid)[104]	1.73
Sum of van der Waals Radii	3.25
	(N·I) Distance (Å)
$(CH_3)_3N \cdot I_2$[78]	2.27
Sum of Covalent Radii	2.03
Sum of van der Waals Radii	3.65

on SO_2 involves pd hybridization on sulfur.[102] In this connection, Figure 27 shows the angles observed in this structure. The nitrogen of the TMA is very nearly in the expected tetrahedral environment with bond distances and angles not much different from those of "free" TMA (d(C-N) = 1.455(2) Å, and (C-N-C) = 111.8(6)).[103] This is consistent with the view that the donation of the electron comes from the non-bonding lone pair of the amine. The sulfur atom might also be viewed as being at the center of a highly distorted tetrahedron with the two oxygen atoms and the nitrogen atom forming the corners of the tetrahedron, while the fourth position is unoccupied. However, the distortion from tetrahedral is significant and this lends support to a hybridization scheme other than sp^3 on sulfur. In the metal-SO_2 complexes, it has been proposed that the observed structure can be rationalized by invoking an approximate sp^3 hybridized vacant orbital on sulfur.[94] In the Ir-SO_2 complex, the angle between the (metal-S) bond and the normal to the SO_2 plane is 33° which is close to the angle expected in the case of tetrahedral bonding.[93] However, in view of the present structure and the results of Dunitz,[102] it seems likely that the hybridization scheme on sulfur is significantly different from sp^3. The importance of including d-orbital character in the higher orbitals of SO_2 has been emphasized in the molecular orbital treatments of this molecule.[105]

The most disturbing features of this structure are the high final R-value and the large anisotropic thermal motion of the atoms. These two results are undoubtedly correlated. The normal scattering factor curves are calculated on the basis of the electron distribution in a stationary atom multiplied by the transform of a smearing function

which accounts for the spread of the electron cloud over a larger volume due to the thermal motion of the atoms.[101] The derivation of the conventional expressions for an atom vibrating in an anisotropic harmonic potential field involves the approximation that the force on an atom is proportional to its relative displacement and independent of the motions of its neighboring atoms. The assumption of independent motion is an oversimplification since the motions of atoms connected by covalent bonds are undoubtedly correlated and neglect of this correlation is valid only in the approximation of very small displacements.[106] In the present structure the thermal displacements are quite large and the independent motion assumption is likely a gross oversimplification. It is suggested that this is the main cause of the high final R-value. For these reasons, the validity of the bond lengths reported for this structure are open to some question.

There are basically two approaches which may be taken to obtain better estimates of the geometry of this complex; (1) the data can be retaken at a lower experimental temperature where it is anticipated that thermal motion is minimized or (2) a detailed analysis of the thermal motions in the structure can be undertaken in order to obtain corrections to the observed geometry. With regard to the first point, attempts to collect data on the TMA·SO_2 complex at lower temperatures were unsuccessful. The inability to maintain the low experimental temperature for the extended periods necessary for data collection and the annoying tendency of the crystals to fracture and resublime when exposed to the repeated thermal shocks accounted for this failure. Concerning the alternate possibility, Busing and Levy[106] have discussed the effects of thermal

motion on bond lengths, emphasizing that the joint distribution of the motions of the atoms must be known if proper corrections are to be made. Rigid body motion is a case where the joint distribution is well defined. However, the components of the TMA·SO_2 complex are connected by a bond which is something less than a normal covalent bond and it seems likely that its motion cannot be described completely in rigid body motion terms. Indeed, the orientation of the individual ellipsoids do not suggest any straightforward center for such motion.

Although the rigid body analysis of the complex is not attempted here, the orientation of the individual ellipsoids with respect to various reference systems is considered in some detail. For these purposes, Table 45 gives the lengths of the principal axes of the ellipsoids and their direction cosines with respect to the unit cell axes. The large B values ($B = 8\pi^2 \bar{\mu}^2$ where $\bar{\mu}^2$ is the mean square amplitude of thermal displacement) give an indication of the large displacements due to thermal motion in this structure. Only for the nitrogen atom are the B values of reasonable magnitude. This may be attributed to the fact that the nitrogen atom is held more or less rigidly in place by its tetrahedral coordination. However, the other atoms are not particularly restricted in their motion either by intramolecular or intermolecular interactions.

Figures 28 and 29 show the orientations of the ellipsoids on the individual atoms. Figure 29 is an ORTEP[119] drawing of the complex showing the orientations of the ellipsoids for all the atoms of the complex. Figure 28 shows the orientation of the principle axes of the ellipsoids of the SO_2 component and Table 46 gives the angles between the axes of the ellipsoids and pertinent vectors. In Figure 28 the SO_2 component is depicted as lying in the plane of the paper and the TMA

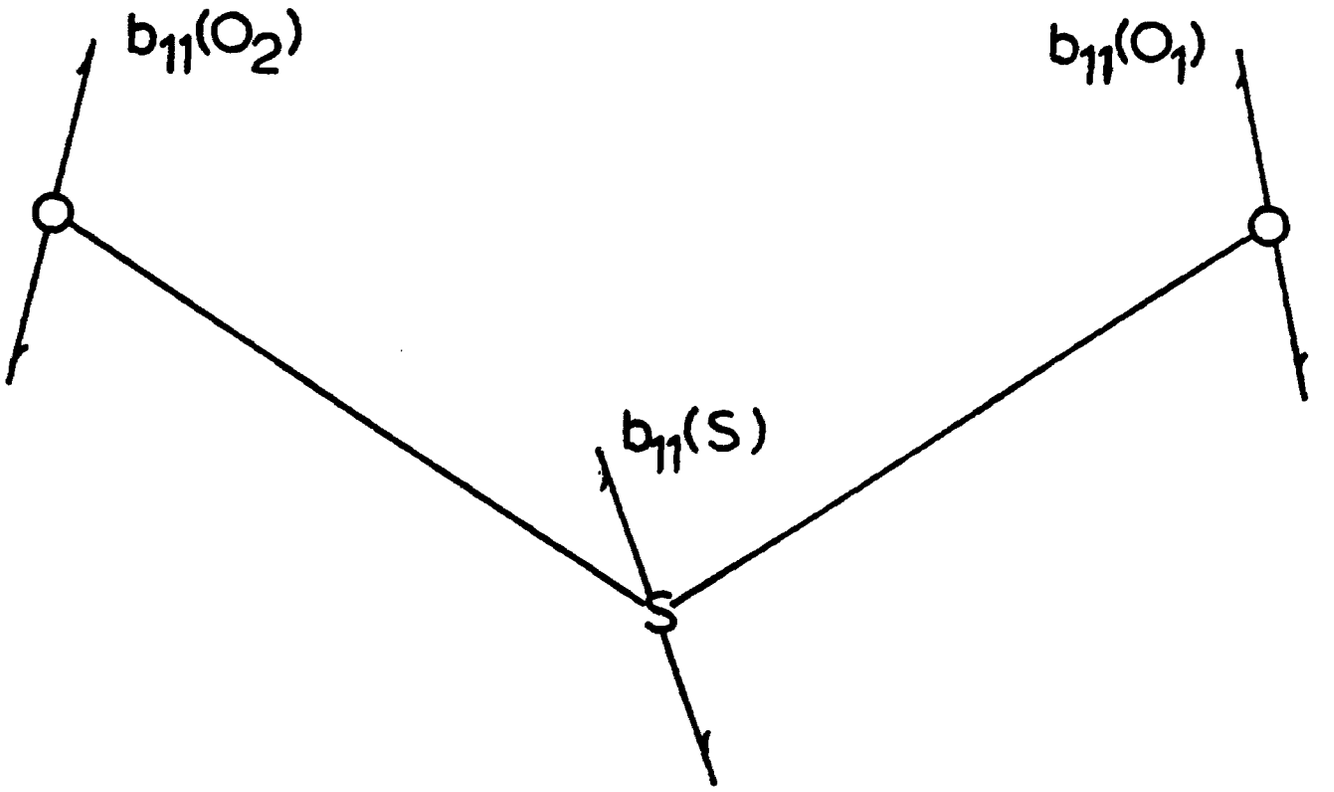

Figure 28. Orientation of the Major Axis of the Thermal Ellipsoids on the SO_2 Component.

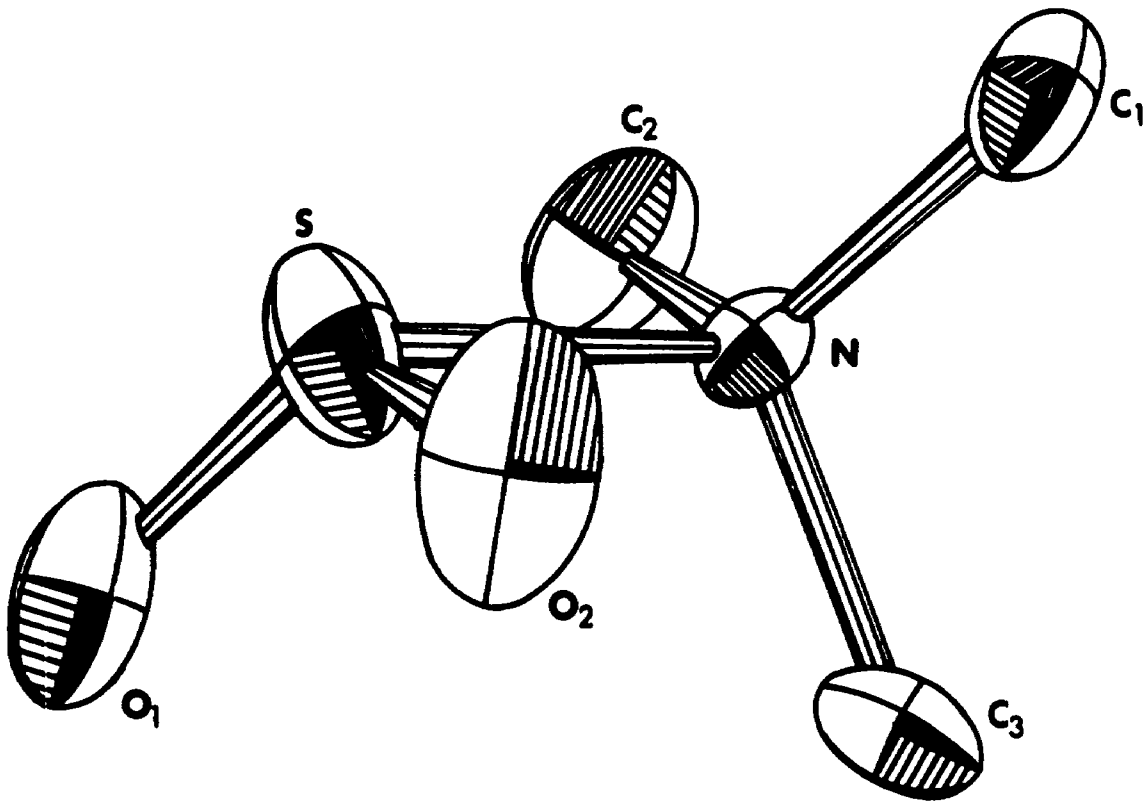

Figure 29. ORTEP Drawing of the TMA·SO_2 Complex Indicating the Orientations of the Various Ellipsoids

TABLE 45

PRINCIPAL AXES AND DIRECTION COSINES OF ANISOTROPIC ELLIPSOIDS

Atom	B	ℓ_1	ℓ_2	ℓ_3
S	11.4	-0.196	0.311	0.943
	6.82	0.848	0.529	-0.271
	3.55	-0.491	0.788	-0.190
O_1	14.6	-0.424	0.388	0.910
	9.05	0.888	0.004	0.148
	3.66	0.175	0.921	-0.385
O_2	22.4	-0.708	0.175	0.875
	8.67	0.198	0.979	-0.107
	4.28	0.676	-0.102	0.471
N	3.98	-0.600	0.777	0.018
	3.49	-0.285	0.007	0.999
	2.99	0.746	0.628	-0.034
C_1	9.69	-0.124	0.451	0.877
	6.88	0.898	-0.328	-0.012
	3.11	0.422	0.830	-0.481
C_2	10.2	-0.791	0.261	0.779
	8.16	-0.033	0.885	-0.429
	3.90	0.611	0.385	0.457
C_3	8.53	0.646	0.754	-0.102
	6.36	0.630	-0.612	0.249
	3.93	-0.429	0.238	0.963

TABLE 46

ANGLES BETWEEN PRINCIPAL AXES OF ANISOTROPIC ELLIPSOIDS AND VARIOUS VECTORS

Atom	Axis	Vector	Angle
S	b_{11}	Normal to the SO_2 Plane	113°
	b_{22}	"	86°
	b_{33}	"	23°
	b_{11}	$S-O_1$	100°
	b_{22}	"	14°
	b_{33}	"	98°
	b_{11}	$S-O_2$	130°
	b_{22}	"	137°
	b_{33}	"	105°
	b_{11}	N-S	88°
	b_{22}	"	86°
	b_{33}	"	176°
	b_{11}	Normal to the SO_2 Plane	100°
	b_{22}	"	127°
	b_{33}	"	39°
	b_{11}	$S-O_1$	111°
	b_{22}	"	37°
	b_{33}	"	59°
	b_{11}	O_1-O_2	80°
	b_{22}	"	40°
	b_{33}	"	52°

TABLE 46 - continued

Atom	Axis	Vector	Angle
O_2	b_{11}	Normal to the SO_2 Plane	98°
	b_{22}	"	57°
	b_{33}	"	124°
	b_{11}	$S-O_2$	110°
	b_{22}	"	145°
	b_{33}	"	58°
	b_{11}	O_1-O_2	102°
	b_{22}	"	41°
	b_{33}	"	52°
	b_{11}	N-S	93°
	b_{11}	C_1-C_2	115°
	b_{11}	C_1-C_3	125°
	b_{11}	N-S	113°
	b_{11}	C_1-C_2	105°
	b_{11}	C_2-C_3	129°
	b_{11}	N-S	100°
	b_{11}	C_1-C_3	56°
	b_{11}	C_2-C_3	116°

component (not shown) lies below the plane. The major axis of the ellipsoids lie in and out of the plane some 10 to 20°. The amplitudes of the major axis for the S and O_1 atoms are not greatly different while the amplitude for O_2 is considerably greater than that of S or O_1 (Table 45). The motion implied in this figure might be viewed as an oscillation of the SO_2 portion about some center located in the area of the center of the S-O_1 bond. This center would account for the similar amplitudes for S and O_1 while the amplitude for O_2, which would be located further from the center, would be anticipated to be larger. The intermolecular distances lend some support to this argument. It should be recalled that O_1 was involved in some seven van der Waals contacts less than 4 Å while O_2 was involved in only three. Thus, O_1 and S are restricted in their motions to a greater extent than O_2. This is consistent with oscillation about the proposed center. The figure also suggests a large translational motion for the SO_2 component in a direction more or less perpendicular to the N-S bond. In addition, it should also be noted the motion implied in Figure 28 corresponds closely to the normal bending vibrational mode of a bent triatomic molecule.[107] It seems possible that this internal vibration could make a contribution to the observed motion since the experimental temperature is not far removed from the melting point of the complex (76°). The observed motion likely consists of some combination of this internal vibration and the motions discussed above.

The motions of the TMA component of this complex consist mainly of a rotary oscillation about the three-fold axis of the amine. When this motion is coupled with that of the SO_2 component, the complex might be viewed as oscillating about the N-S charge transfer bond were it not

for the large thermal motion of the sulfur atom. If the sulfur atom were to lie on the axis of rotation, it would be expected to have a somewhat smaller thermal parameters than observed. The motions of the two components are undoubtedly correlated, since they are connected by the charge-transfer bond. However, the relatively weak nature of this bond probably relaxes the correlation of the two motions. In this connection, the major motions of the SO_2 appear in the plane of that component while there are only small motions in the direction of the N-S bond. This is consistent with the proposed δ-acceptor properties of the SO_2.

In summary, the high thermal motions encountered in this structure are reflected in the relatively large R-value and probably in the reported bond lengths. An extensive analysis of the dynamics of this system has not been attempted in view of the complex nature of the motions involved. Consequently, the corrections to the observed bond lengths due to thermal motions are not known. However, it is recognized that such corrections can be quite large.[108] In spite of this, it is felt the basic features of the structure are correct although the subtle changes in the geometry of the individual components which occur upon complexation cannot be determined with certainty.

The changes in the geometries of the "free" donor and acceptor that occur upon complexation are of particular interest. Indeed one of the goals of the present research was to determine such changes for the components of the TMA·SO_2 complex. Unfortunately, as the previous discussions indicate, these changes are probably obscured by the large thermal motions. However, the results of this determination may be

combined with those from the literature to gain some insight to these changes. Table 47 summarizes some of the literature results which relate to this question. The changes implied in the table are certainly not clear. In the Ir-SO_2 complex, one of the S-O bonds is shortened relative to the corresponding length in "free" SO_2 while the other is evidently lengthened.[93] The significance of the difference between the individual S-O lengths is somewhat doubtful on the basis of the standard deviations. The O-S-O angle decreases slightly from the value in free SO_2. The structure of the dithionite anion consists of two SO_2^{-1} units, joined by a very long S-S bond (2.39 Å) in an eclipsed configuration with the planes of the opposite SO_2^{-1} groups approximately 30° from parallel.[102] The changes in the SO_2 geometry are similar to those observed for the Ir-SO_2 complex except that both S-O bonds are lengthened over those in free SO_2. The structure of $S_2O_4^{-2}$ anion is of particular interest since it provides the only available information concerning the possible structure of SO_2^{-1}. The structure of SO_2^{-1} is interesting since the variations of its geometry from those of free SO_2 might be viewed as an upper limit on the variations in the geometry of SO_2 in its charge-transfer complexes. This is based on the fact that SO_2^{-1} contains one full electron while in its charge transfer complexes SO_2 has only a partial negative charge. The implication is that the addition of a full electron to neutral SO_2 results in a significant lengthening of the S-O bonds and a closing of the O-S-O angle relative to free SO_2. The O-S-O angle in the anion of 108° is approximately tetrahedral but the S-S-O angles (99°) deviate significantly. In the TMA·SO_2 complex the O-S-O angle is smaller than that in free SO_2 but larger than that listed for $S_2O_4^{-2}$. This would be

TABLE 47

SULFUR DIOXIDE GEOMETRIES

Compound	$S-O_1$ (Å)	$S-O_2$ (Å)	Angle (O-S-O)	Reference
SO_2 Solid (-130°C)	1.430(15)	1.430(15)	119.5(1.5)	109
$IrCl(CO)(SO_2)(P(C_6H_5)_3)_2$				
	1.411(23)	1.467(25)	117.8(0.6)	93
$Na_2S_2O_4$	1.496(20)	1.515(20)	108.2(0.6)	102
$TMA \cdot SO_2$	1.401(5)	1.361(6)	116.8(0.3)	

consistent with the transfer of only a partial negative charge to the SO_2 molecule in the complex. The S-O bond lengths are shorter than those in either the anion or free SO_2. However, the large thermal motions prohibit any definite conclusions to be drawn from this observation since these bonds may be considerably foreshortened.[110]

The significance of the difference in the individual S-O bond lengths in either the present structure or those in the table is open to question. The large standard deviations and/or high confidence levels of the determinations make the significance of these differences difficult to determine. On chemical grounds there is no obvious reason to expect these bonds to differ. If the observed difference is real, then it may result from thermal motion and/or packing effects similar to those discussed for the $TMA \cdot SO_2$ complex.

Theoretical Interpretation of the Structure

The orientation of the $TMA \cdot SO_2$ complex is consistent with the qualitative explanations given by Dunitz.[102] In an attempt to explain the structure of the $S_2O_4^{-2}$ anion, Dunitz noted that the lowest unoccupied molecular orbital of SO_2 was like an antibonding orbital involving dp hybridization on the sulfur atom. The combination of d and p orbitals to form this hybrid is shown in Figure 30. The orientation of this orbital would account for the non-zero angle between the N-S bond and the bisector of the O-S-O angle observed in the $TMA \cdot SO_2$ complex.

The descriptions of the lowest unfilled molecular orbital (LUMO) of sulfur dioxide can be placed on a more quantitative basis by considering the molecular orbital description given by Ionov and Porai-Koshits.[111]

They calculated an MO scheme for sulfur dioxide using an SCF LCAO MO method (simplified Roothaan).[120] The fourteen valence electrons which were considered (six from the sulfur and four from each oxygen) were situated in seven MO's. The MO's were constructed from the (3s,3p,3d) AO's of sulfur and the (2p) AO's of the oxygens. Slater-type AO's[121] were used in evaluating the coefficients of the various MO's. According to this calculation the LUMO of SO_2 is given by the expression

$$\psi_{SO_2} = 0.36(3d_{yz})^s - 0.54(3p_y)^s + 0.76\pi^0$$

where $3d_{yz}$ and $3p_y$ are the AO's on sulfur and π^0 refers to a linear combination of $2p_\pi$ type atomic orbitals of the oxygens. This orbital is in essential agreement with that proposed by Dunitz. A graphical illustration of this orbital is given in Figure 30.

Since the observed structure indicated that the bonding was essentially through the sulfur of the SO_2, the hybrid pd orbital localized on that atom is of particular interest. The relative p and d character of this hybrid and the angles θ_1 and θ_2 (Figure 30) can be determined from the coefficients of ψ_{SO_2}. The angle θ_2 is particularly interesting since it gives a theoretical approximation to the angle observed between the N-S bond and the bisector of the O-S-O angle in TMA·SO_2. This is based on the assumption that maximum overlap occurs when the amine approaches the SO_2 along L_2.

Substitution of the normalized spherical harmonic expressions for p_y and d_{yz} in the form

$$p_y = \left(\frac{3}{4\pi}\right)^{\frac{1}{2}} \sin\theta \sin\phi \qquad (13)$$

and

$$d_{yz} = (\frac{15}{4\pi})^{\frac{1}{2}} \sin\theta \cos\theta \sin\phi \qquad (14)$$

into the expression for ψ_{SO_2} gives the angular dependence of that function. In equations (13) and (14) the angles θ and ϕ are the usual spherical coordinates. Here the radial function is ignored since only the orientation of the orbital is of interest. When the angle ϕ is set equal to 90° (the function has its maximum in the yz plane), the resulting expression for ψ_{SO_2} is given by

$$\psi_{SO_2}(\cos\theta) = A \sin\theta \cos\theta - B \sin\theta$$

where

$$A = 0.36(\frac{15}{4\pi})^{\frac{1}{2}} \qquad \text{and } B = 0.54(\frac{3}{4\pi})^{\frac{1}{2}} .$$

The angles θ_1 and θ_2 are found by differentation of this function with respect to $\cos\theta$ and setting the derivative equal to zero. Actually, the derivative of $\psi_{SO_2}^2$ should be considered but ψ_{SO_2} and $\psi_{SO_2}^2$ have their extrema at the same values of θ and either of these functions may be used. This process results in values of 27° and 123° for θ_1 and θ_2, respectively. The value of θ_2 implies an angle of 33° between the normal to the SO_2 plane and the line L_2. This value can be compared with the value of 22° observed in the TMA·SO_2 complex. The agreement between these two angles implies that the description of ψ_{SO_2} given by Ionov and Porai-Koshits is at least compatible with the present structure. The difference between these two angles is probably due to the inaccuracies in ψ_{SO_2}, changes in the geometry of SO_2 on complexation, and errors in the observed structure.

These considerations imply that SO_2 functions virtually as a δ-type acceptor with the main interaction occurring in the present case between

the nonbonding amine lone pair and the portion of the unoccupied MO of SO_2 which is located mainly on the sulfur.

The bonding characteristics of the LUMO of SO_2 are important since they give a theoretical prediction of the changes which may be expected in the SO_2 geometry upon complexation. Dunitz[102] stated that this orbital was antibonding with respect to the S-O bonds and explained the increase in the S-O bond lengths in $S_2O_4^{-2}$ over those of neutral SO_2 on this basis. That this should be the case is certainly not clear in the expression given by Ionov and Porai-Koshits. Figure 30 indicates the p orbital of the sulfur and the p orbitals of the oxygens to be anti-bonding with respect to this bond but the overlap between the p orbital of the oxygens and the d orbital of the sulfur to be bonding. The coefficients of ψ_{SO_2} must be used to derive the relative contributions of each of these terms to the net overlap. Although the nature of this orbital was not discussed in detail by Ionov and Porai-Koshits,[111] it is possible to extend their calculations to show that the π-antibonding contribution (-0.16) is approximately twice as great as the π-bonding contribution (0.07) to the overlap in ψ_{SO_2}. The AO overlaps necessary in these calculations were obtained from the tables of Mulliken[112] and Loftus.[113] They were in essential agreement with those employed by Ionov and Porai-Koshits. This calculation shows ψ_{SO_2} to be slightly antibonding with respect to the S-O bonds. On this basis slight increases in the S-O bond distances are expected to occur on the transfer of an electron to this orbital. It should also be noted that this orbital is slightly O-O bonding (Figure 30) so that the O-S-O angle might be expected to decrease slightly on transfer. These results are

Figure 30

(A) The Formation of a dp Hybrid Orbital

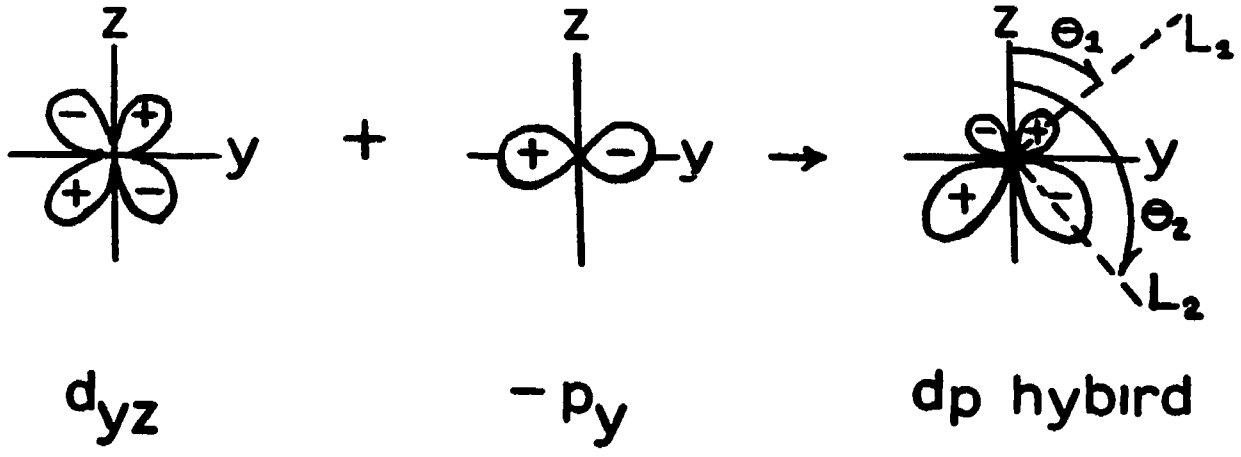

(B) The lowest unoccupied molecular orbital of SO_2 (z-axis) bisects the O-S-O angle; oxygen atoms are located in the XZ-plane).

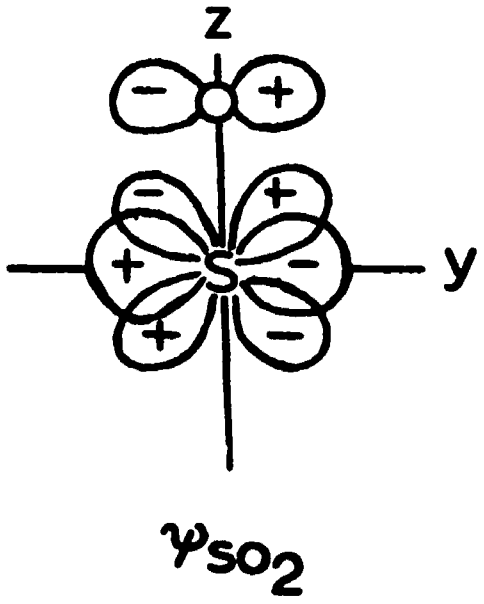

in agreement with the structure of $S_2O_4^{-2}$ and that of the Ir-SO_2 complex (assuming the S-O bond length to be given by the average value 1.439 Å). However, in the present structure, the angle decreases but the bonds appear to shorten. As pointed out previously, the effects of large thermal motion in this structure make the validity of the reported bond lengths questionable. Consequently, the changes in the geometry of SO_2 which occur when it is involved in charge-transfer complexes have not been unambiguously determined. This points out the need for additional studies of this type. In this connection, Dr. Enwall[114] of this laboratory has determined the structure of the complex N,N,N',N'-tetramethylethylenediamine·2SO_2. Preliminary results indicate the basic structure of this complex to be essentially similar to the TMA·SO_2 structure. Enwall reports (S-O) bond distances of 1.42 and 1.46 Å (average 1.44 Å), an O-S-O angle of 113° and an (N-S) bond distance of 2.1 Å. The orientation of the SO_2 with respect to the (N-S) bond is similar to that in TMA·SO_2. These results verify the decrease in the O-S-O angle observed for SO_2 in the complexed form. However, the present (S-O) bond lengths show behavior similar to those of the Ir-SO_2 complex. The average (S-O) bond length (1.44 Å) is slightly longer than that in free SO_2 but again this increase is probably within experimental error.

CHAPTER IX

IMPLICATIONS OF THE STRUCTURE

This chapter is devoted to an interpretation of the structure in terms of the energy parameters defined by Mulliken.[5] The crystal structure is combined with the spectral,[49] thermodynamic,[49] and dielectric properties[67] of this complex to obtain these parameters. This treatment is essentially similar to those Mulliken has employed in studying the iodine complexes. Appendix IV gives an outline of Mulliken's Resonance Theory and defines most of the terms considered here. However, this appendix is necessarily brief and the reader is referred to Mulliken and Person's book Molecular Complexes for a complete description of this theory.[5]

Extent of Charge Transfer

The contribution of the dative structure ($b^2 + abS_{01}$) to the ground state wave function ($\psi_N = a\psi_0 + b\psi_1$) is a measure of the extent of electron transfer from the donor to the acceptor in a complex (see Appendix IV). One common method of estimating this requires knowledge of both the structure and the experimental dipole moment of the complex. The experimental dipole moment is equated to the theoretical dipole moment of the ground state of the complex (Appendix IV).

$$\mu_{exp.} \simeq \mu_N = a^2\mu_0 + b^2\mu_1 + 2ab\mu_{01} \qquad (16)$$

where the terms in this equation represent vectors. The magnitudes of these vectors will be denoted by $|\mu_i|$. If the dipole moment of the ground state is zero ($|\mu_0| = 0$), then this equation can be simplified to give

$$\frac{\mu_N}{\mu_1} = (b^2 + abS_{01}) \ . \qquad (17)$$

The term μ_1 (dipole moment of the dative structure) is estimated by $\mu_1 = e\vec{R}$ (more exactly $\mu_1 = \mu_0 + e\vec{R}$). From the equilibrium geometry of the complex and the charge distributions of the donor and acceptor in the dative structure, μ_1 can be estimated.[5] If the directions of μ_0, μ_1 and μ_N are collinear, e.g., benzene·halogen and amine·halogen, then equation (2) may be used directly to estimate $(b^2 + abS_{01})$ by simply substituting for the vectors their magnitudes. For these complexes μ_0 is assumed to be zero. The term $(b^2 + abS_{01})$ is estimated as 0.1 for benzene·halogen complexes and 0.4 for amine·halogen complexes.[5] The assumption of $\mu_0 = 0$ for the amine complexes is an obvious over-simplification since the amine component usually has a finite dipole moment. Although neither component in the benzene·halogen complexes has a dipole moment, Hanna[28] has shown that the benzene quadrupole-halogen induced dipole interaction leads to a significant value for μ_0 in these complexes. As a result, the value of $(b^2 + abS_{01}) = 0.1$ overestimates the extent of charge transfer by as much as 20 to 80%. However, Person[5] has shown that such effects are negligible in the stronger amine·halogen complexes and that the major stabilization is

due to charge transfer forces.

When μ_0 is not assumed to be zero, equation (1) must be used to calculate $(b^2 + abS_{01})$. The most useful form of this equation is

$$\mu_N = (a^2 + abS_{01})\mu_0 + (b^2 + abS_{01})\mu_1 \qquad (18)$$

which is derived from the expression for μ_{01} in the appendix. The normalization equation for ψ_N

$$a^2 + b^2 + 2abS_{01} = 1 \qquad (19)$$

must now be used in conjunction with equation (18) to obtain $(b^2 + abS_{01})$. The orientation of μ_0 with respect to μ_1 must of course be known.

For the TMA·SO_2 complex, the magnitude of μ_N was taken as 4.95D as determined by Moede and Curran in benzene solvent.[67] Since it has been suggested that the contribution of the dative structure to the ground state increases slightly as the medium is changed from gas (where the theory applies) to solution,[49] this value probably overestimates the gas phase moment. It remains then to evaluate $|\mu_0|$, $|\mu_1|$ and the angle between them. The equilibrium geometry, (Figure 31) as observed in the structure is used to obtain these quantities

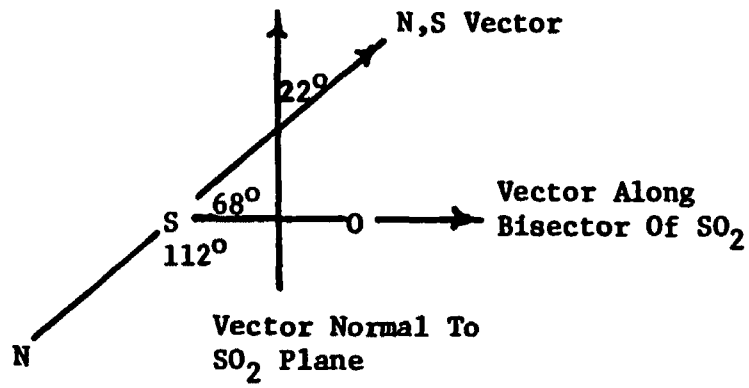

Fig. 31 Geometry of the TMA·SO_2 Complex

To simplify the calculation, the complex is assumed to have exact C_m symmetry and equal S-O bond lengths of 1.4 Å. The dipole moment for the no-bond structure is estimated to be 2.1 D by vector addition of the dipole moments of the component molecules (μ_{TMA} = 0.86D and μ_{SO_2} = 1.6D).[49] The dipole moment of the dative structure is given by

$$\mu_1 = \mu_0 + e\vec{R} \qquad (20)$$

where $e\vec{R}$ is the dipole due to the charge separation. This term is estimated by assuming that the transferred electron of SO_2^{-1} remains localized in the lowest unoccupied orbital of SO_2. Using the population analysis for SO_2 given by Ionov for neutral SO_2,[111] it is possible to calculate the distribution of the electron in SO_2^{-1}. This procedure leads to a prediction of an effective charge of -0.2e on the sulfur and -0.4e on each oxygen. For the purposes of calculation, this is assumed to be equivalent to a negative charge located approximately 4/5 the way down the bisector of the O-S-O angle. The term $e\vec{R}$ then consists of a charge of +1e located approximately on the nitrogen and a charge of -1e located as above with a separation of 2.4 Å. Thus, $|e\vec{R}|$ is 11.3D. The angle between μ_0 and $e\vec{R}$ needed to calculate μ_1 is 150° and thus $|\mu_1|$ is 12.5D. The angle (130°) between μ_0 and μ_1 is calculated from equation (20) in the form

$$\cos\theta = \frac{|e\vec{R}|^2 - |\mu_1|^2 - |\mu_0|^2}{-2|\mu_1||\mu_0|} .$$

Equation (3) in the form

$$|\mu_N|^2 = (a^2 + abS_{01})|\mu_0|^2 + (b^2 + abS_{01})|\mu_1|^2 - 2|\mu_0||\mu_1|$$

$$(a^2 + abS_{01})(b^2 + abS_{01})\cos\theta$$

and the normalization equation

$$a^2 + b^2 + 2abS_{01} = 1$$

can now be combined to give

$$b^2 + abS_{01} = 0.31. \qquad (21)$$

Thus, approximately 30% charge-transfer is predicted for the TMA·SO_2 complex. This value is somewhat lower than that predicted for the amine·I_2 complexes, as might be expected, since the latter complexes are in general somewhat stronger.

Estimation of Mulliken's Resonance Theory Parameters

It is interesting to calculate the energy parameters defined in Mulliken's Resonance Theory (Appendix IV). Equation (18) and the normalization equation may be solved for the coefficients of the ground state wave function (a and b) provided the overlap S_{01} is known. About all that can be done is assume some "reasonable" value for the overlap (S_{01}). For the amine·I_2 complexes, Mulliken[5] assumed values of S_{DA}^* and thus S_{01} (for definitions of these see Appendix IV) of 0.3 and 0.4 respectively while Nagakura[115] assumed values of 0.2 and 0.3. This approximation was made by evaluating the integral

$$S_{DA}^* = \int 2t_e 5p\sigma d\tau$$

where $2t_e$ was the donating atomic orbital on the donor amine approximated as a tetrahedral sp^3 hybrid orbital on nitrogen and $5p\sigma$ refers to the lowest unfilled atomic orbital on the iodine atom. Using Slater type orbitals and the tables prepared by Mulliken, this integral was evaluated

at the equilibrium distance observed in the structure of amine·I_2 complexes. Pilkington[116] has estimated S_{DA}^* to be 0.13 ($S_{01} \simeq 0.2$) for the TMA·SO_2 complex. The difference between this value and that estimated for the amine·I_2 complexes may be due to differences in the sizes of the acceptor orbitals and differences in the equilibrium distances considered. The shorting of the (N-I) distance relative to the van der Waal's (N-I) distance is about 20% greater than the corresponding shorting for TMA·SO_2 (Table 44). The integral evaluated in the TMA·SO_2 case was

$$S_{DA}^* = \int \psi_{SO_2} \psi_{TMA} \, d\tau$$

where

$$\psi_{SO_2} = -0.538(3p_y)^S + 0.362(3d_{yz})^S + 0.761(\pi)^O$$

as suggested by Ionov[111] for the lowest unfilled orbital on SO_2. ψ_{TMA} was approximated from the highest filled molecular orbitals calculated for NH_3 in the planar ($\measuredangle$ H-N-H = 120°) and the equilibrium ($\measuredangle$ H-N-H = 107°) geometries.[117] The wave function resulting from a linear interpolation of the coefficients of the two NH_3 wave functions at the observed C-N-C angle (110°) in TMA was taken as ψ_{TMA}

$$\psi_{TMA} = 0.947(2p_z)^N - 0.236(2s)^N - 0.0385(1s)^N - 0.130(\sigma)^H$$

where $(\sigma)^H$ refers to a linear combination of s atomic orbitals on the hydrogens. The integral was evaluated on the assumption that overlap between nonbonded atoms is zero. Terms involving only s and p atomic orbitals were evaluated at the equilibrium distance using Mulliken's tables[112] and terms involving d atomic orbitals were evaluated using

the tables of Loftus.[113] With this value for S_{01} the coefficient of the ground state wave function

$$\psi_N = a\psi_0 + b\psi_1$$

can be estimated (Table 48). Additional parameters needed to calculate the energy parameters are the energy of the ground state which is set equal to the enthalpy of formation of the gas phase complex

$$W_N = \Delta H = -0.42ev$$

and the energy of the excited state

$$W_V = h\nu_{ct} + W_N = 4.07ev$$

where $h\nu_{ct} = 4.49$ ev for the gas phase complex. With these parameters it was possible to use the relations in the appendix to evaluate the following parameters for various values of the overlap.

TABLE 48

ENERGY PARAMETERS FOR THE TMA·SO_2 COMPLEX

S_{01}	a	b	$b^2 + abS$	β_0	β_1
0.2	0.782	0.486	0.315	-1.84	-2.17
0.3	0.764	0.456	0.315	-1.68	-2.14
0.4	0.746	0.428	0.315	-1.49	-2.05

TABLE 48 - continued

X_0	X_1	W_0	W_1	W_{01}
-1.02	1.85	0.60	2.22	-1.72
-0.85	2.11	0.43	1.96	-1.55
-0.70	2.38	0.28	1.69	-1.38

The rather odd trends in these parameters with increasing overlap is a result of the constraint placed on the values of a and b. That is, the overlap is increased but the percent charge-transfer (b^2 + abS) and the energies (W_N and W_V) are forced to remain constant. The values in this table are comparable in magnitude to those calculated by Nagakura for the amine·I_2 complexes,[115] which might be expected for complexes of comparable strength. It would seem worthwhile to consider the parameters listed for S_{01} = 0.2 since this is the value estimated previously. The energy of the no-bond structure (W_0) is positive as expected due to closed shell repulsion at the equilibrium distance but smaller in magnitude than that for the amine·I_2 complexes. This may be a reflection of the shortening relative to the van der Waals distance mentioned earlier. The rather small value of W_1 (energy of the dative structure) is expected due to the large coulombic attraction at the equilibrium distance. The difference (W_1-W_0) is relatively small, compared to that for the weaker benzene·I_2 complexes,[5] and thus the interaction (W_{01}) and the resonance stabilization energies (X_0 and X_1) are relatively large. The greater destabilization (X_1) of W_1 relative to W_V compared to the stabilization (X_0) of W_0 relative to W_N is

usually explained in terms of a shifting of the minimum of the excited state curve to a distance greater than the equilibrium distance.[5] This is assumed due to the electron being placed more in an antibonding orbital thus decreasing the bond order of the excited complex. The figure in the appendix was constructed to correspond to the energy parameters for the TMA·SO_2 complex.

Although interesting, calculations of this type probably give only very rough estimates of the energy parameters discussed here. The oversimplified theory and errors in the input experimental data (particularly the dipole moments) prohibit any detailed analysis of these results. However, in the development of a more sophisticated theory which predicts parameters as these from first principles, these estimates of their values might prove useful.

APPENDIX I

NON-SPECIFIC EFFECTS ON SOLUBILITY

Attempts have been made to divide the increased solubility of a solute in the presence of dissolved donor molecules owning to specific donor-solute interactions and a part arising from non-specific effects which can be accounted for by using Hildebrand and Scott's solubility parameter theory[19] or other theories of nonelectrolyte solutions. In particular, Mulliken and Person[15] considered activity effects on dissolved solute species which result from the large donor concentrations employed in the conventional experiments of the Benesi-Hildebrand type and concluded that such effects were significant. The following considerations represent an attempt to account for similar effects as encountered in the polyiodide solubility method.

The thermodynamic equilibrium constant in terms of activities is given by

$$K\ (\text{Thermo}) = \frac{a_{DA}}{a_A a_D} = \frac{\gamma_{DA}}{\gamma_D \gamma_A} \frac{C_{DA}}{C_D C_A} = K_\gamma K_c \qquad (1)$$

where the familiar definition of activity ($a_i = \gamma_i C_i$) in terms of the activity coefficient and concentration of species i has been employed. In this treatment, for convenience, the 1M ideal dilute solution standard state is chosen for the components and the complex. In the dilute solution region where Raoult's law holds for the solvent and Henry's law

for the solute, Margules' suggested form for ln γ_i and the Gibbs-Duhem equation may be combined for small $\alpha_i C_D$ to yield the activity coefficient of the ith component in the form[62]

$$\gamma_i = 1 + \alpha_i C_D \tag{2}$$

That is, in the dilute solution region the activity coefficients of all of the solute species are linear functions of the donor concentration. Equation (1) can now be rewritten as

$$K \text{ (Thermo)} = \frac{(1 + \alpha_{DA}C_D)}{(1 + \alpha_A C_D)(1 + \alpha_D C_D)} \frac{C_{DA}}{C_A C_D} \tag{3}$$

which simplifies for small $\alpha_i C_D$ to

$$K \text{ (Thermo)} = 1 + (\alpha_{DA} - \alpha_A - \alpha_D)C_D \frac{C_{DA}}{C_A C_D} \tag{4}$$

or defining $\beta = \alpha_{DA} - \alpha_A - \alpha_D$ to

$$K \text{ (Thermo)} = (1 + \beta C_D) \frac{C_{DA}}{C_A C_D} \tag{5}$$

Thus, the equilibrium constant as determined using the polyiodide solubility method should be written as

$$K \text{ (Thermo)} = (1 + \beta C_D) \frac{f_{I_2} - C_{I_2}}{C_{I_2} C_D} \tag{6}$$

where f_{I_2} is the formal concentration of iodine (complexed and uncomplexed) determined from the absorbance at the isosbestic point and C_{I_2} is the concentration of uncomplexed iodine. In the absence of nonspecific activity effects, C_{I_2} may be assumed to be constant and equal to $C^o_{I_2}$; however in the present treatment, C_{I_2} must be considered a variable, owing to the possibility that activity effects may modify the

solubility of uncomplexed iodine. In light of equation (2), the expression for the activity of iodine in the dilute solution region is given by

$$a_{I_2} = \gamma_{I_2} C_{I_2} = (1 + \alpha_{I_2} C_D) C_{I_2} = C^o_{I_2} \qquad (7)$$

where the activity of the uncomplexed iodine has been set equal to the concentration ($C^o_{I_2}$) of iodine in the heptane blank. This is possible since once this activity is established, it remains constant in all the solutions. As equation (7) implies, the concentration of uncomplexed iodine is not expected to be constant, but the product of activity coefficient and concentration will be constant and equal to $C^o_{I_2}$. Only in the limit as C_D approaches zero will $C_{I_2} = C^o_{I_2}$. Thus, solving equation (7) for C_{I_2} yields,

$$C_{I_2} = \frac{C^o_{I_2}}{(1 + \alpha_{I_2} C_D)} \qquad (8)$$

and substitution of this into equation (7) gives

$$K\ (\text{Thermo}) = \frac{\left(f_{I_2} - \dfrac{C^o_{I_2}}{1 + \alpha_{I_2} C_D}\right)}{\left(\dfrac{C^o_{I_2}}{1 + \alpha_{I_2} C_D}\right) C_D} (1 + \beta C_D) \qquad (9)$$

which can be rearranged to give

$$\frac{f_{I_2} - C^o_{I_2}}{C_D C^o_{I_2}} = \frac{K\ (\text{Thermo})}{(1 + \beta C_D)} + \frac{\alpha_{I_2} f_{I_2}}{C^o_{I_2}} \ . \qquad (10)$$

The limit of this expression corresponds to what has previously been called the 1:1 complex formation constant and will be denoted by K_S. That is,

$$\lim_{C_D \to 0} \left(\frac{f_{I_2} - C^o_{I_2}}{C_D C^o_{I_2}} \right) = K_S = K \text{ (Thermo)} + \alpha_{I_2} \qquad (11)$$

where $\lim_{C_D \to 0} f_{I_2} = C^o_{I_2}$ since the concentration of iodine approaches that of the blank as the donor concentration approaches zero. According to equation (11), the solubility method results in an equilibrium constant which includes both the specific interactions (K (Thermo)) and the non-specific interactions (α_{I_2}) between the donor and acceptor. Thus, in the limit as C_D approaches zero, the non-specific effects are minimized, although not eliminated, and obtaining equilibrium constants by the solubility method which are constant over some finite donor concentration range does not imply the absence of such effects. The relative importance of the two effects then becomes the important question. When the dissolved species have small polarizabilities and/or the specific effect is large, it may intuitively be anticipated that α_{I_2} is negligible compared to K_C because of the weak nature of the non-specific forces. In the case of the pyridine-iodine complex, the non-specific effect is probably very small compared to the specific complex formation effect and neglecting the former is probably justified. However, in the case of very weak complexes such as those encountered in the aromatic hydrocarbon-iodine series, the relative importance of these two effects is difficult to assess, particularly in view of the large polarizability of iodine. The importance of estimating the magnitude of α_{I_2} is therefore quite obvious.

The magnitude of α_{I_2} can be estimated using Hildebrand and Scott's

solubility parameter theory.[19,62] The concept of the "regular solution," upon which this theory is based, is defined as "a solution involving no entropy change when a small amount of one of its components is transferred to it from an ideal solution of the same composition, the total volume remaining unchanged." Simply stated this means that the mixing of the components is completely random, that is, there is no specific tendency for one molecule to be near another. Thus, for a regular solution the excess entropy of mixing is zero and the entropy of mixing is given by the ideal entropy of mixing. Regular solutions are most likely to be formed by non-polar molecules where the interactions between molecules can be described in terms of the nondirectional London dispersion forces. For polar molecules, where interactions between molecules may involve such directionally dependent terms as dipole-dipole and complex formation interactions, the theory does not apply. In fact, any interaction which results in some net ordering effect will not be accounted for by this theory. Hildebrand and Scatchard sought to connect the properties of a liquid mixture with those of its pure components. For a particular mixture these properties were conveniently expressed in terms of "Solubility parameters (δ_i)" which are related to the "cohesive energy density" of its pure components i. The "cohesive energy density" of a pure liquid is a measure of the attractive forces between its molecules and is given by its energy of vaporization per cubic centimeter ($\Delta E_i^{vap}/V_i$) where V_i is the molar volume of pure liquid i. The solubility parameter (δ_i) was defined as $(\Delta E_i^{vap}/V_i)^{\frac{1}{2}}$ and the interaction between different molecules in a mixture was approximated by the geometric mean of their individual solubility parameters

$$\delta_{ij} = \left(\frac{\Delta E_i^{vap}}{V_i} \cdot \frac{\Delta E_j^{vap}}{V_j}\right)^{\frac{1}{2}} \qquad (12)$$

Thus, two substances which have equal cohesion, or solubility parameters, when mixed are expected to form an ideal solution since the interaction between pure component molecules is the same as that between the different molecules in the mixture. As the difference of the solubility parameters of the mixed components increase, the mixture becomes less ideal. Thus, according to this theory, increases in the solubility of iodine, as observed in the solubility method, are predicted whenever the solubility parameter of the donor is greater than that of the solvent and such increases should not be taken as conclusive indication of specific complex formation. Specific complex formation is indicated only by increases in solubility over and above those predicted by the solubility parameter theory. On this basis, the assumption that all increases in the solubility of iodine are attributable to "specific" complex formation is not entirely justifiable. The procedure implied above is that the non-specific effect on solubility must be subtracted from the total increase to obtain that due to specific effects.

In addition to the geometric mean approximation for δ_{ij}, the three other basic assumptions of this theory were as follows: (1) the mutual energy between two molecules depends only on their distance of separation and their relative orientation and not at all on the nature of the molecules between them or on the temperature, (2) the distribution of the molecules in position and orientation is random, (3) the change in volume on mixing is zero. As was demonstrated by Scatchard,[63] these assumptions

alone allow derivation of the following equation for the activity coefficient of iodine dissolved in a mixed solvent

$$\ln\gamma_2 = \frac{v_2\phi_m^{\,2}(\delta_2 - \delta_m)^2}{RT} \qquad (13)$$

In equation (13), v_2 is the molar volume of iodine, ϕ_m is the volume fraction of the mixed solvent, and δ_2 and δ_m are the solubility parameters of iodine and of the mixed solvent. The solubility parameter of the mixed solvent was approximated by

$$\delta_m = \frac{\phi_1\delta_1 + \phi_3\delta_3}{\phi_1 + \phi_3} \qquad (14)$$

where the subscripts refer to the two components of the mixed solvent and will be used to denote the solvent (1) and the donor (3). Equation (14) may be simplified to

$$\delta_m = \delta_1 + (\delta_3 - \delta_1)\phi_3 \qquad (15)$$

since ϕ_2 is always small in the polyiodide solubility method such that $\phi_1 + \phi_3 \approx 1$. Substituting this relation into equation (13) with ϕ_m^2 set equal to 1 and expanding the resulting term in the bracket yeilds

$$\ln\gamma_2 = \frac{v_2}{RT}(\delta_2 - \delta_1)^2 - (\delta_3 - \delta_1)^2\,\phi_3^{\,2} - (2(\delta_2 - \delta_1)(\delta_3 - \delta_1)\,\phi_3) \; . \qquad (16)$$

Differentiation of (16) with respect to ϕ_3 gives

$$\frac{d\ln\gamma_2}{d\phi_3} = \frac{v_2}{RT}\,-2(\delta_3 - \delta_1)^2\phi_3 - 2(\delta_2 - \delta_1)(\delta_3 - \delta_1) \qquad (17)$$

which in the limit as ϕ_3 goes to zero becomes

$$\lim_{\phi_3 \to 0} \frac{d\ln\gamma_2}{d\phi_3} = \frac{-2v_2}{RT} (\delta_2 - \delta_1)(\delta_3 - \delta_1). \tag{18}$$

The relation between the volume fraction of the donor and the corresponding concentration of the donor is given by

$$\phi_3 = \frac{C_D v_3}{1000} : (v_3 = \text{molar volume of the donor}) \tag{19}$$

for dilute solutions of the donor. Using this expression, the implied variable transformation can be made in equation (18) to yield

$$\lim_{C_D \to 0} \frac{d\ln\gamma_2}{dC_D} = \frac{-2v_2 v_3}{1000\ RT} (\delta_2 - \delta_1)(\delta_3 - \delta_1). \tag{20}$$

The right hand side of this equation can be equated to α_{I_2}. This can be shown by taking the natural log of equation (2) to obtain

$$\ln\gamma_{I_2} = \ln (1 + \alpha_{I_2} C_D) , \tag{21}$$

which simplifies for very small $\alpha_{I_2} C_D$,

$$\ln\gamma_{I_2} = \alpha_{I_2} C_D. \tag{22}$$

The derivative of (22) with respect to C_D yields

$$\frac{d(\ln\alpha_{I_2})}{dC_D} = \alpha_{I_2} , \tag{23}$$

which is valid in the limit as C_D approaches zero. The right hand sides of equations (20) and (23) may now be equated to yield

$$\alpha_{I_2} = \frac{-2v_2 v_3}{1000\ RT} (\delta_2 - \delta_1)(\delta_3 - \delta_1) , \tag{24}$$

which gives the correction to K_S necessary to obtain K (Thermo), as

implied in equation (11), in terms of the molar volumes and solubility parameters of the various components. One implication of equation (24) is that activity effects are eliminated in the solubility method whenever the solubility parameters of the donor and solvent are equal (i.e., $\alpha_{I_2} = 0$). This implies that the non-specific interactions between iodine and the donor or solvent are the same, so that whether the iodine molecule is surrounded by pure donor or pure solvent molecules or some admixture of the two is not differentiated by the iodine molecule. Table 11 lists the results obtained by application of equation (24) to estimate the magnitude of the non-specific effects on the solubility of iodine.

One surprising result in Table 11 is the magnitude of the correction term implied by this theory. It amounts to approximately 50% of the total effect observed via the solubility method for the benzene-iodine complex and decreases slightly through the aromatic hydrocarbon series. However, it might be argued that the solubility parameter of iodine used to calculate δ_{I_2} is too high since it was determined by averaging the results obtained from a range of solvents, including some where specific effects are known to exist.[19] Thus, α_{I_2} may include to some extent effects due to both specific and non-specific effects. If δ_{I_2} is too high, the magnitude of α_{I_2} is overestimated to some extent and K(Thermo) is underestimated. Another interesting feature of Table 11 is the agreement between K(Thermo) (the 1:1 complex formation constant corrected for activity effects) and K_{B-H} (the equilibrium constant determined by Benesi-Hildebrand techniques). This agreement might be taken as indication that the conventional spectral techniques fortuitously result in equilibrium constants relatively free from

activity effects. This would imply that K_γ equals approximately one or that γ_{AD} nearly equals the product $\gamma_D\gamma_A$ over the entire donor concentration range employed. However, Mulliken and Person used solubility parameter theory (see Chapter I) to estimate the dependence of K_γ on donor concentration and did not find this result. In fact, they estimated that the equilibrium constant may be underestimated by as much as a factor of two. Thus, the cancellation of activity effects implied by the results in Table 11 are contradicted by Mulliken and Person's calculations. Whether such effects cancel or not is still an unanswered question.

In this connection, it is interesting to note that α_{I_2} is predicted to be zero for the diethyl ether system, which implies the absence of non-specific effects and requires that K_S = K(Thermo). In this case, K_S should agree with the spectrally determined constant K_{B-H}, if indeed the conventional techniques are free of activity effects. However, as seen in the table, these constants do differ by several percent. However, difficulties encountered in studying this particular system probably resulted in large experimental errors in the equilibrium constants and any conclusions are likewise uncertain.

These considerations point out the difficulties encountered in any attempt to separate the specific interactions between components from those which are of a non-specific type. The validity of using any theory to separate these effects is impossible to determine in the absence of experimental methods which measure the two effects separately. Perhaps the only significant result of this treatment is that assigning all increases in the solubility of iodine to complex formation leads to an

equilibrium constant which includes both of these effects. Equilibrium constants derived under such an assumption might be likened to the second virial coefficient used to describe non-ideal gases in that it includes all deviations from ideality regardless of origin. The results obtained with the solubility method are more reasonable than the corresponding properties determined using the conventional techniques and it is very tempting to take the position that the total effect is, in reality, the one of most interest. The reasonable trends in properties derived under this assumption indicate this to be the case.

TABLE 11

CORRECTION OF THE EQUILIBRIUM CONSTANTS DETERMINED WITH THE SOLUBILITY METHOD FOR NON-SPECIFIC EFFECTS

Donor	$v_3(cm^3)$	$\delta_3(cal^{1/2}cm^{-3/2})$	$\alpha^*_{I_2}$	K_s	K(thermo)	K_{B-H}
Benzene	89	9.2	0.22	0.37	0.15	0.20
Toluene	107	8.9	0.22	0.50	0.28	0.32
o-Xylene	121	9.0	0.27	0.64	0.37	0.42
p-Xylene	123	8.8	0.24	0.64	0.40	0.41
m-Xylene	124	8.8	0.24	0.70	0.46	0.54
Mesitylene	140	8.8	0.27	0.98	0.71	0.74
Diethyl ether	105	7.4	0	1.44	1.44	1.23

*In the calculation of α_{I_2} the following parameters were used:

for heptane, $v_1 = 148\ cm^3$, $\delta_1 = 7.4\ cal^{1/2}cm^{-3/2}$

for iodine, $v_2 = 59\ cm^3$, $\delta_2 = 14.5\ cal^{1/2}cm^{-3/2}$.

APPENDIX II

PRIMARY DATA FROM CONVENTIONAL EXPERIMENTS OF THE BENESI-HILDEBRAND TYPE

The data from the conventional spectral investigations described in Chapter IV are presented in this section. C_D refers to the initial donor concentration. ΔA is the observed absorbance of the complex at λ^{ct}, corrected for the absorbance of donor and acceptor by use of the extinction coefficients ε_D and ε_A. Calculated values of ΔA are based on the method described in Chapter IV. The initial iodine concentration is given by $C^o_{I_2}$. A cell pathlength of 1.0 cm. was employed in all of these determinations.

TABLE 12

CONVENTIONAL SPECTRAL DATA FOR THE

BENZENE-IODINE SYSTEM AT 25°C

C_D(mole/ℓ)	ΔA	ΔA(calc.)
0.2236	0.132	0.132
0.4472	0.253	0.254
0.6708	0.363	0.365
0.8944	0.469	0.468
1.118	0.569	0.564
1.565	0.724	0.734
2.012	0.871	0.884
3.354	1.26	1.23
4.472	1.45	1.44
5.600	1.61	1.62

$C_{I_2}^{o}$ (mole/ℓ)	2.16×10^{-4}
λ^{ct} (mμ)	289
ε_D ($\ell mole^{-1}cm^{-1}$)	5.0×10^{-3}
ε_A ($\ell mole^{-1}cm^{-1}$)	80

TABLE 13

CONVENTIONAL SPECTRAL DATA FOR THE

TOLUENE-IODINE SYSTEM AT 25°C

C_D(mole/ℓ)	ΔA	ΔA(calc.)
0.1872	0.113	0.112
0.3744	0.216	0.212
0.5616	0.305	0.302
0.7488	0.391	0.384
0.9360	0.461	0.458
1.123	0.522	0.525
1.498	0.640	0.644
1.872	0.739	0.745
2.808	0.941	0.943
3.744	1.09	1.09
4.680	1.20	1.20

$C_{I_2}^o$ (mole/ℓ)	1.90×10^{-4}
λ^{ct} (mμ)	300
ε_D (ℓmole^{-1}cm^{-1})	9.1×10^{-3}
ε_A (ℓmole^{-1}cm^{-1})	76

TABLE 14

CONVENTIONAL SPECTRAL DATA FOR THE

o-XYLENE-IODINE SYSTEM AT 25°C

C_D(mole/ℓ)	ΔA	ΔA(calc.)
0.1650	0.124	0.121
0.3300	0.227	0.228
0.4950	0.323	0.322
0.6600	0.408	0.406
0.8250	0.482	0.481
0.9900	0.553	0.549
1.320	0.667	0.667
1.650	0.754	0.764
2.475	0.955	0.952
3.300	1.09	1.08

$C_{I_2}^{o}$ (mole/ℓ)	1.93×10^{-4}
λ^{ct} (mμ)	314
ε_D ($\ell mole^{-1} cm^{-1}$)	7.3×10^{-3}
ε_A ($\ell mole^{-1} cm^{-1}$)	41

TABLE 15

CONVENTIONAL SPECTRAL DATA FOR THE

m-XYLENE-IODINE SYSTEM AT 25°C

C_D (mole/ℓ)	ΔA	ΔA(calc.)
0.1620	0.142	0.141
0.3240	0.260	0.260
0.4860	0.365	0.364
0.6480	0.446	0.453
0.8100	0.525	0.532
0.9720	0.611	0.602
1.296	0.724	0.720
1.620	0.827	0.816
2.430	0.973	0.993
3.240	1.12	1.11

$C_{I_2}^{o}$ (mole/ℓ)	1.95×10^{-4}
λ^{ct} (mμ)	314
ε_D ($\ell mole^{-1} cm^{-1}$)	1.1×10^{-2}
ε_A ($\ell mole^{-1} cm^{-1}$)	41

TABLE 16

CONVENTIONAL SPECTRAL DATA FOR THE

p-XYLENE-IODINE SYSTEM AT 25°C

C_D^*(mole/ℓ)	ΔA	ΔA(calc.)
0.1614	0.085	0.082
0.3228	0.155	0.155
0.4842	0.223	0.219
0.6456	0.278	0.277
0.8070	0.328	0.329
0.9684	0.376	0.376
1.291	0.456	0.458
1.614	0.523	0.526
2.424	0.647	0.659
3.228	0.756	0.753

$C_{I_2}^o$ (mole/ℓ)	1.50×10^{-4}
λ^{ct} (mμ)	302
ε_D ($\ell mole^{-1}cm^{-1}$)	2.6×10^{-2}
ε_A ($\ell mole^{-1}cm^{-1}$)	73

TABLE 17

CONVENTIONAL SPECTRAL DATA FOR THE

DIETHYL ETHER-IODINE SYSTEM 15°C

C_D(mole/ℓ)	ΔA	ΔA(calc.)
0.1947	0.191	0.195
0.2922	0.273	0.268
0.3895	0.322	0.328
0.5842	0.428	0.424
0.7789	0.496	0.496
1.169	0.604	0.598
1.558	0.661	0.666

$C_{I_2}^{o}$ (mole/ℓ)	1.98×10^{-4}
λ^{ct} (mμ)	250
ε_D ($\ell mole^{-1} cm^{-1}$)	2.8×10^{-2}
ε_A ($\ell mole^{-1} cm^{-1}$)	440

TABLE 18

CONVENTIONAL SPECTRAL DATA FOR THE

MESITYLENE-IODINE SYSTEM AT 25°C

C_D(mole/ℓ)	ΔA	ΔA(calc.)
0.1433	0.132	0.128
0.2866	0.234	0.233
0.4299	0.327	0.322
0.5732	0.394	0.397
0.7165	0.459	0.461
0.8598	0.513	0.517
1.003	0.565	0.567
1.146	0.611	0.610
1.290	0.651	0.649
1.433	0.686	0.684

$C_{I_2}^{o}$ (mole/ℓ) 1.31×10^{-4}

λ^{ct} (mμ) 327

ε_D ($\ell mole^{-1}cm^{-1}$) 1.1×10^{-2}

ε_A ($\ell mole^{-1}cm^{-1}$) 30

APPENDIX III

PRIMARY DATA FROM THE POLYIODIDE SOLUBILITY METHOD

The data from the solubility experiments described in Chapter IV are presented in this section. Except for the pyridine-iodine system, C_D refers to both the initial and uncomplexed donor concentration. For the pyridine-iodine system, C_D^o refers to the initial donor concentration and C_D to the uncomplexed donor concentration. The calculated values of ΔA^{iso} and ΔA^{ct} are based on the method described in Chapter IV. The general form of the equation employed to fit ΔA^{iso} as a function of C_D was

$$\Delta A^{iso} = K_1 C_D^a + K_2 C_D^b + K_3 C_D^c$$

and the equation employed to fit ΔA^{ct} as a function of ΔA^{iso} was

$$\Delta A^{ct} = K_1 (\Delta A^{iso})^a + K_2 (\Delta A^{iso})^b + K_3 (\Delta A^{iso})^c \ .$$

A particular fit is indicated by the values of a, b and c and the RMSD corresponding to that fit. For example, in Table 19 the fit (1,0,0) corresponds to a fit of ΔA^{iso} as a linear function of the donor concentration. The fit (1,2,0) corresponds to a fit of ΔA^{iso} which includes both linear and second order dependence on C_D. In each case, the intercept of a particular fit is taken as zero. The wavelength

and extinction coefficient at λ^{iso} and the wavelength (λ^{ct}) of the maximum absorbance in the charge-transfer band are listed. Except where indicated, the data are referred to a cell path length of 2.0 cm.

TABLE 19

POLYIODIDE SOLUBILITY DATA FOR THE SYSTEM BENZENE-IODINE AT 25°C (VISIBLE REGION)

C_D(mole/ℓ)	ΔA^{iso}	ΔA^{iso}(calc.)
0.1118	0.014	0.015
0.2236	0.031	0.030
0.3354	0.046	0.046
0.4472	0.063	0.062
0.5590	0.080	0.079
0.6708	0.096	0.097
0.7826	0.113	0.115
0.8944	0.134	0.134
1.006	0.152	0.153
1.118	0.172	0.173
1.342	0.218	0.215
1.789	0.304	0.305

Fit	RMSD x 10^2
a b c	
1 0 0	0.972
1 2 0	0.148
1 2 3	0.155

λ^{iso} (mμ) 520

ε^{iso} (ℓmole^{-1}cm^{-1}) 918

TABLE 20

POLYIODIDE SOLUBILITY DATA FOR THE SYSTEM BENZENE-IODINE AT 25°C (ULTRAVIOLET REGION)

ΔA^{iso}	ΔA^{ct}	ΔA^{ct}(calc.)
0.014	0.133	0.124
0.031	0.274	0.275
0.046	0.413	0.409
0.063	0.558	0.561
0.080	0.711	0.716
0.096	0.867	0.862
0.113	1.02	1.02
0.134	1.21	1.21
0.152	1.38	1.38
0.172	1.57	1.57
0.218	2.01	2.01
0.304	2.85	2.85

Fit			RMSD x 10^2
a	b	c	
1	0	0	2.30
1	2	0	0.433
1	2	3	0.457

λ^{ct} (mμ) 288

TABLE 21

POLYIODIDE SOLUBILITY DATA FOR THE SYSTEM TOLUENE-IODINE AT 25°C (VISIBLE REGION)

C_D(mole/ℓ)	ΔA^{iso}	ΔA^{iso}(calc.)
0.0936	0.019	0.017
0.1872	0.035	0.035
0.2808	0.055	0.053
0.3744	0.071	0.071
0.4680	0.089	0.090
0.5616	0.109	0.109
0.6552	0.126	0.128
0.7488	0.149	0.148
0.8424	0.170	0.169
0.9360	0.189	0.189
1.123	0.230	0.232
1.498	0.325	0.323
1.872	0.420	0.421

Fit	RMSD x 10^2
a b c	
1 0 0	1.08
1 2 0	0.159
1 2 3	0.164

λ^{iso} (mμ) 518

ε^{iso} ($\ell mole^{-1} cm^{-1}$) 913

TABLE 22

POLYIODIDE SOLUBILITY DATA FOR THE SYSTEM TOLUENE-IODINE AT 25°C (ULTRAVIOLET REGION)

ΔA^{iso}	ΔA^{ct}	ΔA^{ct}(calc.)
0.019	0.136	0.144
0.035	0.258	0.266
0.055	0.422	0.419
0.071	0.546	0.542
0.089	0.674	0.681
0.109	0.840	0.837
0.126	0.980	0.969
0.149	1.15	1.15
0.170	1.30	1.32
0.189	1.46	1.47
0.230	1.81	1.79
0.325	2.56	2.56

Fit			RMSD x 10^2
a	b	c	
1	0	0	1.62
1	2	0	0.950
1	2	3	0.975

λ^{ct} (mμ) 300

TABLE 23

POLYIODIDE SOLUBILITY DATA FOR THE SYSTEM o-XYLENE-IODINE AT 25°C (VISIBLE REGION)

C_D(mole/ℓ)	ΔA^{iso}	ΔA^{iso}(calc.)
0.0825	0.019	0.019
0.1650	0.039	0.039
0.2475	0.059	0.060
0.3300	0.082	0.080
0.4125	0.100	0.101
0.4950	0.125	0.124
0.5775	0.144	0.146
0.6600	0.171	0.169
0.7425	0.188	0.192
0.8250	0.215	0.216
0.9900	0.266	0.265
1.320	0.371	0.369
1.650	0.479	0.480

Fit	RMSD x 10^2
a b c	
1 0 0	1.28
1 2 0	0.196
1 2 3	0.198

λ^{iso} (mμ) 519

ε^{iso} ($\ell mole^{-1} cm^{-1}$) 915

TABLE 24

POLYIODIDE SOLUBILITY DATA FOR THE SYSTEM o-XYLENE-IODINE AT 25°C (ULTRAVIOLET REGION)

ΔA^{iso}	ΔA^{ct}	ΔA^{ct}(calc.)
0.019	0.144	0.136
0.039	0.284	0.280
0.059	0.430	0.426
0.082	0.586	0.596
0.100	0.735	0.730
0.125	0.906	0.917
0.144	1.07	1.06
0.171	1.27	1.27
0.188	1.40	1.40
0.215	1.61	1.61
0.266	2.02	2.02

Fit			RMSD x 10^2
a	b	c	
1	0	0	1.72
1	2	0	0.696
1	2	3	0.729

λ^{ct} (mμ) 313

TABLE 25

POLYIODIDE SOLUBILITY DATA FOR THE SYSTEM m-XYLENE-IODINE AT 25°C (VISIBLE REGION)

C_D(mole/ℓ)	ΔA^{iso}	ΔA^{iso}(calc.)
0.0810	0.019	0.021
0.1620	0.044	0.042
0.2430	0.064	0.063
0.3240	0.085	0.085
0.4050	0.109	0.107
0.4860	0.132	0.129
0.5670	0.152	0.152
0.6480	0.174	0.175
0.7290	0.198	0.199
0.8100	0.222	0.223
0.9720	0.271	0.272
1.296	0.374	0.375
1.620	0.484	0.483

Fit	RMSD x 10^2
a b c	
1 0 0	0.967
1 2 0	0.154
1 2 3	0.132

λ^{iso} (mμ) 518

ε^{iso} ($\ell mole^{-1} cm^{-1}$) 913

TABLE 26

POLYIODIDE SOLUBILITY DATA FOR THE SYSTEM m-XYLENE-IODINE AT 25°C (ULTRAVIOLET REGION)

ΔA^{iso}	ΔA^{ct}	ΔA^{ct}(calc.)
0.019	0.136	0.137
0.044	0.318	0.322
0.064	0.476	0.472
0.085	0.646	0.634
0.109	0.818	0.822
0.132	1.00	1.01
0.152	1.17	1.17
0.174	1.36	1.35
0.198	1.55	1.56
0.222	1.76	1.76
0.271	2.20	2.20

Fit	RMSD x 10^2
a b c	
1 0 0	3.30
1 2 0	0.604
1 2 3	0.628

λ^{ct} (mμ) 314

TABLE 27

POLYIODIDE SOLUBILITY DATA FOR THE SYSTEM p-XYLENE-IODINE AT 25°C (VISIBLE REGION)

C_D(mole/ℓ)	ΔA^{iso}	ΔA^{iso}(calc.)
0.08069	0.018	0.019
0.1614	0.038	0.038
0.2421	0.057	0.058
0.3228	0.078	0.078
0.4035	0.098	0.099
0.4842	0.120	0.120
0.5648	0.141	0.141
0.6456	0.162	0.163
0.7262	0.186	0.185
0.8070	0.208	0.208
0.9684	0.256	0.255
1.130	0.302	0.303
1.291	0.352	0.353
1.453	0.406	0.405

Fit	RMSD x 10^3
a b c	
1 0 0	8.99
1 2 0	0.845
1 2 3	0.878

λ^{iso} (mμ) 518 ε^{iso} ($\ell mole^{-1}cm^{-1}$) 913

TABLE 28

POLYIODIDE SOLUBILITY DATA FOR THE SYSTEM p-XYLENE-IODINE AT 25°C (ULTRAVIOLET REGION)

ΔA^{iso}	ΔA^{ct}	ΔA^{ct}(calc.)
0.018	0.118	0.113
0.038	0.240	0.240
0.057	0.366	0.361
0.078	0.498	0.496
0.098	0.630	0.626
0.120	0.768	0.770
0.141	0.912	0.908
0.162	1.05	1.05
0.186	1.20	1.21
0.208	1.36	1.36
0.256	1.68	1.69
0.302	2.02	2.01
0.352	2.37	2.37

Fit	RMSD x 10^2
a b c	
1 0 0	2.24
1 2 0	0.561
1 2 3	0.521

λ^{ct} (mμ) 303

TABLE 29

POLYIODIDE SOLUBILITY METHOD FOR THE SYSTEM PYRIDINE-IODINE AT 25°C (VISIBLE REGION)

C_D^o(mole/ℓ) x 10^2	C_D(mole/ℓ) x 10^2	ΔA^{iso}	ΔA^{iso}(calc.)
0.09804	0.09491	0.026	0.026
0.1961	0.1899	0.054	0.053
0.2941	0.2848	0.080	0.079
0.3922	0.3799	0.106	0.106
0.4902	0.4749	0.132	0.132
0.5882	0.5699	0.158	0.159
0.6863	0.6648	0.185	0.185
0.7843	0.7598	0.211	0.212
0.8824	0.8549	0.237	0.238
0.9804	0.9500	0.262	0.265
1.471	1.425	0.400	0.398
1.961	1.899	0.532	0.530
2.451	2.374	0.664	0.662
2.941	2.849	0.792	0.795

Fit			RMSD x 10^2
a	b	c	
1	0	0	0.169
1	2	0	0.175
1	2	3	0.125

λ^{iso} (mμ) 477 ε^{iso} (ℓmole^{-1}cm^{-1}) 431

TABLE 30

POLYIODIDE SOLUBILITY METHOD FOR THE SYSTEM PYRIDINE-IODINE AT 25°C (ULTRAVIOLET REGION)

ΔA^{iso}	ΔA^{ct}	ΔA^{ct}(calc.)
0.026	2.44	2.49
0.054	5.10	5.17
0.080	7.62	7.66
0.106	10.2	10.1
0.132	12.6	12.6
0.158	15.2	15.1

Fit	RMSD x 10^1
a b c	
1 0 0	0.600
1 2 0	0.478
1 2 3	0.524

λ^{ct} (mμ) 250

TABLE 31

POLYIODIDE SOLUBILITY METHOD FOR THE SYSTEM PYRIDINE-IODINE AT 15°C (VISIBLE REGION)

C_D^o(mole/ℓ) x 10^2	C_D(mole/ℓ) x 10^2	ΔA^{iso}	ΔA^{iso}(calc.)
0.09926	0.09659	0.023	0.0270
0.1985	0.1926	0.051	0.054
0.2977	0.2888	0.077	0.081
0.3971	0.3849	0.105	0.108
0.4963	0.4810	0.132	0.135
0.5955	0.5768	0.161	0.161
0.6948	0.6733	0.185	0.188
0.7940	0.7693	0.213	0.215
0.8933	0.8651	0.243	0.241
1.489	1.443	0.399	0.404
1.989	1.922	0.539	0.537
2.481	2.403	0.671	0.672
2.977	2.883	0.811	0.806

Fit	RMSD x 10^2
a b c	
1 0 0	0.309
1 2 0	0.231
1 2 3	0.240

TABLE 32

POLYIODIDE SOLUBILITY METHOD FOR THE SYSTEM DIETHYL ETHER-IODINE AT 15°C (VISIBLE REGION)

C_D(mole/ℓ)	ΔA^{iso}	ΔA^{iso}(calc.)
0.1948	0.026	0.025
0.2922	0.039	0.037
0.3895	0.052	0.050
0.4871	0.062	0.063
0.5844	0.076	0.076
0.7792	0.102	0.103
0.9740	0.131	0.131
1.364	0.190	0.190
1.910	0.278	0.278

Fit	RMSD x 10^2
a b c	
1 0 0	0.597
1 2 0	0.135
1 2 3	0.131

λ^{iso} (mμ) 494

ε^{iso} ($\ell mole^{-1} cm^{-1}$) 705

cell pathlength (cm) 1.0

TABLE 33

POLYIODIDE SOLUBILITY METHOD FOR THE SYSTEM DIETHYL ETHER-IODINE AT 15°C (ULTRAVIOLET REGION)

ΔA^{iso}	ΔA^{ct}	ΔA^{ct}(calc.)
0.026	0.214	0.213
0.039	0.321	0.321
0.052	0.413	0.430
0.062	0.537	0.514
0.076	0.626	0.634
0.102	0.861	0.859
0.131	1.10	1.12
0.190	1.67	1.65
0.278	2.49	2.49

Fit	RMSD x 10^1
a b c	
1 0 0	0.360
1 2 0	0.142
1 2 3	0.149

λ^{ct} (mμ) 250

cell path length (cm) 1.0

TABLE 34

POLYIODIDE SOLUBILITY DATA FOR THE SYSTEM MESITYLENE-IODINE AT 25°C (VISIBLE REGION)

C_D(mole/ℓ)	ΔA^{iso}	ΔA^{iso}(calc.)
0.07165	0.027	0.025
0.1433	0.052	0.051
0.2150	0.076	0.077
0.2866	0.106	0.104
0.3583	0.133	0.131
0.4299	0.157	0.158
0.5016	0.186	0.186
0.5732	0.214	0.214
0.7165	0.273	0.272
0.8598	0.329	0.332
1.003	0.391	0.393
1.146	0.457	0.456
1.290	0.523	0.521
1.433	0.587	0.588

Fit	RMSD x 10^2
a b c	
1 0 0	1.10
1 2 0	0.171
1 2 3	0.168

λ^{iso} (mμ) 520 ε^{iso} ($\ell mole^{-1}cm^{-1}$) 918

TABLE 35

POLYIODIDE SOLUBILITY DATA FOR THE SYSTEM MESITYLENE-IODINE AT 25°C (ULTRAVIOLET REGION)

ΔA^{iso}	ΔA^{ct}	ΔA^{ct}(calc.)
0.027	0.220	0.228
0.052	0.430	0.441
0.076	0.656	0.647
0.106	0.906	0.907
0.133	1.14	1.14
0.157	1.36	1.35
0.186	1.60	1.61
0.214	1.87	1.86
0.273	2.39	2.39

Fit			RMSD x 10^2
a	b	c	
1	0	0	1.53
1	2	0	0.874
1	2	3	0.896

λ^{ct} (mμ) 327

APPENDIX IV

MULLIKEN'S VALENCE BOND (RESONANCE) THEORY

"General Theory"

According to Mulliken's theory,[5] the ground state wave function for a complex is expressed as

$$\psi = a\psi_o(D,A) + b\psi_1(D^+ - A^-) + \ldots\ldots \qquad (1)$$

where $\psi_o(D,A)$ is the "no-bond" wave function corresponding to a hypothetical state where D (donor) and A (acceptor) are pressed together in the configuration they have in the complex. It contains all the "classical" interactions expected of two closed shell molecules in such a situation. The term $\psi_1(D^+ - A^-)$ corresponds to a situation in which an electron has been completely transferred from D to A. The contribution of this term to the ground state gives that state some charge transfer character. That is, there is a partial transfer of an electron from the donor to the acceptor in the complex. The wave function (1) should also contain other terms as (DA^*), (D^*A), (D^{+*}, A^-), etc., corresponding to locally excited states on the donor and/or acceptor. In the first approximation such terms are usually ignored. As Hanna has shown, this can result in large errors for some complexes.[26] The excited state of the complex is given by

$$\psi_v = -b^*\psi_0(D,A) + a^*\psi_1(D^+ - A^-) + \ldots\ldots \quad (2)$$

where the coefficients b^* and a^* are determined by the requirement that the excited state be orthogonal to the ground state

$$\int \psi_N \psi_v d\tau = 0 \quad (3)$$

The charge transfer transition corresponds to the transition

$$\psi_N \xrightarrow{h\nu_{ct}} \psi_v \cdot \quad (4)$$

It is required that ψ_N, ψ_v, ψ_0 and ψ_1 be normalized

$$\int \psi_N^2 d\tau = 1 = a^2 + b^2 + 2abS_{01} \quad (5)$$

$$\int \psi_v^2 d\tau = 1 = a^{*2} + b^{*2} - 2a^*b^*S_{01} \quad (6)$$

$$\int \psi_0^2 d\tau = 1 \quad (7)$$

and

$$\int \psi_1^2 d\tau = 1 \quad (8)$$

where

$$S_{01} = \int \psi_0 \psi_1 d\tau \quad (9)$$

Using (3) with (5) and (6) the relation

$$a^*(b + aS_{01}) = b^*(bS + a) \quad (10)$$

can be derived.

The overlap (S_{01}) between the no-bond and dative wave functions is expressed as

$$S_{01} = \int \psi_0 \psi_1 d\tau \simeq \sqrt{2}\,\frac{S_{DA}^*}{\sqrt{1 + S_{DA}^2}}$$

where S^{*}_{DA} refers to the overlap between the highest filled molecular orbital of the donor and the lowest unfilled orbital of the acceptor in the complex. The derivation of this relationship is outlined in some detail by Mulliken and Person[5] and is not reproduced here. It should be noted that this expression for S_{01} does include the assumption that donor and acceptor orbitals not involved in the charge-transfer are unchanged by the electron transfer.

The contribution of the dative structure to the ground state is usually taken as $(b^2 + abS_{01})$ by assigning half of the term $2abS_{01}$ in (5) to the donor and half to the acceptor. That is

$$F_0 = (a^2 + abS_{01})$$

and $$F_1 = (b^2 + abS_{01})$$

where $F_0 + F_1 = 1$ and F_0 and F_1 are then taken as measures of the weight of the no-bond and dative structures respectively.

Application of the linear variation method in which the energy of the ground state

$$W_N = \frac{\int \psi_N H \psi_N d\tau}{\int \psi_N^2 d\tau} \qquad (12)$$

is minimized with respect to a and b results in the following secular determinant

$$\begin{vmatrix} (W_0 - W_N) & (W_{01} - W_N S_{01}) \\ (W_{01} - W_N S_{01}) & (W_1 - W_N) \end{vmatrix} = 0$$

or $$(W_N - W_0)(W_N - W_1) = (W_{01} - W_N S_{01})^2 \qquad (13)$$

where

$W_0 = \int \psi_0 H \psi_0 d\tau$ (Energy of the no-bond structure)

$W_1 = \int \psi_1 H \psi_1 d\tau$ (Energy of the dative structure)

$W_{01} = \int \psi_0 H \psi_1 d\tau$ (Resonance or interaction energy of the no-bond and dative structures).

Solution of (13) for W_N yields

$$W_N = \frac{\frac{1}{2}(W_0 + W_1) - S_{01}W_{01} - (\frac{\Delta}{2})^2 + B_0B_1}{(1 - S_{01}^2)}$$

where $B_0 \equiv W_{01} - W_0S_{01}$,

$B_1 \equiv W_{01} - W_1S_{01}$

and $\Delta = W_1 - W_0$.

A similar procedure for W_E gives

$$W_E = \frac{\frac{1}{2}(W_0 + W_1) - S_{01}W_{01} + (\frac{\Delta}{2})^2 + B_0B_1}{(1 - S_{01}^2)}$$

The energy of the charge-transfer band is then

$$h\nu_{ct} = W_V - W_N = \frac{2(\frac{\Delta}{2})^2 + B_0B_1}{(1 - S_{01}^2)}$$

Substitution of W_N or W_E into the secular equations which make up the determinates and solving for the ratios b/a and b^*/a^* yields

$$\rho = \frac{b}{a} = -\frac{(W_0 - W_N)}{(W_{01} - S_{01} - W_N)} = -\frac{(W_{01} - S_{01}W_N)}{(W_1 - W_N)}$$

and

$$\rho^* = \frac{b^*}{a^*} = \frac{(W_{01} - S_{01}W_V)}{(W_{01} - S_{01}W_N)} = \frac{(W_1 - W_V)}{(W_{01} - S_{01}W_V)}$$

From these relations for ρ and ρ^* the following useful relationships can be developed

$$W_0 = \frac{(\rho S_{01} + 1)W_N + (\rho^* - S_{01})\rho W_V}{\rho\rho^* + 1}$$

$$W_1 = \frac{(\rho^* S_{01} - 1)W_V - (\rho + S_{01})\rho^* W_N}{-(\rho\rho^* + 1)}$$

and

$$W_{01} = -\rho W_1 + \rho W_N + S_{01} W_N$$

or

$$W_{01} = \rho^* W_0 - \rho^* W_V + S_{01} W_V.$$

The dipole moment of the ground state is given by

$$\mu_N = \int \psi_N \mu_{op} \psi_N d\tau = a^2 \mu_0 + b^2 \mu_1 + 2ab\mu_{01}$$

where μ_N, μ_{op}, μ_o, etc. are vectors defined as

μ_o = dipole moment of the ground state

μ_1 = dipole moment of the excited state

μ_{op} = dipole moment operator

μ_{01} = overlap dipole moment.

The overlap dipole moment has been approximated by Mulliken to be

$$\mu_{01} = \tfrac{1}{2}(\mu_1 - \mu_0)S_{01} + S_{01}\mu_0.$$

The potential surface diagrams are very useful in discussing charge-transfer complexes. It is common practice to take a cross section through such a diagram which corresponds to changing only one of the normal coordinates, namely the internuclear charge transfer distance. Figure 32 is such a diagram constructed to correspond roughly to the

parameters estimated for $TMA \cdot SO_2$ with $S_{01} = 0.2$. I_D and E_A are the ionization potential of TMA and electron affinity of SO_2 respectively. X_1 and X_0 are the resonance stabilization energies of the dative and no-bond states defined by

$$X_1 = W_V - W_1$$

$$X_0 = W_N - W_0.$$

The other terms are as defined previously.

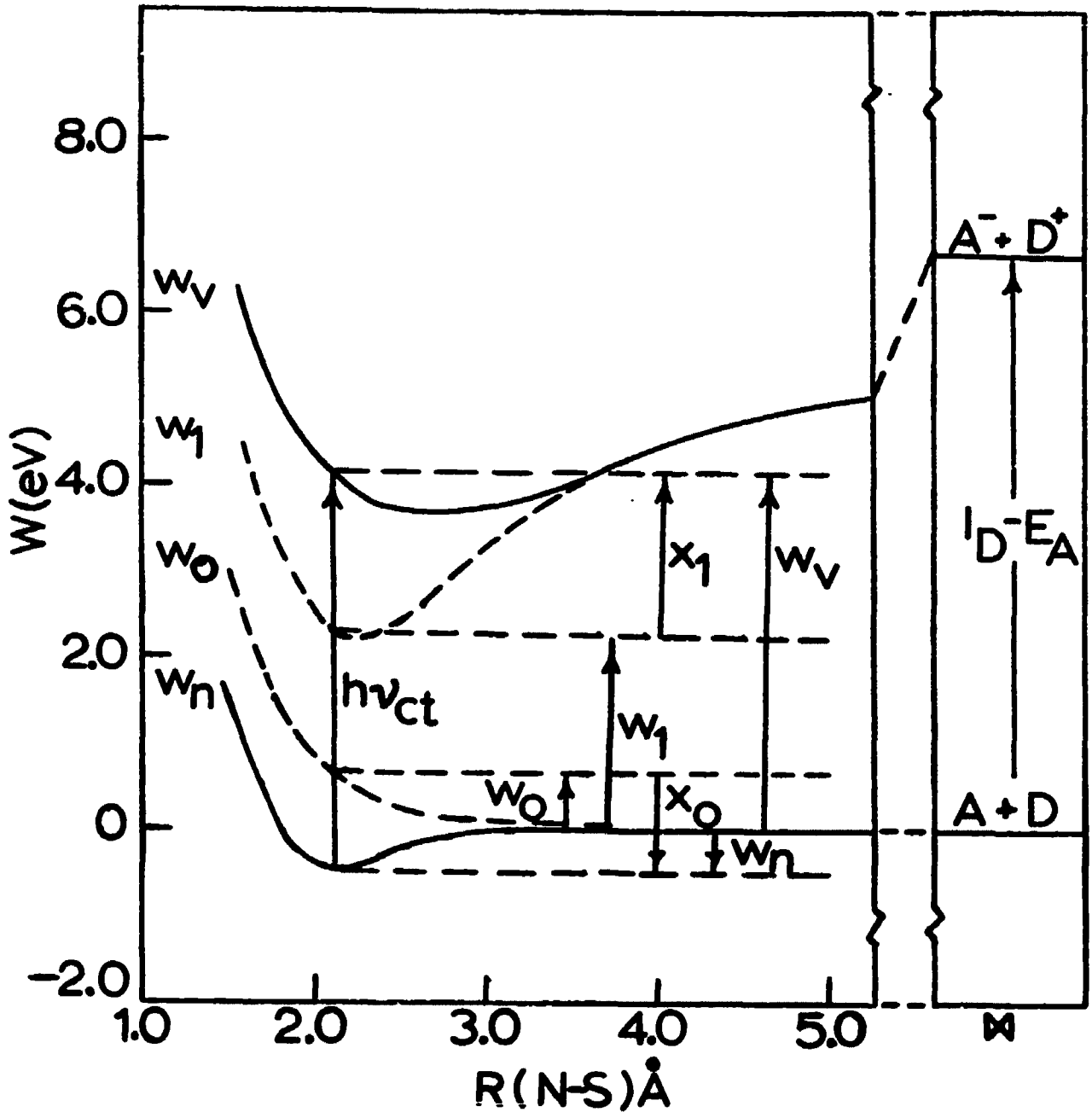

Figure 32. Energy Diagram for the TMA·SO_2 Complex for S_{01} = 0.2.

BIBLIOGRAPHY

1. Benesi, H. A. and Hildebrand, J. H., J. Amer. Chem. Soc., 71, 2703 (1949).

2. Mulliken, R. S., J. Amer. Chem. Soc., 72, 600 (1950).

3. Briegleb, G., "Elektronen-Donator-Acceptor-Komplexe," Springer-Verlag, Berlin, (1961).

4. Foster, R., "Organic Charge-Transfer Complexes," Academic Press, London and New York, (1969).

5. Mulliken, R. S. and Person, W. B., "Molecular Complexes," Wiley-Interscience, New York, (1969).

6. Scott, R. L. and Fenby, D. V., Ann. Rev. Phys. Chem., 20, 111 (1969).

7. Reid, C. and Mulliken, R. S., J. Amer. Chem. Soc., 76, 3869 (1954).

8. Mulliken, R. S., J. Amer. Chem. Soc., 91, 1237 (1969).

9. Scott, R. L., Rec. Trav. Chim., 75, 787 (1956).

10. Christian, S. D., J. Chem. Educ., 45, 713 (1968).

11. Person, W. B., J. Amer. Chem. Soc., 87, 167 (1965).

12. Peters, J. and Person, W. B., J. Amer. Chem. Soc., 86, 10 (1964).

13. Christian, S. D. and Tucker, E. E., J. Phys. Chem., 74, 214 (1970).

14. Carter, S., Murrell, J. N., and Rosch, E. J., J. Chem. Soc., 2048 (1965).

15. Mulliken, R. S. and Person, W. B., "Molecular Complexes," Wiley-Interscience, New York, (1969), Chapter 7.

16. Drago, R. S., Bolles, T. F., and Niedzielski, J. Amer. Chem. Soc., 88, 2717 (1966).

17. Christian, S. D., Taha, A. A., and Gash, B. W., Quart. Rev., 24, 20 (1970).

18. Mulliken, R. S., J. Amer. Chem. Soc., 74, 811 (1952).

19. Hildebrand, J. H. and Scott, R. L., "Regular Solutions," Prentice-Hall, Englewood Cliffs, N. J., (1962).

20. Orgel, L. E. and Mulliken, R. S., J. Amer. Chem. Soc., 79, 4839 (1957).

21. Deranleau, D., J. Amer. Chem. Soc., 88, 2717 (1966).

22. Scatchard, G., Ann. N. Y. Acad. Sci., 51, 660 (1949).

23. Evans, D. F., J. Chem. Phys., 23, 1426 (1954).

24. Rice, O. K., Int. J. Quantum Chem., IIS, 219 (1968).

25. Atack, D. and Rice, O. K., J. Phys. Chem., 58, 1017 (1954).

26. Mulliken, R. S. and Person, W. B., "Molecular Complexes," Wiley-Interscience, New York, (1969), Chapter 11.

27. Christian, S. D., Grundnes, J., and Cheam, V., Acta Chem. Scand., 24, 1836 (1970).

28. Hanna, M. W., J. Amer. Chem. Soc., 90, 285 (1968).

29. Christian, S. D., Affsprung, H. E., Johnson, J. R., and Worley, J. D., J. Chem. Educ., 40, 419 (1963).

30. Kortüm, G. and Vogel, W. M., Z. Electrochem., 59, 16 (1955).

31. Kortüm, G. and Kortüm-Seiler, M., Z. Naturforsch, 5a, 544 (1950).

32. Andrews, L. J. and Keefer, R. M., J. Amer. Chem. Soc., 74, 4500 (1952).

33. Tamres, M. and Searles, S., J. Amer. Chem. Soc., 75, 4358 (1953).

34. van de Stolpe, C., Ph.D. Dissertation, Amsterdam, 1953.

35. Plucknett, K. and Richards, H. L., J. Chem. Eng., 8, 234 (1963).

36. Bhowik, B. B., Spectro. Acta, 27A, 321 (1971).

37. Brandon, S. M., Tamres, M., and Searles, S., J. Amer. Chem. Soc., 82, 2129 (1960).

38. Reid, C. and Mulliken, R. S., J. Amer. Chem. Soc., 76, 3869 (1954).

39. McKinney, W. J. and Popov, A. I., J. Amer. Chem. Soc., 91, 5215 (1969).

40. Bist, H. D. and Person, W. B., J. Phys. Chem., 71, 2750 (1967).

41. Ham, J., J. Amer. Chem. Soc., 76, 3875 (1954).

42. Gregory, M. D., Ph.D. Dissertation, The University of Oklahoma, 1968.

43. Chattaway, F. D. and Hoyle, G., J. Chem. Soc., 123, 654 (1923).

44. Farnham, S. B., Ph.D. Dissertation, The University of Oklahoma, 1970.

45. Foote, H. W. and Fleisher, M., J. Phys. Chem., 37, 21 (1933); 57, 122 (1953).

46. Timmermans, J., "Physico-Chemical Constants of Pure Organic Compounds," Elsevier Publishing Company, Amsterdam-London-New York (1965).

47. Sanborn, R. H. and Orlemann, E. F., J. Amer. Chem. Soc., 77, 3724 (1955).

48. Sillén, L. S., Acta Chem. Scand., 18, 1085 (1965).

49. Christian, S. D. and Grundnes, J., J. Amer. Chem. Soc., 90:9, 2239 (1968).

50. Wilde, D. J., "Optimum Seeking Methods," Prentice-Hall, Inc., Englewood Cliffs, N. J. (1964).

51. Tamres, M. and Bhat, S. N., J. Phys. Chem., 75, 1057 (1971).

52. (a) Halpern, A. M. and Wiess, K., J. Amer. Chem. Soc., 90:23, 6297 (1968);
(b) De Maine, P. A. D., J. Chem. Phys., 26, 1192 (1957).

53. Ham, J. S., Platt, J. R., and McConnell, H., J. Chem. Phys., 19, No. 10, 1301 (1951).

54. Mulliken, R. S. and Person, W. B., "Molecular Complexes," Wiley-Interscience, New York, (1969), Chapter 1.

55. (a) Lin, T. F., Ph.D. Dissertation, The University of Oklahoma (1966).

(b) Tucker, E. E., Ph.D. Dissertation, The University of Oklahoma (1969).

(c) Morrow, J. K., Ph.D. Dissertation, The University of Oklahoma (1971).

56. Ketelaar, J. A. A., van de Stople, C., Goudsmit, A., and Dzcubas, W., Recueil, 1104, 71 (1952).

57. Ling, C., Ph.D. Dissertation, The University of Oklahoma, (1964).

58. Mulliken, R. S. and Person, W. B., "Molecular Complexes," Wiley-Interscience, New York, (1969), Chapter 10.

59. Bitaskar, K. R. and Singh, S., Spectro. Acta, 23A, 1155 (1967).

60. Waikley, J., Glew, D. N., and Hildebrand, J. H., J. Chem. Phys., 33, 621 (1960).

61. Duerksen, W. K. and Tamres, M., J. Amer. Chem. Soc., 90, 1379 (1968).

62. Hildebrand, J. H. and Scott, R. L., "The Solubility of Nonelectrolytes," Reinhold Publishing Company, New York, (1950), Chapter III.

63. Scatchard, G., Chem. Rev., 8, 321 (1931).

64. Byrd, W. E., Inorg. Chem., 1, 762 (1962).

65. Burg, A. B., J. Amer. Chem. Soc., 65, 1629 (1943).

66. Sim, G. A., Acta Cryst., 10, 177 (1957); Parthasirathyl, S., Acta Cryst., 18, 1022 (1965).

67. Moede, J. A. and Curran, C., J. Amer. Chem. Soc., 71, 852 (1949).

68. Hata, T., Tohoku Dalgaku Fisuiyoeki Kagaku Kenhyusho Hokoku, 16, 131 (1967).

69. Anderson, J. and Savoie, R., Can. J. Chem., 43(8), 2271 (1965).

70. Tramer, A., Bull. de L'Acad. Pol. Scie., Cl III, 5, 501 (1957).

71. Andrews, L. J. and Keefer, R. M., J. Amer. Chem. Soc., 73, 4169 (1951); Scott, R. L., J. Amer. Chem. Soc., 75, 1550, (1953).

72. De Maine, P. A. D., J. Chem. Phys., 26, 1036 (1957).

73. Booth, D., Dainton, E. S., and Irvin, K. J., Trans. Faraday Soc., 55, 1293 (1959).

74. Drago, R. S. and Wenz, D. A., J. Amer. Chem. Soc., 84, 526 (1962).

75. De Maine, P. A. D., J. Chem. Phys., 26, 1024 (1957).

76. Pout, C. K. and Wright, J. D., Angewandte Chemie, 7, 659 (1968).

77. Hassel, O. and Rømming, C., Quart. Rev., 16, 1 (1962).

78. Strømme, K., Acta Chem. Scand., 13, 268 (1959).

79. Hassel, O. and Hope, H., Acta Chem. Scand., 14, 391 (1960).

80. Hassel, O. and Hope, H., Acta Chem. Scand., 15, 407 (1961).

81. Hassel, O. and Rømming, C., Acta Chem. Scand., 15, 967 (1961).

82. Dahl, T. and Hassel, O., Acta Chem. Scand., 21, 592 (1967).

83. Marstokk, K. and Strømme, K., Acta Cryst., B24, 71 (1968).

84. Hassel, O. and Huosiet, E., Acta Chem. Scand., 8, 873 (1954).

85. Hassel, O. and Strømme, K., Acta Chem. Scand., 13, 275 (1959).

86. Rømming, C., Acta Chem. Scand., 14, 2145 (1960).

87. Hassel, O. and Strømme, K., Acta Chem. Scand., 12, 1146 (1958).

88. Hassel, O., Acta Chem. Scand., 13, 1781 (1959).

89. Strieter, F. J. and Templeton, J., J. Chem. Phys., 37, 161 (1962).

90. Wallwork, S. C., J. Chem. Soc., 494 (1961).

91. Shipley, G. G. and Wallwork, S. C., Acta Cryst., 22, 593 (1967).

92. Vogt, L. H., Katz, J. L., and Wiblerley, S. E., Inorg. Chem., 4, 1157 (1965).

93. La Placa, J. J. and Ibers, J. A., Inorg. Chem., 5, 405 (1966).

94. Shriver, D. F., Accounts Chem. Res., 3, 231 (1970).

95. Margenau, H. and Murphy, G. M., "The Mathematics of Physics and Chemistry," D. van Nostrand Co., 2nd ed., New Jersey, (1956).

96. Lipson, H. and Cochran, W., "The Determination of Crystal Structures, Vol. III," Cornell University Press, New York (1966).

97. "International Tables for X-Ray Crystallography," Vol. III, Kynoch Press, England (1962).

98. Ahmed, F. R., Structure Factor and Least Squares Computer Program, NRC-10, Ottawa: National Research Council, 1966.

99. Nicholas, H. Ph.D. Dissertation, The University of Oklahoma, 1968.

100. Ahmed, F. R., Fourier Computer Program for Distorted and Undistorted Nets, NRC-8, Ottawa: National Research Council, 1966.

101. Cruichshank, D. W. J., Acta Cryst., 9, 747 (1956).

102. Dunitz, J. D., Acta Cryst., 9, 579 (1956).

103. Beagley, B., Trans. Faraday Soc., 64(10), 2561 (1968).

104. Kanda, F. A. and King, A. J., J. Amer. Chem. Soc., 73, 2315 (1951).

105. Pauling, L., J. Phys. Chem., 56, 361 (1952); Moffitt, W. E., Proc. Roy. Soc. (London), A200, 409 (1950).

106. Busing, W. R. and Levy, H. A., Acta Cryst., 17, 142 (1964).

107. King, G. W., "Spectroscopy and Molecular Structure," Holt, Rinehart and Winston, Inc., New York, Chicago, San Francisco, (1964).

108. Cox, E. G., Cruichshank, D. W. J., and Smith, J. A. S., Proc. Roy. Soc., 247A, 1 (1958).

109. Post, B., Schwartz, R. S., and Frankuchen, I., Acta Cryst., 5, 372 (1952).

110. Shoemaker, V. and Trueblood, K. N., Acta Cryst., B24, 63 (1968).

111. Ionov, S. P. and Porai-Koshits, M. A., Zhurnal Strukturnoi Khimii, 7, No. 2, 252 (1966).

112. Mulliken, R. S., J. Chem. Phys., 23, 1833 (1955).

113. Lofthus, A., Mol. Phys., 6, 115 (1963).

114. Enwall, E., Private Communication of work to be published.

115. Kobinata, S. and Nagakura, S., J. Amer. Chem. Soc., 88, 3905 (1966).

116. Pilkington, P., Private Communication.

117. Kaplan, H., J. Chem. Phys., 26, 1704 (1957).

118. Harker, D., J. Chem. Phys., 4, 381 (1936).

119. Johnson, C. K., Ortep: A Fortran Thermol-Ellipsoid Plot Program for Crystal Structure Illustrations, ORNL-3794, Oak Ridge National Laboratory: Tennessee, 1965.

120. Roothaan, C. C. J., Revs. Modern Phys., 23, 69 (1951).

121. Palke, W. E. and Lipscomb, W. N., J. Amer. Chem. Soc., 88, 2384 (1966).